Dissertation ETH No.16569

Cellular translocation, trafficking and metabolic cleavage of novel cell penetrating peptides

A dissertation submitted to the

Swiss Federal Institute of Technology Zurich

for the degree of

Doctor of Sciences

(Dr. sc. ETH)

presented by

Christina Förg

Pharmacist

Julius-Maximilians-Universität Würzburg

born on Dec 16th, 1977

citizen of Germany

accepted on the recommendation of

Prof. Dr. H.P. Merkle, examiner

Prof. Dr. Ernest Giralt, co-examiner

Dr. Urs Ziegler, co-examiner

2006

CONTENTS

ABBREVIATIONS

AcCN	acetonitrile
Antp	Antennapedia
BBB	blood brain barrier
BSA	bovine serum albumin
Calu-3	human Caucasian lung adenocarcinoma cell line
CF	5(6)carboxyfluoresceine
CHO	chinese hamster ovary cell line
CLSM	confocal laser scanning microscopy
CPPs	cell-penetrating peptides
CsA	cyclosporine A
DOG	2-deoxyglucose
DMEM	Dulbecco's modified Eagle's medium
DPM	disintegrations per minute
DNA	desoxyribonucleic acid
EEA1	early endosome antigen-1
ECM	extracellular matrix
EthD-1	ethidium homodimer-1
FACS	fluorescence-activated cell sorting
FCS	foetal calf serum
FITC	fluorescein isothiocyanate
GalR-1	galanin receptor-1
Gal T	galactosyltransferase
GFP	green fluorescent protein
HBSS	Hank`s balanced salt solution
hCT	human calcitonin
HeLa	human cervix epithelial adenocarcinoma cell line
HIV	human immune deficiency virus
HPLC	high performance liquid chromatography
HS	heparin sulphate
HSV-1	Herpes simplex virus type 1
HP-γ-CD	hydroxypropyl- γ-cyclodextrin
IBD	Inflammatory Bowel Disease

MALDI-TOF MS	matrix assisted laser desorption and ionization time of flight mass spectrometry
MDCK	Madin Darby canine kidney cell line
M-β-CD	methyl- β -cyclodextrin
MTS	3-(4,5-dimethylthiazol-2-yl)-5-(3-carboxymethoxy-phenyl)-2-(4-sulfophenyl)-2H-tetrazolium
NaN_3	sodium azide;
NLS	nuclear localization sequence
PBS	phosphate buffered saline
PFA	paraformaldehyde
PNA	peptide nucleic acids
PTD	protein transduction domain
SAP	sweet arroz peptide
SV40	Simian virus 40
TAMRA	carboxytetramethylrhodamine
Tat	trans-activating transduction
Tc	Technetium
TEER	transepithelial electrical resistance
TFA	trifluoroacetic acid
TGN	trans-Golgi network
TJ	tight junctions
TRITC	tetramethyl rhodamine isothiocyanate
pVEC	vascular endothelial cadherin
VP22	virion phosphoprotein
ZO-1	zonula occludens protein-1

BACKGROUND AND PURPOSE

Cellular uptake of biopharmaceuticals, such as peptides, proteins and nucleic acid based pharmaceuticals, represents a crucial prerequisite when it comes to reach intracellular targets and exert therapeutic activity. Nevertheless, cellular barriers often restrict sufficient cellular entry, in particular through the lipophilic nature of the biological membrane, the charge of biopharmaceuticals, and the metabolic cleavage of the molecules before they reach their intracellular target. Therefore, the cellular bioavailability of such biomacromolecules is often poor, compromising their otherwise promising therapeutic potential. The discovery of various 10 to 30-mer peptides with the ability to cross cellular membranes has opened a new horizon in the delivery of biopharmaceuticals. Chemical ligation or physical assembly of these so-called cell penetrating peptides (CPPs) with biopharmaceuticals of poor cellular access have been suggested to mediate the non-invasive import of such problematic cargoes into the cells. In fact, in vivo studies in mice with Tat, a polycationic CPP derived from the human immunodeficiency virus (HIV) Tat protein, triggered great expectation, as it appeared to help a marker protein pass several biological barriers, even the blood brain barrier, and distribute into virtually every organ [1, 2].

Over the last decade, a variety of CPPs has been discovered that translocate cellular membranes successfully and deliver their cargos into the cytoplasm and/or the nucleus. Most of the currently recognized CPPs are of cationic nature and derived from viral, insect or mammalian proteins endowed with membrane translocation properties. A prominent CPP – commonly referred to as penetratin - that has been first reported in 1994, derives from the third helix of the Antennapedia protein homeodomain [3]. Penetratin, together with Tat derived peptides [4] and the chimeric peptide transportan [5], is one of the most extensively investigated CPPs today. Besides, several other CPPs such as peptides from the MPG family [6], CPPs with antimicrobial properties [7], pVEC [8] and VP22 [9] have been identified and are well described in the literature. More recently, SAP, a linear trimer of repetitive VRLPPP domains, and conceived as an amphipathic version of a polyproline sequence related to γ-zein, a storage protein of maize, has been identified as CPP [10-12]. Besides these oligocationic peptides, enhanced translocation of the cellular membrane has also been reported for weakly cationic peptides, such as a new group of peptide sequences derived from the C-terminal domain of human calcitonin (hCT) [13-15]. Of particular advantage of the recently developed CPPs SAP and the branched hCT(9-32)-br are their negligible cytotoxicity, even at high concentrations, as compared to other CPPs, as well as their high metabolic stability when in

contact with epithelial cell cultures. These advantages may be crucial with respect to their therapeutic application of cell-penetrating peptides in the future.

In an introductory chapter, the present PhD thesis revisits the performance of cell penetrating peptides for drug delivery. To this aim we cover both accomplishments and failures and report on new prospects of the CPP approach. Further on, our investigations on cellular translocation efficiency and translocation mechanisms of the CPPs SAP and hCT(9-32)-br in epithelial cell cultures aim to contribute to a better understanding of the translocation process of cell penetrating peptides across the plasma membrane. As the metabolic stability of CPPs is an important biopharmaceutical factor for cellular bioavailability, we studied the metabolic degradation of four recently developed CPPs, namely SAP, hCT(9-32)-br, [Pα] and [Pβ], when in contact with three epithelial cell cultures, consisting of either subconfluent HeLa or confluent MDCK or Calu-3 cells. Additionally, through analysis of their cellular translocation, we aim to reveal a possible relationship between metabolic stability and translocation efficiency. Another important aspect of the present PhD thesis is to demonstrate the impact of the respective cell line, the cellular differentiation state and the formation of tight junctions upon the translocation efficiency of CPPs. According to an increasing trend in literature for CPP translocation to occur via endocytic processes, we aim to elucidate the underlying cellular mechanisms for endocytosis. Furthermore, in the context of the observed barriers for CPP translocation into epithelia, we also comment on potential niches for the therapeutic application of CPPs in drug delivery, including the use of CPP for delivery into inflammatory epithelia.

1. Schwarze, S.R., et al., *In vivo protein transduction: delivery of a biologically active protein into the mouse.* Science, 1999. **285**(5433): p. 1569-72.
2. Schwarze, S.R., K.A. Hruska, and S.F. Dowdy, *Protein transduction: unrestricted delivery into all cells?* Trends Cell Biol, 2000. **10**(7): p. 290-5.
3. Derossi, D., et al., *The third helix of the Antennapedia homeodomain translocates through biological membranes.* J Biol Chem, 1994. **269**(14): p. 10444-50.
4. Vives, E., P. Brodin, and B. Lebleu, *A truncated HIV-1 Tat protein basic domain rapidly translocates through the plasma membrane and accumulates in the cell nucleus.* J Biol Chem, 1997. **272**(25): p. 16010-7.
5. Pooga, M., et al., *Cell penetration by transportan.* Faseb J, 1998. **12**(1): p. 67-77.

6. Chaloin, L., et al., *Design of carrier peptide-oligonucleotide conjugates with rapid membrane translocation and nuclear localization properties.* Biochem Biophys Res Commun, 1998. **243**(2): p. 601-8.
7. Frank, R.W., et al., *Amino acid sequences of two proline-rich bactenecins. Antimicrobial peptides of bovine neutrophils.* J Biol Chem, 1990. **265**(31): p. 18871-4.
8. Elmquist, A., et al., *VE-cadherin-derived cell-penetrating peptide, pVEC, with carrier functions.* Exp Cell Res, 2001. **269**(2): p. 237-44.
9. Elliott, G. and P. O'Hare, *Intercellular trafficking of VP22-GFP fusion proteins.* Gene Ther, 1999. **6**(1): p. 149-51.
10. Crespo, L., et al., *Peptide dendrimers based on polyproline helices.* J Am Chem Soc, 2002. **124**(30): p. 8876-83.
11. Fernandez-Carneado, J., et al., *Potential Peptide Carriers: Amphipathic Proline-Rich Peptides Derived from the N-Terminal Domain of gamma-Zein.* Angew Chem Int Ed Engl, 2004. **43**(14): p. 1811-1814.
12. Fernandez-Carneado, J., et al., *Amphipathic peptides and drug delivery.* Biopolymers, 2004. **76**(2): p. 196-203.
13. Krauss, U., et al., *In vitro gene delivery by a novel human calcitonin (hCT)-derived carrier peptide.* Bioorg Med Chem Lett, 2004. **14**(1): p. 51-4.
14. Machova, Z., et al., *Cellular internalization of enhanced green fluorescent protein ligated to a human calcitonin-based carrier peptide.* Chembiochem, 2002. **3**(7): p. 672-7.
15. Trehin, R., et al., *Cellular internalization of human calcitonin derived peptides in MDCK monolayers: a comparative study with Tat(47-57) and penetratin(43-58).* Pharm Res, 2004. **21**(1): p. 33-42.

Seite Leer /
Blank leaf

ABSTRACT

Over the last decade, marked improvements in the cellular delivery of various biologically active molecules have been achieved upon chemical or physical ligation to so-called cell-penetrating peptides (CPPs), denoting peptides with the capacity to translocate the plasma membrane of mammalian cells. This PhD thesis mainly studies two recently developed CPPs, namely SAP and hCT(9-32)-br. For comparison, other established CPPs are also included, namely the Tat peptide as well as the linear hCT derived peptide hCT(9-32), and two members of the MPG family, [Pα] and [Pβ].

The *first chapter* presents a selection of representative CPP families and cargo molecules that have been efficiently delivered by the CPP approach. From this perspective, mechanisms of internalization as well as intracellular trafficking routes were considered. The focus of this review is to revisit the performance of cell penetrating peptides for drug delivery. To this aim we cover both accomplishments and failures and we report on new prospects of the CPP approach. Besides a selection of successful case histories of CPPs we also review the limitations of CPP mediated translocation. In particular, we comment on the impact of (i) metabolic degradation, (ii) the cell line and cellular differentiation state dependent uptake of CPPs as well as (iii) the regulation of their endocytic traffic by Rho-family GTPases. Further on, we aim at the identification of promising niches for CPP application in drug delivery. In this context, as inspired by current literature, we focus on three principal areas: (i) the delivery of antineoplastic agents, (ii) the delivery of CPPs as antimicrobials, and (iii) the potential of CPPs to target inflammatory tissue.

Despite increasing evidence for the involvement of endocytosis in the internalization of CPPs, the exact mechanism underlying the translocation of CPPs across the cellular membrane is still not completely understood. In the *second chapter* of the PhD thesis, we study translocation efficiency and mechanism as well as intracellular trafficking of SAP and hCT(9-32)-br into HeLa cells using biochemical markers in combination with quenching and colocalization approaches. Both peptides were readily internalized by HeLa cells through interaction with the extracellular matrix followed by lipid raft-mediated endocytosis. This was confirmed by reduced uptake at lower temperatures, in the presence of endocytosis inhibitors and through cholesterol depletion by methyl-β-cyclodextrin, supported by colocalization with markers for clathrin-independent pathways. In contrast to the oligocationic CPPs SAP and hCT(9-32)-br, interaction with the extracellular matrix, however, was no prerequisite for the observed lipid raft-mediated uptake of the weakly cationic, unbranched hCT(9-32). Transient involvement of endosomes in the intracellular trafficking of SAP and hCT(9-32)-br prior to

endosomal escape of both peptides was revealed by colocalization and pulse-chase studies of the peptides with the early endosome antigen1.

Metabolic stability of CPPs is an important biopharmaceutical factor for cellular bioavailability, since the peptides should be stable enough to carry their cargo to the target before they are metabolically cleaved. Therefore, we studied in the *third chapter* of this thesis the metabolic degradation of four recently developed CPPs. Besides SAP and hCT(9-32)-br, we investigated [Pα] and [Pβ], when in contact with three epithelial cell cultures, consisting of either subconfluent HeLa or confluent MDCK or Calu-3 cells. Additionally, through analysis of their cellular translocation, we aimed to reveal possible relation between metabolic stability and translocation efficiency. Between HeLa, MDCK and Calu-3 we found the levels of proteolytic activities to be highly variable. However, for each peptide, the individual patterns of metabolic degradation were quite similar. The metabolic stability of the investigated CPPs was in the order of CF-SAP = CF-hCT(9-32)-br > [Pβ]−IAF > [Pα]. We were further able to identify specific cleavage sites for each of the four peptides. For all investigated CPPs, we observed higher translocation efficiencies into HeLa cells as compared to MDCK and Calu-3, corresponding to the lower state of differentiation of HeLa cell cultures. For the four CPPs, there was no direct relation between metabolic stability and translocation efficiency. These results indicate that metabolic stability is not a main limiting factor for efficient cellular translocation. Nevertheless, the translocation of individual CPPs may be improved by structural modifications aiming at increased metabolic stability.

In the *forth chapter* of this thesis, we emphasize the importance of differentiated cell models to study CPP translocation, and, moreover, we point towards inflamed epithelia as potential niches for CPP application in drug delivery. We observed marked endocytic uptake of the two CPPs SAP and hCT(9-32)-br into proliferating MDCK cells by a mechanism involving both lipid rafts and clathrin-coated pits. In well-differentiated, confluent MDCK monolayers, however, we noted a massive slow-down of compound-unspecific endocytosis. The underlying mechanism is the down-regulation of endocytosis by Rho-GTPases that have been previously identified to be intimately involved in endocytic traffic. In fact, we found a correlation between endocytic translocation and active form Rho-A, as well as a correlation between cell density, cellular differentiation and endocytic slow-down on the one hand, and active form Rac-1 on the other. To our knowledge, this is the first study to cast light on the underlying mechanisms for the differentiation-restricted translocation of CPPs into epithelial cell models. Our findings were further elaborated using an inflammatory epithelial, IFN-γ/TNF-α induced MDCK model mimicking inflammatory epithelial diseases. CPP

translocation in the inflammatory model was enhanced in a cytokine concentration-dependent way, resulting in maximum enhancement rates of up to 90 %. Interestingly, our observations suggest a cytokine-induced redistribution of lipid rafts in confluent MDCK layers to be involved in the observed enhancement of CPP translocation.

In conclusion, we describe in this PhD thesis the cellular translocation mechanism, the intracellular trafficking and the metabolic cleavage of two recently developed CPPs, SAP and hCT(9-32)-br, into epithelial cell cultures. As compared to other CPPs, e.g. the Tat peptide, both peptides show the advantage of negligible cytotoxicity and high metabolic stability. The finding of their lipid raft-mediated uptake into HeLa cells adds evidence to the suggestion of a common endocytic translocation mechanism of CPPs. With regard to cellular barriers to CPP internalization, we suggest inflamed epithelia as potential niches for a therapeutic application of CPPs in drug delivery.

ZUSAMMENFASSUNG

Im Laufe des letzten Jahrzehnts konnte die gezielte zelluläre Freisetzung verschiedener biologisch aktiver Moleküle dadurch verbessert werden, dass sie auf chemischem oder physikalischem Wege an sogenannte Zellpenetrierende Peptide (ZPPs) gekoppelt wurden. Diese Zellpenetrierenden Peptide sind in der Lage, die Plasmamembran von Säugetierzellen zu überwinden. Die vorliegende Dissertation befasst sich vornehmlich mit den beiden neu entwickelten ZPPs SAP und hCT(9-32)-br. Andere, bereits gut erforschte, ZPPs wie das Tat-Peptid, das lineare hCT(9-32) sowie die zwei MPG Peptide [Pα] und [Pβ] wurden zu Vergleichszwecken herangezogen.

Das erste Kapitel stellt eine Auswahl etablierter ZPP-Familien dar und präsentiert eine Reihe von „Cargo-Molekülen", die bereits effizient durch ZPPs in Zellen transportiert werden konnten. In diesem Zusammenhang werden Aufnahmemechanismen sowie die intrazelluläre Wanderung der Peptide betrachtet. Dieses Überblickskapitel beschäftigt sich hauptsächlich mit der Effizienz von ZPPs bei der gezielten zellulären Freisetzung biologisch aktiver Moleküle. Dabei gehen wir neben einer Auswahl an positiven Beispielen auch auf die Grenzen des ZPP-Ansatzes ein. Insbesondere interessiert uns hierbei der Einfluss auf die ZPP-Aufnahme, den (i) die Metabolisierung, (ii) die jeweiligen Zellinien und der zellulären Differenzierungsstatus sowie (iii) die Regulierung der Endozytose durch Rho-GTPasen haben. Im Ausblick präsentieren wir weiterhin viel versprechende Nischen für die zukünftige Anwendung von ZPPs. Bezug nehmend auf aktuelle Literatur beschäftigen wir uns dabei hauptsächlich mit den drei Gebieten Antitumortherapie, antimikrobieller Anwendung sowie dem Potential von ZPPs im Einsatz gegen entzündete Epithelien.

Trotz vermehrter Hinweise auf die Beteiligung von Endozytose an der zellulären Aufnahme von ZPPs ist der genaue Mechanismus, der diesem Prozess zugrunde liegt, noch nicht vollständig geklärt. Im 2. Kapitel dieser Arbeit beschäftigen wir uns mit Aufnahmeeffizienz und –mechanismus sowie mit der Wanderung der Peptide SAP und hCT(9-32)-br in HeLa Zellen. Hierbei wurden Zellorganellen biochemisch gekennzeichnet und „Quenching"- und Kollokalisationsmethoden herangezogen. Beide Peptide wurden nach Wechselwirkung mit der extrazellulären Matrix und der folgenden „lipid raft"-Endozytose effizient in HeLa Zellen aufgenommen. Dies wurde bestätigt durch reduzierte Aufnahme bei niedrigen Temperaturen, bei Zugabe von Endozytose-Hemmstoffen und bei einer Verringerung des Cholesterinanteils. Weitere Belege für diese These liefern Kollokalisationsstudien mit Fluoreszenzmarkern für einen Clathrin-unabhängigen Endozytoseweg. Im Unterschied zu den oligokationischen ZPPs SAP und hCT(9-32)-br ist

jedoch die Wechselwirkung mit der extrazellulären Matrix keine Notwendigkeit für die Aufnahme des schwach kationischen, linearen hCT(9-32) via „lipid raft"-Endozytose.
Die vorübergehende Aufnahme von SAP und hCT(9-32)-br in Endosomen und ihre nachfolgende Freisetzung wurde durch Kollokalisations- und „Pulse-chase"-Studien der Peptide mit dem „early endosome antigen 1" deutlich gemacht.

Unter dem Gesichtspunkt der metabolischen Stabilität der ZPPs betrachtet, sollten die Peptide in der Lage sein, Ihr Cargo zum Zielort zu transportieren, bevor sie gespalten werden. Daher untersuchen wir im 3. Kapitel dieser Arbeit den metabolischen Abbau der vier neu entwickelten ZPPs SAP, hCT(9-32)-br, [Pα] sowie [Pβ], auf den drei epithelialen Zellkulturen HeLa, Calu-3 und den konfluenten MDCK Zellen. Zusätzlich versuchen wir herauszufinden, ob bei den Peptiden eine Beziehung zwischen ihrer metabolischen Stabilität und ihrer zellulären Aufnahmeeffizienz besteht. Das Ausmaß an proteolytischer Aktivität variiert stark zwischen HeLa, MDCK und Calu-3 Zellen. Die jeweiligen metabolischen Abbaumuster der einzelnen ZPPs auf den Zellen sind dagegen sehr ähnlich. CF-SAP und CF-hCT(9-32)-br weisen die größte metabolische Stabilität der untersuchten ZPPs auf, weniger stabil ist [Pβ]–IAF und [Pα] stellt das am wenigsten stabile Peptid dar. Wir konnten weiterhin spezifische Abbaustellen für jedes der vier ZPPs identifizieren. Alle vier weisen in HeLa Zellen eine höhere Aufnahmeeffizienz auf als in MDCK und Calu-3 Zellen. Dies entspricht auch dem niedrigeren Differenzierungsstatus von HeLa-Zellkulturen. Für alle vier ZPPs lässt sich keine direkte Beziehung zwischen metabolischer Stabilität und Aufnahmeeffizienz ableiten. Dieses Ergebnis deutet darauf hin, dass die metabolische Stabilität kein limitierender Faktor für effiziente zelluläre Aufnahme ist. Nichtsdestotrotz könnte die Aufnahme der einzelnen ZPPs durch strukturelle Modifizierung mit dem Ziel erhöhter metabolischer Stabilität weiter verbessert werden.

Das 4. Kapitel dieser Arbeit untersucht den Einfluss differenzierter Zellmodelle auf Aufnahmestudien und stellt entzündete Epithelien als mögliche Nischen für die Anwendung von ZPPs vor. SAP und hCT(9-32)-br werden effizient in proliferierende MDCK-Zellen aufgenommen. Hierbei ist unseren Ergebnissen zufolge sowohl Endzytose über „clathrin-coated pits" als auch über „lipid rafts" involviert. In ausdifferenzierten, konfluenten MDCK-Zellen beobachten wir jedoch eine stark verminderte Endozytoseaktivität, unabhängig vom jeweils getesteten, aufzunehmenden Stoff. Beim hier zugrunde liegende Mechanismus scheint es sich um die Herabregulierung der Endozytoseaktivität durch Rho-GTPasen zu handeln, welche bekanntermaßen bei Endozytose-Prozessen eine wichtige Rolle spielen. Tatsächlich können wir eine Korrelation zwischen endozytotischer Aufnahme und aktiver Rho-A GTPase,

sowie eine Korrelation zwischen Zelldichte, zellulärer Differenzierung und endozytotischer Herabregulierung auf der einen Seite und aktiver Rac-1 GTPase auf der anderen Seite beobachten. Nach unserem Kenntnisstand ist dies die erste Studie, die den Mechanismus differenzierungsabhängiger Aufnahme von ZPPs in epitheliale Zellmodelle aufdeckt. Diese Erkenntnisse wurden für weitere Studien an MDCK-Modellen genutzt, welche mit IFN-γ/TNF-α behandelt werden, um epitheliale Entzündung zu simulieren. Die Aufnahme der ZPPs in diese Entzündungsmodelle war in Abhängigkeit des Zytokingehalts erhöht, die maximale Steigerung lag bei bis zu 90%. Interessanterweise legen unsere Beobachtungen nahe, dass eine Zytokin-induzierte Umverteilung der "lipid-rafts" in konfluenten MDCK-Zellen an der beobachteten Erhöhung der ZPP-Aufnahme beteiligt ist.

Insgesamt beschreiben wir in dieser Dissertation die zellulären Aufnahmemechanismen, die intrazelluläre Wanderung und den metabolischen Abbau der zwei neu entwickelten ZPPs SAP and hCT(9-32)-br in epithelialen Zellkulturen. Im Vergleich zu anderen ZPPs, z.B. dem Tat-Peptid, weisen diese beiden Peptide den Vorteil vernachlässigbarer Toxizität und hoher metabolischer Stabilität auf. Zusätzlich ist die Erkenntnis ihrer Aufnahme über "lipid-raft"-Endozytose ein starkes Indiz für einen gemeinsamen Aufnahmemechanismus von ZPPs mittels Endozytose. Im Hinblick auf Beschränkungen bei der Aufnahme von ZPPs schlagen wir entzündete Epithelien als Perspektive für einen therapeutischen Anwendungsbereich vor.

CHAPTER I

On the biomedical promise of cell penetrating peptides: limits versus prospects

Christina Foerg[1] and Hans P. Merkle[1]

[1] Department of Chemistry and Applied Biosciences, Institute of Pharmaceutical Sciences, ETH Zurich, Switzerland

ABSTRACT

The cell membrane poses a substantial hurdle to the use of pharmacologically active biomacromolecules that are not *per se* actively translocated into cells. An appealing approach to deliver such molecules involves tethering them to so-called cell penetrating peptides (CPPs) that are able to cross plasma membranes. This CPP approach is currently a main avenue in engineering delivery systems that could mediate the non-invasive import of problematic cargos into cells. The large number of different cargo molecules that have been efficiently delivered by CPPs ranges from small molecules to proteins and particles. Today, there is increasing evidence for the involvement of endocytosis as a major mechanism for cellular internalization. Moreover, in terms of intracellular trafficking, current data argue for the transport to acidic early endosomal compartments with cytosolic release mediated via retrograde delivery through the Golgi apparatus and the endoplasmic reticulum.

The focus of this review is to revisit the performance of cell penetrating peptides for drug delivery. To this aim we cover both accomplishments and failures and report on new prospects of the CPP approach. Besides a selection of successful case histories of CPPs we also review the limitations of CPP mediated translocation. In particular, we comment on the impact of (i) metabolic degradation, (ii) the cell line and cellular differentiation state dependent uptake of CPPs as well as (iii) the regulation of their endocytic traffic by Rho-family GTPases. Further on, we aim at the identification of promising niches for CPP application in drug delivery. In this context, as inspired by current literature, we focus on three principal areas: (i) the delivery of antineoplastic agents, (ii) the delivery of CPPs as antimicrobials, and (iii) the potential of CPPs to target inflammatory tissue.

INTRODUCTION

The full therapeutic potential of peptide-, protein- and nucleic acid-based drugs is frequently compromised by their limited ability to cross the plasma membrane of mammalian cells, resulting in poor cellular access and inadequate therapeutic efficacy [1, 2]. Today this hurdle represents a major challenge for the biomedical and commercial development of many biopharmaceuticals. Over the past decade, however, attractive propects for a massive improvement in the cellular delivery of such molecules have been announced that were to result from physical assembly or chemical ligation to so-called *cell penetrating peptides* (CPPs), also denoted as *protein-transduction domains* (PTDs). CPPs represent short peptide sequences of ten to about thirty amino acids which can cross the plasma membrane of mammalian cells and may thus offer unprecedented opportunities for cellular drug delivery. In fact, in a widely recognized landmark study in mice, the intraperitoneal injection of a fusion protein conjugated to Tat(47-57), an oligocationic CPP derived from human immunodeficiency virus (HIV) Tat protein, was found to let the ligated protein overcome several biological barriers, distribute into virtually every organ and even pass the blood brain barrier [3]. Nevertheless, the biomedical promise of CPPs is still far from clinical implementation. Whereas most of the scientific motivation in the field of the CPPs derives from the appealing perspectives for their biomedical use, much of the actual research is still very much focused on more fundamental aspects as to their biochemical, biophysical and cell biological assessment. Clinically relevant contributions appear to be rare.

This review focuses on the biomedical promise of cell penetrating peptides. By revisiting the performance of CPPs for drug delivery, we cover both accomplishments and failures and report on new prospects of the CPP approach. Besides a selection of successful case histories, we also point out limitations of CPP mediated translocation. Major obstacles to CPP mediated drug delivery consist in (i) their metabolic degradation (ii) the cell line and cellular differentiation state dependent uptake of CPPs as well as (iii) the regulation of their endocytic traffic by Rho-family GTPases. In the final section, we aim at the identification of promising niches for CPP application in drug delivery. In this context, as inspired by current literature, we focus on three principal areas: (i) the delivery of antineoplastic agents, (ii) the delivery of CPPs as antimicrobials, and (iii) the potential of CPPs to target inflammatory tissue.

Selected CPP families and cargo molecules

Most of the currently recognized CPPs are of oligocationic nature and derived from viral, insect or mammalian proteins endowed with membrane translocation properties. One of the first CPPs, reported as early as 1994, derived from the third helix of the Antennapedia protein homeodomain of *Drosophila* [4]. Today, this peptide is commonly referred to as penetratin and, together with oligopeptides of the Tat family [5] and the chimeric peptide transportan [6], one of the most widely investigated CPPs. As for the third α-helix (residues 43-58) of the Antennapedia protein homeodomain the minimal sequence responsible for the cellular translocation of the Tat protein has also been identified and is represented by the predominantly cationic residues 47-57 [7]. In addition, a wealth of further oligocationic CPPs has been revealed and described in the literature [8, 9]. Prominent examples are the peptides of the so-called MPG family [10], antimicrobial-derived CPPs [11-15], pVEC [16, 17] and VP22 [18-20]. Expectedly, by genomic exploration more and more CPP sequences are currently being uncovered.

Besides oligocationic CPPs, enhanced translocation of the cellular membrane has also been reported for weakly cationic peptides, e.g., a family of peptide sequences derived from the C-terminal domain of human calcitonin (hCT) [21-23]. The discovery of this CPP class stemmed from the observation that a C-terminal fragment of hCT was subject to endocytosis when exposed to excised nasal epithelium [24]. More recently, SAP, a linear trimer of moderately cationic, repetitive VRLPPP domains, and conceived as an amphipathic version of a polyproline sequence related to γ-zein, a storage protein of maize, has been identified as CPP [25-27]. A selection of names, origins and sequences of representative CPP families are shown in Table 1.

The large number of different cargo molecules that have been efficiently delivered by the CPP approach includes biologics like peptides [28-30], proteins [31-34], antisense oligonucleotides [35-38], siRNA [39, 40], plasmid DNA [41-44], as well as model drugs [45, 46]. Even particulate systems such as liposomes [47], and microparticles [48-50] could be delivered. A more detailed overview over various cargos delivered by CPPs was recently presented by Jarver et al. [51]. A representative selection of model cargoes and related references is part of Table 1.

Table I Selection of representative CPP families, model cargoes and related references.

Name	Origin	Sequence	References	Cargo/Reference
Tat family				
Tat (48-60)	HIV-1 protein	GRKKRRQRRRPPQQ	[3, 52-55]	β-Galactosidase [3]
Oligoarginine	Tat derivative	R_n	[56-59]	Cyclosporin A [60]
Penetratin family				
pAntp	Antennapedia homeodomain	RQIKIWFQNRRMKWKK	[4, 61-63]	Polo-box [30]
pIsl	Isl-1 homeodomain	RVIRVWFQNKRCKDKK	[64-66]	Biotin / avidin [65]
Chimeric CPPs				
Transportan	(galanin-mastoparan)	GWTLNSAGYLLGKINLKALAALAKKIL	[6, 67]	GalR-1 (Antisense) [68]
MPG peptides			[10, 69]	siRNA [39, 40]
[Pβ]	(gp41-SV40)	GALFLGFLGAAGSTMGAWSQPKKKRKV	[69, 70]	fluorophore (Chaper III)
[Pα]	(gp41-SV40)	GALFLAFLAAALSLMGLWSQPKKKRKV	[71, 72]	fluorophore (Chaper III)
Pep-1	(Trp-rich motif-SV40)	KETWWETWWTEWSQPKKKRKV	[72, 73]	proteins [73]
Antimicrobial-derived CPPs				
Buforin 2	Toad stomach	TRSSRAGLQWPVGRVHRLLRK	[11, 74]	GFP [74]
Bac715-24	Bactenecin family	PRPLPFPRPG	[12, 14]	NeutrAvidin [75]
SynB(1)	Protegrin 1	RGGRLSYSRRRFSTSTGR	[15, 76]	Doxorubicin [76]
Other CPPs				
pVEC	Murine VE-cadherin	LLIILRRRIRKQAHAHSK	[17, 77]	fluorophore [17]
VP22	Viral protein (HSV-1)	DAATATRGRSAASRPTE– –RPRAPARSASRPRRPVE	[18, 19]	GFP [18]
hCT-derived peptides			[78]	
hCT(9-32)	Human calcitonin	LGTYTQDFNKFHTFPQTAIGVGAP	[22-24, 79]	GFP [22]
hCT(9-32)-br	Human calcitonin, SV40	LGTYTQDFNKFHTFPQTAIGVGAP | AFGVGPDEVKRKKKP-NH_2	[21, 80]	GFP [21]
SAP	Modified maize	VRLPPP-VRLPPP-VRLPPP	[25-27]	fluorophore [26]
Protamin	Salmon roe	Mixture of protamin 1-4	[81]	fluorophore [81]

Mechanisms of internalization

The exact mechanisms underlying the internalization of CPPs across the cellular membrane still await complete understanding. During the pioneering phase, the cellular translocation of penetratin and Tat peptides was frequently (but not exclusively) assigned to a passive, temperature-independent process [4, 5, 57] that was to be insensitive to endocytosis inhibitors [5, 61]. These observations were thought to be consistent with various theoretical models for a CPP-induced physical perturbation of the lipid membrane leading to a direct translocation of the plasma membrane into the cytosol without prior compartmentalization into subcellular vesicles [4, 5, 61]. More recently, however, the related hypotheses involving direct translocation have been widely challenged following several reports on artifactual results that were caused by cell fixation protocols prior to confocal laser scanning microscopy (CLSM) of cells incubated with fluorescence-labeled CPPs. Another source of misinterpretation was found to derive from experimental difficulties to distinguish cell surface-associated CPPs from CPPs internalized in cytoplasmic compartments [82]. Unequivocal discrimination between associated and internalized fluorescence, however, is a prerequisite to interpret both CLSM and fluorescence-activated cell sorting (FACS) analysis with fluorescence labelled CPPs [80]. In contrast to initial reports, more recent work demonstrated clearly an involvement of endocytosis in the internalization of a Tat-derived peptide [82] and penetratin [83]. Prior to endocytosis, both peptides were shown to first interact electrostatically with the extracellular matrix (ECM) of the cell surface through binding to negatively charged glycosaminoglycans [84]. In a yet early stage we proposed an endocytic mechanism for a hCT derived CPP [24] possibly owing to a β-sheet induced aggregation on the cell surface. In fact, to date endocytic uptake is the accepted pathway for many of the currently known CPPs, though with some exceptions [61, 72]. Endocytosis may involve several pathways [80]. So far, many classical studies focused on uptake via clathrin-coated pits [85, 86]. Meanwhile, however, technologies and reagents are available that can cast light on non-classical, clathrin-independent pathways such as macropinocytosis and endocytosis via lipid rafts [87-91]. A number of excellent reviews report on pathways of cellular CPP internalization [9, 90, 92]. Below we present an updated overview of the field.

Intracellular trafficking routes of CPPs

Very little information is available regarding the downstream fate of CPPs after endocytic capture at the plasma membrane. Thus, towards future therapeutic implementation, the mechanisms of CPP internalization and the pursued intracellular trafficking routes need to

be studied in more detail. Increasing evidence for endocytic uptake mechanisms of CPPs caused concern that the vectors might be trapped in endosomes, rendering them unable to release their cargo. Wadia et al. [91] suggested the rate-limiting step of drug delivery by CPPs to be the escape from the macropinosomal vesicle. Having entered cells by lipid raft macropinocytosis, most of the studied Tat(48-57)-Cre peptide remained trapped in macropinosomes, even after 24 hours, indicating that escape from macropinosomes is an inefficient process. Chloroquine, an ion-transporting ATPase inhibitor that disrupts endosomes by preventing their acidification, enhanced Tat-Cre release from macropinosomes but was associated with extremely high cytotoxicity. To circumvent these deficiencies, the authors developed a transducible, pH-sensitive fusogenic dTat-HA2 peptide that markedly enhanced the release of Tat-Cre from macropinosomes [91]. HA2 is a well-characterized, pH sensitive fusogenic peptide that destabilizes lipid membranes at low pH [91].

Fischer et al. suggested that CPPs do not necessarily end up for good in endosomes but, after a certain endosomal sojourn, move on to other organelles within the cell. [93]. Their data point towards a shift into acidic early endosomal compartments followed by a retrograde delivery through the Golgi apparatus and the endoplasmic reticulum, and a final release into the cytosol. The authors also reported about similarities of the oligocationic CPPs Tat and penetratin, respectively, with toxins that are known to be transported by means of the retrograde pathway [93]. These toxins, such as ricin and Shigella toxin, reach the cytosol of eukaryotic cells after binding to the cell surface, endocytosis by different mechanisms and retrograde transport to the Golgi apparatus and the endoplasmic reticulum [94-96].

To improve insight into the intracellular trafficking pathways of two recently developed CPPs, SAP and hCT(9-32)-br, a branched hCT derived CPP, we performed CLSM based colocalization studies with the early endosomal antigen 1 (EEA1), a protein associated with early endosomes [80]. The resulting overlays revealed that early endosomes were involved in the uptake and initial intracellular trafficking of the two oligocationic peptides. However, after an incubation time of 3 h, most of the internalized CF-SAP or CF-hCT-(9-32)-br were no longer present in early endosomes but moved to other compartments within the cytosol [80].

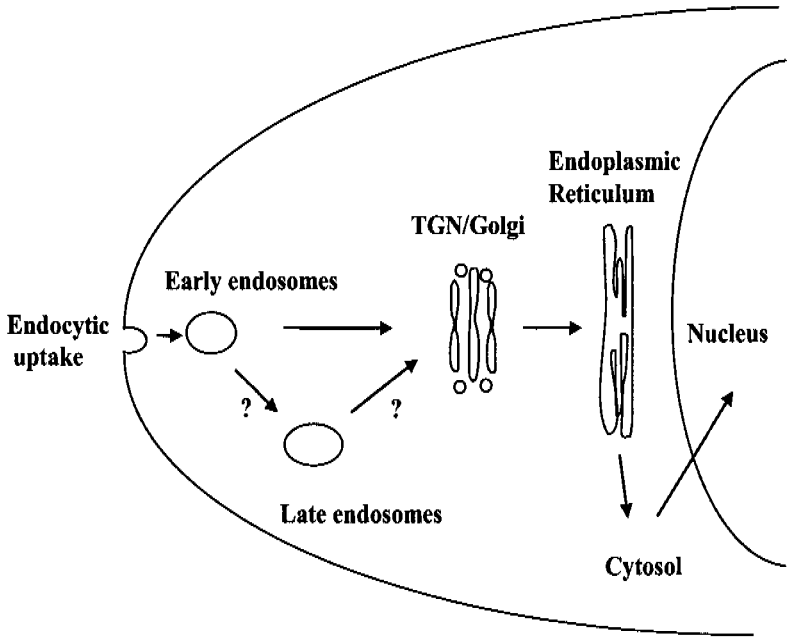

Figure 1. Scheme of the potential retrograde pathway of CPPs as reported by Fischer et al. [93].

When we tested whether the peptides may have entered the endoplasmic reticulum or the Golgi network, none of the related experiments yielded unequivocal results, neither in favor nor against the hypothesis [80]. More recently, Jones et al. (abstract book, pepvec meeting August 2005, Montpellier, France) presented direct evidence for the localization of Tat and octaarginine (R_8), after endocytic uptake, in late endosomes and lysosomes. In two leukaemia cell lines with different endocytic profiles, and in epithelial cells, a significant fraction of internalized Tat and R_8 entered lysosomal compartments within 60 min of internalization. No effects on the cellular distribution of the peptides with agents that disrupt the morphology of the Golgi and the endoplasmic reticulum could be observed (abstract book, pepvec meeting August 2005, Montpellier, France)., These findings shift evidence from the retrograde pathway of CPPs involving cytosolic release, to their entry into lysosomal compartments which is likely to be followed by CPP degradation. Obviously, this would have a negative impact on the integrity of the CPPs and, most likely, also on the delivery of their cargoes to the respective intracellular targets.

ACCOMPLISHMENTS AND FAILURES. REVISITING THE PERFORMANCE OF CPPs FOR DRUG DELIVERY

Successful delivery by the CPP approach

The following section covers selected examples of successful drug (or model drug) delivery by the CPP approach. In particular, we focus on distinct *in vivo* studies, whereas a more detailed outline is given in the review of Dietz et al. [8]. A pioneering piece of work on the CPP mediated cellular delivery of heterologous proteins was authored by Fawell et al. [53]. The authors chemically linked Tat peptides to β-galactosidase, horseradish peroxidase, RNase A, and domain III of Pseudomonas exotoxin A, and monitored uptake colorimetrically or by cytotoxicity. The Tat chimeras were effective on all cell types tested, and stainings showed uptake into virtually every cell in each experiment. In mice, treatment with Tat-β-galactosidase chimeras resulted in delivery to various tissues, with high levels in heart, liver and spleen, low-to-moderate levels in lung and skeletal muscle, and little or no activity in the kidney and in the brain [53].

In rats, constructs of CPPs with antisense PNA (peptide nucleic acid) have been shown to regulate galanin receptor levels and modify pain transmission [38]. Intrathecal administration of a CPP-PNA construct, consisting of penetratin coupled to an antisense PNA targeting the galanin receptor, was shown to modify galanin-mediated pain and reduced the levels of ^{125}I-galanin binding in the dorsal horn of the spinal cord, although the presence of the penetratin-PNA construct within the cell was not demonstrated [38].

Another *in vivo* study demonstrated the cellular delivery of the caveolin-1 scaffolding domain, resulting in the inhibition of nitric oxide synthesis and the reduction of inflammation [97]. A chimeric peptide consisting of the caveolin-1 scaffolding domain peptide attached to penetratin was successfully taken up into blood vessel endothelial tissue from isolated mouse aorta rings, resulting in an inhibition of acetylcholine-induced vasodilatation and nitric oxide production [97]. Moreover, the chimeric peptide showed suppression of acute inflammation and a vascular leak when used systemically in mice. The suppression was as efficient as glucocorticoid or endothelial nitric oxide synthetase inhibitors [97].

New advances in the transport of doxorubicin through the blood-brain barrier (BBB) by a CPP mediated strategy were shown by Rousselle et al. [13]. The ability of doxorubicin to cross the BBB was studied using an in situ rat brain perfusion technique and also by i.v. injection in mice. When doxorubicin was coupled to either D-penetratin or SynB1, its uptake was increased by a factor of 6, as compared to free doxorubicin. Moreover, using a capillary

depletion method, coupling of doxorubicin to either one of the two CPPs led to a 20-fold increase in the amount of doxorubicin transported into brain parenchyma, demonstrating that the two CPPs enhance the delivery of doxorubicin across the BBB [13].

Advantages and versatility of protein transduction over viral transgene delivery were demonstrated by van der Noel et al. when they compared the *in vivo* transduction of Tat-β-galactosidase in rat salivary gland cells with retroviral gene delivery [98]. The authors found that in contrast to viral transduction, having a limited capacity to infect non-dividing cells, all cell types were susceptible to Tat-mediated protein transduction. Moreover, the authors were able to achieve equal cellular concentrations of Tat-β-galactosidase in 100% of the cells whereas with viral delivery a transduction efficiency of only 30-50% was achieved [98].

More recently, Cao et al. [99] created a Bcl-xL fusion protein, denoted as PTD-HA-Bcl-xL, containing the protein transduction domain derived from the human immunodeficiency TAT protein. Bcl-xL is a well-characterized anti-apoptotic protein that may enhance cell survival. The Bcl-xL fusion protein was shown to be highly efficient in transducing primary neurons in cultures and potently inhibited staurosporin-induced neuronal apoptosis. Furthermore, intraperitoneal injection of PTD-HA-Bcl-xL into mice resulted in robust protein transduction in neurons in various brain regions and decreased cerebral infarction in a dose-dependent manner [99].

Finally, in a highly recognized study in mice, Schwarze et al. [3] demonstrated the intraperitoneal delivery of a fusion protein, Tat(47-57)-β-galactosidase (Tat-β-gal), to result in an uptake into almost every organ or tissue, as detected by significant local β-gal activities. Although substantially less intense as compared to organs close to the peritoneum, even the blood-brain barrier could be overcome showing β-gal activity in sagittal brain sections of the mice. Importantly, Tat-β-gal could not disrupt the blood-brain barrier as was observed after a treatment with protamine as positive control. As late as in 2000, Schwarze et al. [55] claimed that such protein-transduction domains (PTDs) can efficiently deliver protein cargoes into virtually the entire organism.

Limitations of CPP mediated translocation

Nevertheless, in contrast to the promise of these reports, the literature also provides evidence that the hypothesis of CPPs as unrestricted delivery tools should be challenged. In fact, the alleged universality of CPPs as a delivery tool has recently come under scrutiny. For instance, Koppelhus et al. [100] investigated the translocation of Tat and penetratin in five

different cell cultures, namely HeLa (cervical carcinoma), SK-BR-3 (breast carcinoma), IMR-90 (fetal lung fibroblast), H9 (lymphoid) and U937 (monocytic) cells. The two CPPs demonstrated either poor or no uptake in the investigated five cell lines. This observation was explained to potentially result from either a very low CPP translocation efficiency, or from quick cleavage of fluorescence labelled CPPs in the cells. Moreover, the authors demonstrated that Tat and penetratin showed distinct differences in their uptake patterns relative to the tested cell line. Therefore, they concluded that the internalization of the CPPs could be limited to certain cell types and depend on cell-specific membrane components or lipid composition [100]. Likewise, CLSM studies by Kramer et al. [101] showed that Tat(44-57) carrying a fluorescent tag, Tat(44-57)-fluorescein, did not enter MDCK cells with intact plasma membranes but accumulated at their basal side. Only cells permeable for ethidium homodimer-1 (EthD-1), a marker for plasma membrane impairment, showed uptake and intracellular accumulation of Tat(44-57). A similar phenomenon was found by Violini et al. [102]. The authors demonstrated a complete lack of intracellular accumulation of fluorescein-conjugated Tat(48-57) peptide in confluent, tight junction forming epithelial MDCK and CaCo-2 monolayers. Membranes of epithelial cells that are known not to form tight junctions such as HeLa cells, however, could be efficiently translocated. Previous studies in our group revealed the efficiency of CPP uptake to depend strongly on the investigated cell line [23]. Fully polarized and organized MDCK cells that efficiently mimic epithelial barriers demonstrated only slight translocation of linear human calcitonin derived peptides, Tat(47-57) and penetratin(43-58) as compared to more "leaky" HeLa cells [23].

Furthermore, to evaluate the efficiency of CPP mediated delivery into the cytosol, Falnes et al. [103] fused Tat peptide to the diphtheria toxin A-fragment (dtA), an extremely potent inhibitor of protein synthesis. The Tat–dtA fusion protein avidly bound to the cell surface but failed to show detectable cytotoxicity of the toxin which would preclude uptake. Equally, a fusion protein of VP22 and dtA showed association with cells in the absence of a cytotoxic effect, indicating inefficient transport of dtA into cells by Tat or VP22 [103]. The authors used a much lower concentration as commonly applied for the cellular delivery of biologically active molecules by CPPs and argued that, since relatively high CPP concentrations were required to elicit biological effects, CPPs may not yet represent sufficiently established and efficient vehicles for the intracellular delivery of macromolecules. Also, the authors questioned relevant intrinsic membrane penetrating activities of CPPs and claimed that while CPPs may elicit massive association with the cell surface, possibly through interaction with cell-surface heparans, only a very small fraction of the cell-associated

molecules may be able to cross the cell membrane. Poor efficiency of Tat-mediated cell transduction has also been reported by other groups. Zhang et al. [104], e.g., recently demonstrated that a retro-inverso form of Tat(49-57) CPP, named RI-Tat-9 did not enter confluent MDCK and Caco-2 cells but only translocated into non-epithelial T lymphatic MT2 and HeLa cells. Therefore, a cell type-specific barrier was suggested to control the uptake of RI-Tat-9 by HeLa, MT2, MDCK and Caco-2 cells. Furthermore, the authors hypothesized that oral and dermal delivery by the used CPPs would be inefficient owing to the observed low permeability of epithelia and the repulsion of free RI-Tat-9 molecules by molecules bound at the monolayer surface [104].

Several studies reported on the limited *in vivo* applicability of the CPP approach. Caron and co-workers [105] showed that the direct delivery of a Tat-eGFP fusion protein to muscle tissue, using subcutaneous or intra-arterial injections, led to only few positive fibers in the muscle periphery or surrounding the blood vessels. Muscles injected with Tat-eGFP showed intense labelling of the extracellular matrix (ECM), suggesting that Tat binds to components of the ECM surrounding myofibers which could interfere with the intracellular transduction process [105].

Moreover, radiolabeled [^{99m}Tc] Tat peptide instilled directly into the urinary bladder of rats failed to show any distribution into the body [102]. In fact, Violini et al. demonstrated in rats that a Tat peptide was retained by the epithelium of the bladder, an uroepithelial tissue of similar embryonic origin as MDCK cells [102]. Furthermore, Niesner et al. [106] showed efficient *in vitro* translocation of D- or L-amino acid Tat(49-57) into target cells when conjugated to fluorophores and/or antibody fragments, suggesting receptor-independent cell entry mechanisms. However, an *in vivo* study in mice revealed that conjugation of a human antibody fragment to Tat peptides resulted in a severely reduced tumor targeting performance compared to the unconjugated antibody. Apparently, the antibody-Tat conjugate was not able to cross endothelia of tumor blood vessels. The authors, therefore, suggested CPPs to lack an *in vitro-in vivo* correlation for drug delivery [106]. Leifert et al. [107] came to similar results and concluded from an *in vivo* study with Tat(47-57) and VP22 in mice or in live MC57 cells, respectively, that these peptides would neither enhance translocation into cells nor exhibit enhanced immunogenicity.

A study by Xia et al. [108] tested how the Tat(47-57) motif affected uptake and biodistribution of the lysosomal enzyme β-glucuronidase when expressed from recombinant viral vectors. The continuous *in vivo* production of Tat-β-glucuronidase from adenovirally transduced hepatocytes only led to a moderately increased uptake of the enzyme in certain

tissues [108]. Lee et al. [109] examined pharmacokinetics and organ uptake of Tat(48-58) and Tat-protein conjugates in rats. The effect of Tat peptide on the plasma AUC of the model protein streptavidin as well as the extent to which changes in the plasma AUC influence its uptake into other organs were analyzed. The study revealed rapid clearance of the Tat-biotin conjugate in rats and no enhancement of bioavailability of the protein when bound to the conjugate.

Tseng et al. investigated the cellular translocation of liposomes by penetratin and Tat(47-60) [110]. The authors demonstrated that both Tat and penetratin enhanced the translocation efficiency of liposomes in proportion to the number of CPP units ligated to the liposomal surface. However, the improvement of uptake of liposomal doxorubicin was not reflected by the observed cytotoxicity *in vitro* or tumor control *in vivo*, demonstrating that merely adding CPPs to a liposome encapsulating anticancer drug was inadequate to improve its antitumor activity.

Further support for this trend was provided by several other *in vivo* studies showing that Tat conjugates did not change the common distribution pattern of macromolecular cargoes that was heavily skewed towards the organs of the mononuclear phagocytic system or the organs of waste elimination [53, 109, 111]. It needs to be pointed out that these reports do not dispute the cellular entry of CPPs per se or the validity of CPP-assisted cargo delivery that is based on the cargo's functionality. More likely, differences in the experimental settings including the use of *in vitro* or *in vivo* experiments, the used cell lines, cellular differentiation states, enzymatic activity and metabolic stability of the CPPs and the type of CPPs itself may be of great importance for the efficiencies of CPPs in translocation studies. Or in other words, the concept of CPPs as a universal tool had to be abandoned.

CELLULAR BARRIERS LIMITING CPP TRANSLOCATION

Metabolic degradation

A major obstacle to CPP mediated drug delivery consists in the often rapid metabolic clearance of the peptides when in contact or passing the enzymatic barriers of epithelia and endothelia. Koppelhus et al. [100], for example, reported that the observed poor intracellular uptake of CPPs might results from quick degradation of the fluorescence labelled CPPs in the cells. Until today, however, despite its general relevance, information on the momentous subject of enzymatic stability and degradation of CPPs is rare and only few studies have so far investigated the cellular metabolism of CPPs. Elmquist et al. [17] studied the pVEC peptide on human aorta endothelial cells and murine A9 fibroblasts in order to evaluate its potential usability as a vector for drug delivery. As a result, pVEC was found to be rapidly degraded when incubated with both cellular models. By contrast, when replacing all L-amino acid residues of its sequence by their non-natural D-counterparts, pVEC was no longer subject to any metabolic degradation [16]. Another related study focused on the metabolic stability of transportan, a transportan analogue, and penetratin when in contact with a Caco-2 human colon cancer cell line. The stability of the peptides was shown to be in the order of transportan > TP10 > penetratin [112]. At least ten degradation products were found for both transportan and TP10 and the identified cleavage products were shown not to penetrate cell membranes [113]. In a former study we analyzed the metabolic degradation kinetics and the cleavage patterns of selected CPPs, namely human calcitonin (hCT) derived peptides, Tat(47-57) and penetratin(43-58) by incubation with three epithelial models, MDCK, Calu-3 and TR 146 cell layers [114]. The proteolytic activities among the different epithelial models and the CPPs were highly variable, whereas the individual patterns between the three models for metabolic degradation of each peptide were quite similar or even congruent [114]. The stability of Tat was superior to that of hCT-derived CPPs, such as hCT(9-32), and penetratin. According to identified cleavage sites of hCT(9-32), stabilization as well as enhanced translocation efficiency of this peptide were achieved by modification through a side branch carrying the oligocationic, SV40 large T antigen to the main peptide chain, resulting in the novel hCT-derived CPP, hCT(9-32)-br [21] [80] (Chapter III). Moreover, our group envisaged to explore a potential relation between the metabolic stability of CPPs and their translocation capacity (Chapter III). To this end we focused on (i) metabolic degradation kinetics and cleavage patterns of four oligocationic CPPs, namely SAP, hCT(9-32)-br, [Pα] and [Pβ], when in contact with three epithelial cell cultures, consisting of either subconfluent HeLa or confluent

MDCK or Calu-3 cells, and on (ii) their cellular uptake. CF-SAP and CF-hCT(9-32)-br demonstrated marked metabolic stability under all experimental conditions, whereas, in contrast, [Pα] and [Pβ]-IAF showed drastic enzymatic degradation, and decomposed quickly even when incubated in serum free medium. Moreover, we were able to identify specific cleavage sites for each of the four peptides. Emphasizing the relevance of the chosen cellular models, we found the uptake efficiencies of all four CPPs to be strongly cell line dependent. No direct relation between metabolic stability and translocation efficiency was observed for the investigated CPPs, indicating that metabolic stability is not an absolute prerequisite for efficient cellular translocation. Nevertheless, for individual CPPs we still expect structural modifications aiming at increased metabolic stability to provide an option for improved translocation. A recent study by Holm et al. [115] reported about uptake and metabolic stability of CPPs in two yeast species, *Saccharomyces cervisiae* and *Candida albicans*. The intracellular degradation from the three investigated CPPs, namely pVEC, penetratin and $(KFF)_3K$, varied from complete stability to complete degradation. Moreover, the authors showed that intracellular degradation into membrane impermeable products could significantly contribute to the fluorescence signal which is an issue that needs to be taken into consideration when data from uptake studies are interpreted.

In conclusion, metabolic stability of CPPs is an important biopharmaceutical factor for their cellular bioavailability. For the development of optimized CPP sequences, a balance between two features is required: On the one hand, for successful therapeutic application of CPPs, CPPs need to be stable enough to carry their cargo to the target before they are metabolically cleaved. On the other hand, right upon cellular uptake, CPPs ligated to a therapeutic agent must be cleaved off the drug and, subsequently, cleared from the site before they may accumulate and reach toxic levels.

Cell line and differentiation state dependent uptake

Increasing numbers of contributions to the field report about a cell line and differentiation state dependence of the translocation efficiency of CPPs [23, 79, 102, 104] (Chapter III and IV). In particular, massive differences in CPP translocation between "leaky" and "non-leaky" cell culture models were demonstrated [23, 79, 102, 104] (Chapter IV). "Leaky" cell culture models, such as HeLa cells, lack the ability to form tight junctions and, therefore, grow into rather leaky and highly permeable monolayers [104]. On the other hand, when grown to "non-leaky" epithelial type cell cultures, as represented by confluent MDCK monolayers, cells are connected by junctional complexes encircling the apex of each cell. Tight junctions constitute

the most apical element of the junctional complex which also includes adherens junctions, desmosomes and gap junctions. Tight junctions form an efficient barrier to the paracellular diffusion of molecules from the lumen to the tissue parenchyma (gate function) and restrict the diffusion and exchange of lipids and proteins between the apical and basolateral domains of the plasma membrane (fence function) [116-120].

The relevance of tight junction formation for the translocation of CPPs has been reported on several occasions. For instance, Violini et al. [102] found a plasma membrane-mediated permeation barrier to Tat(48-57) related cationic peptides in selected well-differentiated epithelial cells. L- and D-stereoisomers of Tat(48-57) peptide conjugates labelled with ^{99m}Tc were quantitatively analyzed in confluent monolayers of MDCK renal epithelia and CaCo-2 colonic carcinoma cells forming tight junctions, and compared to HeLa and KB 3-1 cells repesenting epithelial cell lines that do not form tight junctions in monolayer culture. In confluent MDCK and CaCo-2 monolayers, the transepithelial permeability of the investigated vectors was comparable to that of inulin as a macromolecular marker of very low paracellular permeability, but much less than that of propanolol, a highly permeable marker compound for transcellular permeability. Additionally, confluent MDCK and CaCo-2 cells showed a complete lack of intracellular accumulation of fluorescein-conjugated Tat peptide. By contrast, in "leaky" HeLa and KB 3-1 cell cultures, baseline cytoplasmic and nucleolar accumulation was readily observed. These data suggest a cell-type specific, tight junction-dependent barrier for the investigated CPPs.

Similar findings were obtained in a prior study of our group [23]. Using linear human calcitonin derived peptides, Tat(47-57) and penetratin(43-58), we found the efficiency of CPP uptake to depend strongly on the investigated cell line. For all peptides, HeLa cells demonstrated a greater uptake potential as compared to confluent MDCK cells. [23]. Further evidence of a cell type-specific barrier was recently given by the study of Zhang et al. [104] showing the uptake of the retro-inverso form of Tat(49-57), namely RI-Tat-9, to depend on the cell-type specific barrier properties of HeLa, MT2, MDCK and Caco-2 cell cultures. Again, significantly limited CPP uptake was observed in cell cultures with tight junctions.

In a yet unpublished study we investigated in detail the impact of cellular differentiation upon efficiency and mechanism of CPP translocation (Chapter IV). We observed that progressive cellular differentiation of the MDCK cells, such as the formation of tight junctions, correlated well with an endocytic slow-down and a marked drop in the cellular uptake of CPPs. The observed endocytic slow-down was not specific for the investigated CPPs, namely CF-SAP and CF-hCT(9-32)-br. Instead, its mechanism was compound unspecific as it was generally

observed for several markers of endocytosis. Both CPPs were readily taken up by HeLa cells through lipid raft-mediated endocytosis followed by endosomal escape [80]. However, for the translocation of CF-SAP and CF-hCT(9-32)-br in proliferating MDCK cells, we observed the involvement of both lipid raft-mediated as well as clathrin-dependent endocytosis. After reaching confluence, translocation of the investigated CPPs into MDCK monolayers dropped markedly. In fact, when confluent, MDCK monolayers widely lost their capacity for translocation via lipid rafts. The large differences in the translocation efficiencies of the CPPs between "leaky" HeLa and "non-leaky" MDCK cell cultures on the one hand, as well as between "leaky" MDCK cells shortly after seeding, and "non-leaky", well-differentiated MDCK monolayers on the other, demonstrate the crucial impact of confluence upon CPP uptake. Epithelial type cell cultures, such as confluent MDCK cells, feature important elements of polarized epithelia, and represent a more stringent and realistic model to test the potential for therapeutic applications of CPPs as compared to "leaky" cell cultures without tight junctional complexes such as HeLa, KB 3-1, Bowes Human Melanoma or MC57 fibrosarcoma cells [93, 102, 121-123].

Regulation of endocytic activity by Rho-GTPases

Within the context of increasing evidence for endocytosis as an underlying mechanism for the cellular translocation of many CPPs, a more detailed understanding of the cell biology involved in this process is indispensable. As documented in literature, members of the Rho-family of small GTPases are intimately involved in the regulation of endocytic activity [124-126]. Rho-GTPases are ubiquitously expressed across eukaryotes where they act as molecular switches, cycling between an active GTP-bound state and an inactive GDP-bound state [125, 127, 128]. Rho GTPases are activated in response to extracellular cues, allowing the potential for dynamic regulation of membrane-trafficking processes in response to the extracellular environment [129]. Activation enables Rho GTPases to interact with a multitude of effectors that relay upstream signals to cytoskeletal and other components, eliciting rearrangements of the actin cytoskeleton and diverse other responses. Rho GTPases regulate a variety of cellular events such as actin polymerization, cell morphology and polarity, cell growth control, transcription, and membrane trafficking events such as endocytosis [125, 126, 128, 130-133]. Apparently, Rho-GTPases mediate the signalling interface between endocytic traffic and actin cytoskeleton as increasing connections between endocytic traffic and the actin cytoskeleton are revealed [134]. In Swiss 3T3 fibroblasts, RhoA controls the assembly of actin stress fibres

and focal adhesion, Rac1 promotes the formation of lamellipodia and Cdc42 regulates filopodium formation [133, 135, 136]. Cross-talk between Rho proteins has been observed; in particular, Cdc42 is a strong activator of Rac, such that filopodial extensions are usually seen associated with lamellipodial protrusions [133, 136, 137]. On the other hand, opposing activites of Rho versus Rac and Cdc42 GTPases on several cellular functions, such as actin reorganization and endocytosis could be observed [125, 138, 139].

In confluent MDCK cells, RhoA activation has been found to stimulate apical and basolateral endocytosis whereas Rac1 activation led to a drop in endocytosis [138, 139]. Moreover, confluent MDCK cells have been found to feature elevated Rac1 and Cdc42 activity but decreased RhoA activity compared to subconfluent cultures [140]. During the formation of epithelia, Cdc42 and Rac-1 seem to have a prominent role in the generation of intimate cell-to-cell contact [141, 142]. Overexpression of constitutively active Rac1 or Cdc42 increased E-cadherin localization and actin accumulation at cell-cell junctions, whereas these events were inhibited by dominant negative mutants of Rac1 and Cdc42 [141-144]. Kazmierczak et al. [145, 146] suggested that incompletely polarized MDCK cells possess a pathway for the internalization of *Pseudomonas aeruginosa* which is then downregulated during the acquisition of polarity. This pathway is sensitive to actin depolymerising agents and requires activity of a Rho-A small GTPase but not of Rac-1 or Cdc42. Incompletely polarized MDCK cell monolayers (day 1) efficiently internalized apically applied *P. aeruginosa* via a pathway that required actin polymerization and activation of Rho-family GTPases, and was accompanied by an increase in activated RhoA. In contrast, the entry of *P. aeruginosa* into highly polarized MDCK monolayers (day 3) was 10- to 100-fold less efficient and insensitive to inhibitors of actin polymerization or of Rho-family activation. RhoA was not activated. Instead, Cdc42-GTP levels increased significantly [145, 146].

With respect to the cellular uptake of selected CPPs, recent findings in our group indicate an intimate involvement of Rho-family GTPases in the differentiation restricted regulation of endocytic traffic (Chapter IV). In fact, the extent of CPP endocytosis correlated directly with active form Rho-A, whereas active form Rac-1 correlated with endocytic slow-down, cell density and cellular differentiation. The results reflect the above mentioned inverse roles of Rho-A and Rac-1 in the regulation of endocytosis. To our knowledge, this is the first study to cast light on the cell line and differentiation restricted translocation of CPPs into epithelial cell models and its underlying cellular mechanism.

NEW PERSPECTIVES FOR APPLICATION OF CPPs IN DRUG DELIVERY

As a consequence of the described limitations of CPP mediated translocation, e.g. the dependence on the state of cellular differentiation, in this final section we aim at the identification of promising niches for CPP application in drug delivery. Ideally, these approaches should either overcome or bypass the given limitations of CPP mediated delivery described above and, thus, offer a realistic avenue how to promote the therapeutic usage of CPPs. As inspired by current literature we will focus on three principal areas: (i) the delivery of antineoplastic agents, (ii) the delivery of CPPs as antimicrobials, and (iii) the potential of CPPs to target inflammatory tissue.

Delivery of antineoplastic agents through CPP-mediated translocation

The rationale of antineoplastic therapy, i.e. to specifically eradicate proliferating tumor tissue while leaving healthy tissue unharmed, is notoriously difficult to accomplish. Traditional chemotherapy is often poorly specific, making the search for more targeted treatments quite attractive. The reconstitution of tumor-suppression following the mutation or deletion of tumor-suppressor proteins, such as p53, is often considered a prime goal for effective antineoplastic treatment [90]. Recently, various studies revealed the potential of the HIV-1 Tat protein transduction domain to modulate the cell biology of living organisms by the direct cellular delivery of proteins and peptides [90, 147, 148]. In the first example of using CPP mediated transduction to deliver a p53 peptide in vitro, Selinova et al. [149] linked a C-terminal p53 peptide, which was previously shown to activate wild type p53 and several DNA-contact mutant forms of p53 [150], to the Antennapedia transduction domain and found that the conjugate induced p53-dependent apoptosis in several tumor cell lines. Normal cells, being wild type for p53, were resistant to the p53 peptide [149]. Recently, Dowdy et al. used Tat mediated protein transduction to deliver structurally modified p53 C-terminal fragments, resistant to degradation, into ovarian tumor bearing mice [151]. Although the Tat-p53C` peptide was able to enter all cells, p53-specific genes were only activated within cancer cells but not in normal cells. The potential of this approach was further illustrated by *in vivo* experiments where intraperitoneal injection of Tat-p53C` for 12 days caused a significant reduction in tumor growth and a six-fold extension in lifespan, with some mice remaining free of the disease for more than 200 days [151]. Another strategy for the delivery of an antineoplastic agent using CPP mediated transduction is the regulation of the cell cycle. In order to reconstitute tumor suppressor function, p27 was synthesized together with the Tat

transduction domain and tested in human Jurkat cells in culture [152]. Transduced Tat-p27 was found to bind to Cdk2 in the cells, and loss of Cdk2 kinase activity compared to control cells was demonstrated. Moreover, treatment of cells with Tat-p27 resulted in a substantial, dose-dependent, G1 phase cell cycle arrest [152]. Another study from Guis et al. [153] demonstrated that covalent linkage of the p16 peptide to the Tat transduction domain was sufficient to control its intracellular accumulation, subsequent inhibition of cyclin D:Cdk4/6 activity, and G1 arrest in synchronized human keratinocytes [153]. The observations showed that both, transducible peptides and proteins, were capable to target active cyclin:Cdk complexes. Since cell cycle control genes are deregulated in the vast majority of human tumors, the targeting of these genes and/or their products is now under investigation as potential antineoplastic therapy [154]. In an excellent review on various strategies for the application of Tat protein transduction, Wadia et al. [90] focused on technologies to deliver peptides and proteins in the treatment of cancer.

Delivery of CPPs as antimicrobials

The functions of CPPs have been extensively studied in cell cultures of various mammalian cells, but there are only few reports on their ability to overcome the membranes of bacteria and yeast. Given the fact that many CPPs are cationic and often amphipathic, similar to membrane active antimicrobial peptides, Nekhotiaeva et al. [155] examined CPP as to their antimicrobial potency. Two CPPs, TP10 and pVEC, were found to pass the membranes of bacteria and fungi. The observed uptake route involved rapid surface accumulation within minutes followed by microbial entry. TP10 inhibited the growth of *Candida albicans* and *Staphylococcus aureus*, and pVEC inhibited *Mycobacterium smegmatis* growth at low doses, below the levels that harmed human HeLa cells. Therefore, although TP10 and pVEC entered all cell types tested, they preferentially damaged microbes. Indeed, this effect was sufficient to clear HeLa cell cultures from *S. aureus* infection. Also, when exposed to TP10 the cytoplasmic conversion of the marker dye SYTOX Green demonstrated a rapid and lethal permeabilization of the plasma membrane of *S. aureus*. Furthermore, pVEC permeabilized *M. smegmatis*, but not HeLa cells. Therefore, TP10 and pVEC may enter both mammalian and microbial cells, but preferentially permeabilized the microbial rather than the mammalian plasma membrane [155].

Very recently, the uptake of three CPPs, namely pVEC, penetratin and $(KFF)_3K$, into two yeast species, *Saccharomyces cervisiae* and *Candida albicans* was studied by Holm et al. [115]. By comparing the capacity of the investigated CPPs to traverse the yeast cell envelope

the authors could show that the cellular uptake of the peptides varied widely. pVec and $(KFF)_3K$ displayed the highest translocation into yeast, although being partly degraded. Considering the stability of pVEC in both yeast species, it was suggested as attractive candidate for further studies [115]. Nevertheless, to date, the therapeutic value of CPP based antimicrobials has yet to be established.

Potential of CPPs to target inflammatory tissue

In a recent study in our laboratory we observed that a marked drop in the cellular uptake of CPPs into MDCK cells correlated directly with a general slow-down in their endocytic activity, and inversely with the cellular differentiation of the MDCK cells (Chapter IV). Our findings were further corroborated in an inflammatory epithelial model which was induced by pretreatments of confluently grown MDCK monolayers with a mix of IFN-γ and TNF-α. Inflammatory epithelial conditions such as inflammatory bowel diseases, e.g. Crohn`s disease and ulcerative colitis [156-159], or inflammatory airway diseases associated with cystic fibrosis [160] or asthma bronchiale [161], typically feature increased cytokine production, and significant barrier dysfunction. Correspondingly, we found the translocation efficiencies of selected CPPs in the IFN-γ/TNF-α induced inflammatory model to be significantly enhanced as compared to untreated MDCK monolayers as negative control. In a cytokine concentration dependent manner, endocytosis rates of CPPs were boosted by up to 90% in this model. The findings led us to propose that – under inflammatory conditions – the redistribution of tight junction proteins associated with lipid raft microdomains [162, 163] reopens a lipid raft-mediated pathway for CPPs in confluent MDCK cells. The results appear to be of particular interest in the context of a CPP mediated delivery of anti-inflammatory drugs.

The potential of this approach was demonstrated by the CPP mediated delivery of cyclosporin A for the treatment of cutaneous inflammation [60], or caveolin-1 scaffolding domain against vasodilatation and nitric oxide production [97]. In fact, Bucci et al. [97] demonstrated that the CPP mediated *in vivo* delivery of the caveolin-1 scaffolding domain inhibited nitric oxide synthesis and reduced inflammation [97]. A chimeric peptide consisting of the caveolin-1 scaffolding domain peptide ligated to penetratin was successfully taken up into blood vessel endothelial tissue from isolated mouse aorta rings, resulting in an inhibition of acetylcholine-induced vasodilatation and nitric oxide production [97]. Moreover, when used systemically in mice, the chimeric peptide showed suppression of acute inflammation and vascular leak. The

suppression was as efficient as glucocorticoid or endothelial nitric oxide synthetase inhibitors [97].

A further example for an anti-inflammatory application of CPPs was recently presented by Rothbard et al. [60]. The authors studied the topical delivery of cyclosporine A by conjugating an arginine heptamer to cyclosporine A through a pH-sensitive linker, resulting in R7-CsA. In contrast to unmodified cyclosporine A, which failed to penetrate skin, topically applied R7-CsA was efficiently transported into mouse and human skin. R7-CsA reached dermal T lymphocytes and inhibited cutaneous inflammation. The data provides a novel approach to the topical treatment of inflammatory skin disorders [60].

5. Conclusion

Over more than a decade, a broad variety of CPPs has been evaluated as to their capacity for cellular delivery of therapeutics that do normally not cross the cellular membrane. Although a number of landmark studies in the field claimed a practically unrestricted cellular access of CPPs and CPP associated cargos, crucial limitations to these shuttles have been pointed out more recently. In this review, we attempted to review distinct aspects of CPP mediated cellular delivery. Besides the wealth of data that demonstrates what has so far been achieved in the field, we also report in more detail about cellular barriers to CPP uptake and the resulting hurdles for the use of CPPs in drug delivery. In particular, we emphasize the massive impact of (i) metabolic degradation, (ii) cell line and cellular differentiation dependent effects, as well as (iii) the role of Rho GTPase signalling upon CPP translocation. Despite critical aspects, which need to be considered with regard to future therapeutic applications of CPPs, we also discuss a number of potential niches for CPP mediated drug delivery, including the cellular delivery of antineoplastic drugs, or the delivery of antimicrobials and anti-inflammatory medications.

6. References

1. Juliano, R.L., et al., *Antisense pharmacodynamics: critical issues in the transport and delivery of antisense oligonucleotides.* Pharm Res, 1999. **16**(4): p. 494-502.
2. Gewirtz, A.M., D.L. Sokol, and M.Z. Ratajczak, *Nucleic acid therapeutics: state of the art and future prospects.* Blood, 1998. **92**(3): p. 712-36.
3. Schwarze, S.R., et al., *In vivo protein transduction: delivery of a biologically active protein into the mouse.* Science, 1999. **285**(5433): p. 1569-72.
4. Derossi, D., et al., *The third helix of the Antennapedia homeodomain translocates through biological membranes.* J Biol Chem, 1994. **269**(14): p. 10444-50.
5. Vives, E., P. Brodin, and B. Lebleu, *A truncated HIV-1 Tat protein basic domain rapidly translocates through the plasma membrane and accumulates in the cell nucleus.* J Biol Chem, 1997. **272**(25): p. 16010-7.
6. Pooga, M., et al., *Cell penetration by transportan.* Faseb J, 1998. **12**(1): p. 67-77.
7. Schwarze, S.R. and S.F. Dowdy, *In vivo protein transduction: intracellular delivery of biologically active proteins, compounds and DNA.* Trends Pharmacol Sci, 2000. **21**(2): p. 45-8.
8. Dietz, G.P. and M. Bdeltahr, *Delivery of bioactive molecules into the cell: the Trojan horse approach.* Mol Cell Neurosci, 2004. **27**(2): p. 85-131.
9. Magzoub, M. and A. Graslund, *Cell-penetrating peptides: small from inception to application.* Q Rev Biophys, 2004. **37**(2): p. 147-95.
10. Chaloin, L., et al., *Design of carrier peptide-oligonucleotide conjugates with rapid membrane translocation and nuclear localization properties.* Biochem Biophys Res Commun, 1998. **243**(2): p. 601-8.
11. Park, C.B., H.S. Kim, and S.C. Kim, *Mechanism of action of the antimicrobial peptide buforin II: buforin II kills microorganisms by penetrating the cell membrane and inhibiting cellular functions.* Biochem Biophys Res Commun, 1998. **244**(1): p. 253-7.
12. Frank, R.W., et al., *Amino acid sequences of two proline-rich bactenecins. Antimicrobial peptides of bovine neutrophils.* J Biol Chem, 1990. **265**(31): p. 18871-4.
13. Rousselle, C., et al., *New advances in the transport of doxorubicin through the blood-brain barrier by a peptide vector-mediated strategy.* Mol Pharmacol, 2000. **57**(4): p. 679-86.

14. Skerlavaj, B., D. Romeo, and R. Gennaro, *Rapid membrane permeabilization and inhibition of vital functions of gram-negative bacteria by bactenecins.* Infect Immun, 1990. **58**(11): p. 3724-30.

15. Sokolov, Y., et al., *Membrane channel formation by antimicrobial protegrins.* Biochim Biophys Acta, 1999. **1420**(1-2): p. 23-9.

16. Elmquist, A. and U. Langel, *In vitro uptake and stability study of pVEC and its all-D analog.* Biol Chem, 2003. **384**(3): p. 387-93.

17. Elmquist, A., et al., *VE-cadherin-derived cell-penetrating peptide, pVEC, with carrier functions.* Exp Cell Res, 2001. **269**(2): p. 237-44.

18. Cashman, S.M., et al., *Intercellular trafficking of adenovirus-delivered HSV VP22 from the retinal pigment epithelium to the photoreceptors--implications for gene therapy.* Mol Ther, 2002. **6**(6): p. 813-23.

19. Elliott, G. and P. O'Hare, *Intercellular trafficking of VP22-GFP fusion proteins.* Gene Ther, 1999. **6**(1): p. 149-51.

20. Normand, N., H. van Leeuwen, and P. O'Hare, *Particle formation by a conserved domain of the herpes simplex virus protein VP22 facilitating protein and nucleic acid delivery.* J Biol Chem, 2001. **276**(18): p. 15042-50.

21. Krauss, U., et al., *In vitro gene delivery by a novel human calcitonin (hCT)-derived carrier peptide.* Bioorg Med Chem Lett, 2004. **14**(1): p. 51-4.

22. Machova, Z., et al., *Cellular internalization of enhanced green fluorescent protein ligated to a human calcitonin-based carrier peptide.* Chembiochem, 2002. **3**(7): p. 672-7.

23. Trehin, R., et al., *Cellular internalization of human calcitonin derived peptides in MDCK monolayers: a comparative study with Tat(47-57) and penetratin(43-58).* Pharm Res, 2004. **21**(1): p. 33-42.

24. Schmidt, M.C., et al., *Translocation of human calcitonin in respiratory nasal epithelium is associated with self-assembly in lipid membrane.* Biochemistry, 1998. **37**(47): p. 16582-90.

25. Crespo, L., et al., *Peptide dendrimers based on polyproline helices.* J Am Chem Soc, 2002. **124**(30): p. 8876-83.

26. Fernandez-Carneado, J., et al., *Potential Peptide Carriers: Amphipathic Proline-Rich Peptides Derived from the N-Terminal Domain of gamma-Zein.* Angew Chem Int Ed Engl, 2004. **43**(14): p. 1811-1814.

27. Fernandez-Carneado, J., et al., *Amphipathic peptides and drug delivery.* Biopolymers, 2004. **76**(2): p. 196-203.

28. Borsello, T., et al., *A peptide inhibitor of c-Jun N-terminal kinase protects against excitotoxicity and cerebral ischemia.* Nat Med, 2003. **9**(9): p. 1180-6.

29. Giorello, L., et al., *Inhibition of cancer cell growth and c-Myc transcriptional activity by a c-Myc helix 1-type peptide fused to an internalization sequence.* Cancer Res, 1998. **58**(16): p. 3654-9.

30. Yuan, J., et al., *Efficient internalization of the polo-box of polo-like kinase 1 fused to an Antennapedia peptide results in inhibition of cancer cell proliferation.* Cancer Res, 2002. **62**(15): p. 4186-90.

31. Ezhevsky, S.A., et al., *Differential regulation of retinoblastoma tumor suppressor protein by G(1) cyclin-dependent kinase complexes in vivo.* Mol Cell Biol, 2001. **21**(14): p. 4773-84.

32. Harada, H., M. Hiraoka, and S. Kizaka-Kondoh, *Antitumor effect of TAT-oxygen-dependent degradation-caspase-3 fusion protein specifically stabilized and activated in hypoxic tumor cells.* Cancer Res, 2002. **62**(7): p. 2013-8.

33. Klekotka, P.A., et al., *Mammary epithelial cell-cycle progression via the alpha(2)beta(1) integrin: unique and synergistic roles of the alpha(2) cytoplasmic domain.* Am J Pathol, 2001. **159**(3): p. 983-92.

34. Lissy, N.A., et al., *A common E2F-1 and p73 pathway mediates cell death induced by TCR activation.* Nature, 2000. **407**(6804): p. 642-5.

35. Astriab-Fisher, A., et al., *Antisense inhibition of P-glycoprotein expression using peptide-oligonucleotide conjugates.* Biochem Pharmacol, 2000. **60**(1): p. 83-90.

36. Cutrona, G., et al., *Effects in live cells of a c-myc anti-gene PNA linked to a nuclear localization signal.* Nat Biotechnol, 2000. **18**(3): p. 300-3.

37. Moulton, H.M., et al., *HIV Tat peptide enhances cellular delivery of antisense morpholino oligomers.* Antisense Nucleic Acid Drug Dev, 2003. **13**(1): p. 31-43.

38. Pooga, M., et al., *Cell penetrating PNA constructs regulate galanin receptor levels and modify pain transmission in vivo.* Nat Biotechnol, 1998. **16**(9): p. 857-61.

39. Simeoni, F., et al., *Insight into the mechanism of the peptide-based gene delivery system MPG: implications for delivery of siRNA into mammalian cells.* Nucleic Acids Res, 2003. **31**(11): p. 2717-24.

40. Simeoni, F., et al., *Peptide-Based Strategy for siRNA Delivery into Mammalian Cells.* Methods Mol Biol, 2005. **309**: p. 251-60.

41. Branden, L.J., A.J. Mohamed, and C.I. Smith, *A peptide nucleic acid-nuclear localization signal fusion that mediates nuclear transport of DNA.* Nat Biotechnol, 1999. **17**(8): p. 784-7.

42. Ignatovich, I.A., et al., *Complexes of plasmid DNA with basic domain 47-57 of the HIV-1 Tat protein are transferred to mammalian cells by endocytosis-mediated pathways.* J Biol Chem, 2003. **278**(43): p. 42625-36.

43. Rudolph, C., et al., *Oligomers of the arginine-rich motif of the HIV-1 TAT protein are capable of transferring plasmid DNA into cells.* J Biol Chem, 2003. **278**(13): p. 11411-8.

44. Tung, C.H., S. Mueller, and R. Weissleder, *Novel branching membrane translocational peptide as gene delivery vector.* Bioorg Med Chem, 2002. **10**(11): p. 3609-14.

45. Krauss, U., F. Kratz, and A.G. Beck-Sickinger, *Novel daunorubicin-carrier peptide conjugates derived from human calcitonin segments.* J Mol Recognit, 2003. **16**(5): p. 280-7.

46. Mazel, M., et al., *Doxorubicin-peptide conjugates overcome multidrug resistance.* Anticancer Drugs, 2001. **12**(2): p. 107-16.

47. Torchilin, V.P., et al., *TAT peptide on the surface of liposomes affords their efficient intracellular delivery even at low temperature and in the presence of metabolic inhibitors.* Proc Natl Acad Sci U S A, 2001. **98**(15): p. 8786-91.

48. de la Fuente, J.M. and C.C. Berry, *Tat Peptide as an efficient molecule to translocate gold nanoparticles into the cell nucleus.* Bioconjug Chem, 2005. **16**(5): p. 1176-80.

49. Koch, A.M., et al., *Uptake and Metabolism of a Dual Fluorochrome Tat-nanoparticle in HeLa Cells.* Bioconjug Chem, 2003. **14**(6): p. 1115-1121.

50. Lewin, M., et al., *Tat peptide-derivatized magnetic nanoparticles allow in vivo tracking and recovery of progenitor cells.* Nat Biotechnol, 2000. **18**(4): p. 410-4.

51. Jarver, P. and U. Langel, *The use of cell-penetrating peptides as a tool for gene regulation.* Drug Discov Today, 2004. **9**(9): p. 395-402.

52. Ensoli, B., et al., *Release, uptake, and effects of extracellular human immunodeficiency virus type 1 Tat protein on cell growth and viral transactivation.* J Virol, 1993. **67**(1): p. 277-87.

53. Fawell, S., et al., *Tat-mediated delivery of heterologous proteins into cells.* Proc Natl Acad Sci U S A, 1994. **91**(2): p. 664-8.

54. Frankel, A.D. and C.O. Pabo, *Cellular uptake of the tat protein from human immunodeficiency virus.* Cell, 1988. **55**(6): p. 1189-93.

55. Schwarze, S.R., K.A. Hruska, and S.F. Dowdy, *Protein transduction: unrestricted delivery into all cells?* Trends Cell Biol, 2000. **10**(7): p. 290-5.

56. Futaki, S., *Arginine-rich peptides: potential for intracellular delivery of macromolecules and the mystery of the translocation mechanisms.* Int J Pharm, 2002. **245**(1-2): p. 1-7.

57. Futaki, S., et al., *Arginine-rich peptides. An abundant source of membrane-permeable peptides having potential as carriers for intracellular protein delivery.* J Biol Chem, 2001. **276**(8): p. 5836-40.

58. Mitchell, D.J., et al., *Polyarginine enters cells more efficiently than other polycationic homopolymers.* J Pept Res, 2000. **56**(5): p. 318-25.

59. Wender, P.A., et al., *The design, synthesis, and evaluation of molecules that enable or enhance cellular uptake: peptoid molecular transporters.* Proc Natl Acad Sci U S A, 2000. **97**(24): p. 13003-8.

60. Rothbard, J.B., et al., *Conjugation of arginine oligomers to cyclosporin A facilitates topical delivery and inhibition of inflammation.* Nat Med, 2000. **6**(11): p. 1253-7.

61. Derossi, D., et al., *Cell internalization of the third helix of the Antennapedia homeodomain is receptor-independent.* J Biol Chem, 1996. **271**(30): p. 18188-93.

62. Drin, G., et al., *Physico-chemical requirements for cellular uptake of pAntp peptide. Role of lipid-binding affinity.* Eur J Biochem, 2001. **268**(5): p. 1304-14.

63. Joliot, A., et al., *Antennapedia homeobox peptide regulates neural morphogenesis.* Proc Natl Acad Sci U S A, 1991. **88**(5): p. 1864-8.

64. Karlsson, O., et al., *Insulin gene enhancer binding protein Isl-1 is a member of a novel class of proteins containing both a homeo- and a Cys-His domain.* Nature, 1990. **344**(6269): p. 879-82.

65. Kilk, K., et al., *Cellular internalization of a cargo complex with a novel peptide derived from the third helix of the islet-1 homeodomain. Comparison with the penetratin peptide.* Bioconjug Chem, 2001. **12**(6): p. 911-6.

66. Pugliese, L., et al., *Three-dimensional structure of the tetragonal crystal form of egg-white avidin in its functional complex with biotin at 2.7 A resolution.* J Mol Biol, 1993. **231**(3): p. 698-710.

67. Pooga, M., et al., *Cellular translocation of proteins by transportan.* Faseb J, 2001. **15**(8): p. 1451-3.

68. Pooga, M., et al., *Novel galanin receptor ligands.* J Pept Res, 1998. **51**(1): p. 65-74.

69. Morris, M.C., et al., *A new peptide vector for efficient delivery of oligonucleotides into mammalian cells.* Nucleic Acids Res, 1997. **25**(14): p. 2730-6.

70. Vidal, P., et al., *Solid-phase synthesis and cellular localization of a C- and/or N-terminal labelled peptide.* J Pept Sci, 1996. **2**(2): p. 125-33.

71. Deshayes, S., et al., *On the mechanism of non-endosomial peptide-mediated cellular delivery of nucleic acids.* Biochim Biophys Acta, 2004. **1667**(2): p. 141-7.

72. Deshayes, S., et al., *Insight into the mechanism of internalization of the cell-penetrating carrier peptide Pep-1 through conformational analysis.* Biochemistry, 2004. **43**(6): p. 1449-57.

73. Morris, M.C., et al., *A peptide carrier for the delivery of biologically active proteins into mammalian cells.* Nat Biotechnol, 2001. **19**(12): p. 1173-6.

74. Takeshima, K., et al., *Translocation of analogues of the antimicrobial peptides magainin and buforin across human cell membranes.* J Biol Chem, 2003. **278**(2): p. 1310-5.

75. Sadler, K., et al., *Translocating proline-rich peptides from the antimicrobial peptide bactenecin 7.* Biochemistry, 2002. **41**(48): p. 14150-7.

76. Rousselle, C., et al., *Enhanced delivery of doxorubicin into the brain via a peptide-vector-mediated strategy: saturation kinetics and specificity.* J Pharmacol Exp Ther, 2001. **296**(1): p. 124-31.

77. Herbig, M.E., et al., *Bilayer interaction and localization of cell penetrating peptides with model membranes: a comparative study of a human calcitonin (hCT)-derived peptide with pVEC and pAntp(43-58).* Biochim Biophys Acta, 2005. **1712**(2): p. 197-211.

78. Silverman, S.L., *Calcitonin.* Am J Med Sci, 1997. **313**(1): p. 13-6.

79. Trehin, R., et al., *Cellular uptake but low permeation of human calcitonin-derived cell penetrating peptides and Tat(47-57) through well-differentiated epithelial models.* Pharm Res, 2004. **21**(7): p. 1248-56.

80. Foerg, C., et al., *Decoding the entry of two novel cell-penetrating peptides in HeLa cells: lipid raft-mediated endocytosis and endosomal escape.* Biochemistry, 2005. **44**(1): p. 72-81.

81. Reynolds, F., R. Weissleder, and L. Josephson, *Protamine as an efficient membrane-translocating Peptide.* Bioconjug Chem, 2005. **16**(5): p. 1240-5.

82. Richard, J.P., et al., *Cell-penetrating peptides. A reevaluation of the mechanism of cellular uptake.* J Biol Chem, 2003. **278**(1): p. 585-90.

83. Drin, G., et al., *Studies on the internalization mechanism of cationic cell-penetrating peptides.* J Biol Chem, 2003. **278**(33): p. 31192-201.

84. Console, S., et al., *Antennapedia and HIV transactivator of transcription (TAT) "protein transduction domains" promote endocytosis of high molecular weight cargo upon binding to cell surface glycosaminoglycans.* J Biol Chem, 2003. **278**(37): p. 35109-14.

85. Schmid, S.L., *Clathrin-coated vesicle formation and protein sorting: an integrated process.* Annu Rev Biochem, 1997. **66**: p. 511-48.

86. Vendeville, A., et al., *HIV-1 Tat enters T cells using coated pits before translocating from acidified endosomes and eliciting biological responses.* Mol Biol Cell, 2004. **15**(5): p. 2347-60.

87. Nichols, B.J., et al., *Rapid cycling of lipid raft markers between the cell surface and Golgi complex.* J Cell Biol, 2001. **153**(3): p. 529-41.

88. Pelkmans, L., J. Kartenbeck, and A. Helenius, *Caveolar endocytosis of simian virus 40 reveals a new two-step vesicular-transport pathway to the ER.* Nat Cell Biol, 2001. **3**(5): p. 473-83.

89. Puri, V., et al., *Clathrin-dependent and -independent internalization of plasma membrane sphingolipids initiates two Golgi targeting pathways.* J Cell Biol, 2001. **154**(3): p. 535-47.

90. Wadia, J.S. and S.F. Dowdy, *Transmembrane delivery of protein and peptide drugs by TAT-mediated transduction in the treatment of cancer.* Adv Drug Deliv Rev, 2005. **57**(4): p. 579-96.

91. Wadia, J.S., R.V. Stan, and S.F. Dowdy, *Transducible TAT-HA fusogenic peptide enhances escape of TAT-fusion proteins after lipid raft macropinocytosis.* Nat Med, 2004. **10**(3): p. 310-5.

92. Vives, E., *Cellular uptake [correction of utake] of the Tat peptide: an endocytosis mechanism following ionic interactions.* J Mol Recognit, 2003. **16**(5): p. 265-71.

93. Fischer, R., et al., *A stepwise dissection of the intracellular fate of cationic cell-penetrating peptides.* J Biol Chem, 2004. **279**(13): p. 12625-35.

94. Lord, J.M. and L.M. Roberts, *Toxin entry: retrograde transport through the secretory pathway.* J Cell Biol, 1998. **140**(4): p. 733-6.

95. Sandvig, K. and B. van Deurs, *Entry of ricin and Shiga toxin into cells: molecular mechanisms and medical perspectives.* Embo J, 2000. **19**(22): p. 5943-50.

96. Sandvig, K. and B. van Deurs, *Membrane traffic exploited by protein toxins.* Annu Rev Cell Dev Biol, 2002. **18**: p. 1-24.

97. Bucci, M., et al., *In vivo delivery of the caveolin-1 scaffolding domain inhibits nitric oxide synthesis and reduces inflammation.* Nat Med, 2000. **6**(12): p. 1362-7.

98. Barka, T., E.W. Gresik, and H. van Der Noen, *Transduction of TAT-HA-beta-galactosidase fusion protein into salivary gland-derived cells and organ cultures of the developing gland, and into rat submandibular gland in vivo.* J Histochem Cytochem, 2000. **48**(11): p. 1453-60.

99. Cao, G., et al., *In Vivo Delivery of a Bcl-xL Fusion Protein Containing the TAT Protein Transduction Domain Protects against Ischemic Brain Injury and Neuronal Apoptosis.* J Neurosci, 2002. **22**(13): p. 5423-31.

100. Koppelhus, U., et al., *Cell-dependent differential cellular uptake of PNA, peptides, and PNA-peptide conjugates.* Antisense Nucleic Acid Drug Dev, 2002. **12**(2): p. 51-63.

101. Kramer, S.D. and H. Wunderli-Allenspach, *No entry for TAT(44-57) into liposomes and intact MDCK cells: novel approach to study membrane permeation of cell-penetrating peptides.* Biochim Biophys Acta, 2003. **1609**(2): p. 161-9.

102. Violini, S., et al., *Evidence for a plasma membrane-mediated permeability barrier to Tat basic domain in well-differentiated epithelial cells: lack of correlation with heparan sulfate.* Biochemistry, 2002. **41**(42): p. 12652-61.

103. Falnes, P.O., J. Wesche, and S. Olsnes, *Ability of the Tat basic domain and VP22 to mediate cell binding, but not membrane translocation of the diphtheria toxin A-fragment.* Biochemistry, 2001. **40**(14): p. 4349-58.

104. Zhang, X., et al., *Quantitative assessment of the cell penetrating properties of RI-Tat-9: evidence for a cell type-specific barrier at the plasma membrane of epithelial cells.* Mol Pharm, 2004. **1**(2): p. 145-55.

105. Caron, N.J., et al., *Intracellular delivery of a Tat-eGFP fusion protein into muscle cells.* Mol Ther, 2001. **3**(3): p. 310-8.

106. Niesner, U., et al., *Quantitation of the tumor-targeting properties of antibody fragments conjugated to cell-permeating HIV-1 TAT peptides.* Bioconjug Chem, 2002. **13**(4): p. 729-36.

107. Leifert, J.A., S. Harkins, and J.L. Whitton, *Full-length proteins attached to the HIV tat protein transduction domain are neither transduced between cells, nor exhibit enhanced immunogenicity.* Gene Ther, 2002. **9**(21): p. 1422-8.

108. Xia, H., Q. Mao, and B.L. Davidson, *The HIV Tat protein transduction domain improves the biodistribution of beta-glucuronidase expressed from recombinant viral vectors.* Nat Biotechnol, 2001. **19**(7): p. 640-4.

109. Lee, H.J. and W.M. Pardridge, *Pharmacokinetics and delivery of tat and tat-protein conjugates to tissues in vivo.* Bioconjug Chem, 2001. **12**(6): p. 995-9.

110. Tseng, Y.L., J.J. Liu, and R.L. Hong, *Translocation of liposomes into cancer cells by cell-penetrating peptides penetratin and tat: a kinetic and efficacy study.* Mol Pharmacol, 2002. **62**(4): p. 864-72.

111. Polyakov, V., et al., *Novel Tat-peptide chelates for direct transduction of technetium-99m and rhenium into human cells for imaging and radiotherapy.* Bioconjug Chem, 2000. **11**(6): p. 762-71.

112. Lindgren, M.E., et al., *Passage of cell-penetrating peptides across a human epithelial cell layer in vitro.* Biochem J, 2004. **377**(Pt 1): p. 69-76.

113. Soomets, U., et al., *Deletion analogues of transportan.* Biochim Biophys Acta, 2000. **1467**(1): p. 165-76.

114. Trehin, R., et al., *Metabolic Cleavage of Cell Penetrating Peptides in Contact with Epithelial Models: Human Calcitonin (hCT) Derived Peptides, Tat(47-57) and Penetratin(43-58).* Biochem J, 2004. **Pt**.

115. Holm, T., et al., *Uptake of cell-penetrating peptides in yeasts.* FEBS Lett, 2005.

116. Cereijido, M., et al., *Cell-to-cell communication in monolayers of epithelioid cells (MDCK) as a function of the age of the monolayer.* J Membr Biol, 1984. **81**(1): p. 41-8.

117. Cereijido, M., et al., *Role of tight junctions in establishing and maintaining cell polarity.* Annu Rev Physiol, 1998. **60**: p. 161-77.

118. Harhaj, N.S. and D.A. Antonetti, *Regulation of tight junctions and loss of barrier function in pathophysiology.* Int J Biochem Cell Biol, 2004. **36**(7): p. 1206-37.

119. van Meer, G., B. Gumbiner, and K. Simons, *The tight junction does not allow lipid molecules to diffuse from one epithelial cell to the next.* Nature, 1986. **322**(6080): p. 639-41.

120. van Meer, G. and K. Simons, *The function of tight junctions in maintaining differences in lipid composition between the apical and the basolateral cell surface domains of MDCK cells.* Embo J, 1986. **5**(7): p. 1455-64.

121. Ferrari, A., et al., *Caveolae-mediated internalization of extracellular HIV-1 tat fusion proteins visualized in real time.* Mol Ther, 2003. **8**(2): p. 284-94.

122. Hallbrink, M., et al., *Cargo delivery kinetics of cell-penetrating peptides.* Biochim Biophys Acta, 2001. **1515**(2): p. 101-9.

123. Tyagi, M., et al., *Internalization of HIV-1 tat requires cell surface heparan sulfate proteoglycans.* J Biol Chem, 2001. **276**(5): p. 3254-61.

124. Ellis, S. and H. Mellor, *Regulation of endocytic traffic by rho family GTPases.* Trends Cell Biol, 2000. **10**(3): p. 85-8.

125. Etienne-Manneville, S. and A. Hall, *Rho GTPases in cell biology.* Nature, 2002. **420**(6916): p. 629-35.

126. Van Aelst, L. and C. D'Souza-Schorey, *Rho GTPases and signaling networks.* Genes Dev, 1997. **11**(18): p. 2295-322.

127. Bourne, H.R., *GTPases. A turn-on and a surprise.* Nature, 1993. **366**(6456): p. 628-9.

128. Hall, A., *Rho GTPases and the actin cytoskeleton.* Science, 1998. **279**(5350): p. 509-14.

129. Qualmann, B. and H. Mellor, *Regulation of endocytic traffic by Rho GTPases.* Biochem J, 2003. **371**(Pt 2): p. 233-41.

130. Rivero, F. and B.P. Somesh, *Signal transduction pathways regulated by Rho GTPases in Dictyostelium.* J Muscle Res Cell Motil, 2002. **23**(7-8): p. 737-49.

131. Symons, M. and N. Rusk, *Control of vesicular trafficking by Rho GTPases.* Curr Biol, 2003. **13**(10): p. R409-18.

132. Fukata, M., M. Nakagawa, and K. Kaibuchi, *Roles of Rho-family GTPases in cell polarisation and directional migration.* Curr Opin Cell Biol, 2003. **15**(5): p. 590-7.

133. Nobes, C.D. and A. Hall, *Rho, rac, and cdc42 GTPases regulate the assembly of multimolecular focal complexes associated with actin stress fibers, lamellipodia, and filopodia.* Cell, 1995. **81**(1): p. 53-62.

134. Qualmann, B., M.M. Kessels, and R.B. Kelly, *Molecular links between endocytosis and the actin cytoskeleton.* J Cell Biol, 2000. **150**(5): p. F111-6.

135. Chimini, G. and P. Chavrier, *Function of Rho family proteins in actin dynamics during phagocytosis and engulfment.* Nat Cell Biol, 2000. **2**(10): p. E191-6.

136. Nobes, C.D. and A. Hall, *Rho GTPases control polarity, protrusion, and adhesion during cell movement.* J Cell Biol, 1999. **144**(6): p. 1235-44.

137. Mackay, D.J. and A. Hall, *Rho GTPases.* J Biol Chem, 1998. **273**(33): p. 20685-8.

138. Jou, T.S., et al., *Selective alterations in biosynthetic and endocytic protein traffic in Madin-Darby canine kidney epithelial cells expressing mutants of the small GTPase Rac1.* Mol Biol Cell, 2000. **11**(1): p. 287-304.

139. Leung, S.M., et al., *Modulation of endocytic traffic in polarized Madin-Darby canine kidney cells by the small GTPase RhoA.* Mol Biol Cell, 1999. **10**(12): p. 4369-84.

140. Noren, N.K., et al., *Cadherin engagement regulates Rho family GTPases.* J Biol Chem, 2001. **276**(36): p. 33305-8.

141. Kuroda, S., et al., *Regulation of cell-cell adhesion of MDCK cells by Cdc42 and Rac1 small GTPases.* Biochem Biophys Res Commun, 1997. **240**(2): p. 430-5.

142. Takaishi, K., et al., *Regulation of cell-cell adhesion by rac and rho small G proteins in MDCK cells.* J Cell Biol, 1997. **139**(4): p. 1047-59.

143. Ridley, A.J., P.M. Comoglio, and A. Hall, *Regulation of scatter factor/hepatocyte growth factor responses by Ras, Rac, and Rho in MDCK cells.* Mol Cell Biol, 1995. **15**(2): p. 1110-22.

144. Jou, T.S. and W.J. Nelson, *Effects of regulated expression of mutant RhoA and Rac1 small GTPases on the development of epithelial (MDCK) cell polarity.* J Cell Biol, 1998. **142**(1): p. 85-100.

145. Kazmierczak, B.I., et al., *Rho GTPase activity modulates Pseudomonas aeruginosa internalization by epithelial cells.* Cell Microbiol, 2001. **3**(2): p. 85-98.

146. Kazmierczak, B.I., K. Mostov, and J.N. Engel, *Epithelial cell polarity alters Rho-GTPase responses to Pseudomonas aeruginosa.* Mol Biol Cell, 2004. **15**(2): p. 411-9.

147. Wadia, J.S. and S.F. Dowdy, *Protein transduction technology.* Curr Opin Biotechnol, 2002. **13**(1): p. 52-6.

148. Wadia, J.S. and S.F. Dowdy, *Modulation of cellular function by TAT mediated transduction of full length proteins.* Curr Protein Pept Sci, 2003. **4**(2): p. 97-104.

149. Selivanova, G., et al., *Restoration of the growth suppression function of mutant p53 by a synthetic peptide derived from the p53 C-terminal domain.* Nat Med, 1997. **3**(6): p. 632-8.

150. Hupp, T.R., A. Sparks, and D.P. Lane, *Small peptides activate the latent sequence-specific DNA binding function of p53.* Cell, 1995. **83**(2): p. 237-45.

151. Snyder, E.L., et al., *Treatment of terminal peritoneal carcinomatosis by a transducible p53-activating peptide.* PLoS Biol, 2004. **2**(2): p. E36.

152. Nagahara, H., et al., *Transduction of full-length TAT fusion proteins into mammalian cells: TAT-p27Kip1 induces cell migration.* Nat Med, 1998. **4**(12): p. 1449-52.

153. Gius, D.R., et al., *Transduced p16INK4a peptides inhibit hypophosphorylation of the retinoblastoma protein and cell cycle progression prior to activation of Cdk2 complexes in late G1.* Cancer Res, 1999. **59**(11): p. 2577-80.

154. Ortega, S., M. Malumbres, and M. Barbacid, *Cyclin D-dependent kinases, INK4 inhibitors and cancer.* Biochim Biophys Acta, 2002. **1602**(1): p. 73-87.

155. Nekhotiaeva, N., et al., *Cell entry and antimicrobial properties of eukaryotic cell-penetrating peptides.* Faseb J, 2004. **18**(2): p. 394-6.

156. Orlando, R.C., *Mechanisms of epithelial injury and inflammation in gastrointestinal diseases.* Rev Gastroenterol Disord, 2002. **2 Suppl 2**: p. S2-8.

157. Sanders, D.S., *Mucosal integrity and barrier function in the pathogenesis of early lesions in Crohn's disease.* J Clin Pathol, 2005. **58**(6): p. 568-72.

158. Schmitz, H., et al., *Epithelial barrier and transport function of the colon in ulcerative colitis.* Ann N Y Acad Sci, 2000. **915**: p. 312-26.

159. Siccardi, D., J.R. Turner, and R.J. Mrsny, *Regulation of intestinal epithelial function: a link between opportunities for macromolecular drug delivery and inflammatory bowel disease.* Adv Drug Deliv Rev, 2005. **57**(2): p. 219-35.

160. Coyne, C.B., et al., *Regulation of airway tight junctions by proinflammatory cytokines.* Mol Biol Cell, 2002. **13**(9): p. 3218-34.

161. Trautmann, A., et al., *Apoptosis and Loss of Adhesion of Bronchial Epithelial Cells in Asthma.* Int Arch Allergy Immunol, 2005. **138**(2): p. 142-150.

162. Bruewer, M., et al., *Proinflammatory cytokines disrupt epithelial barrier function by apoptosis-independent mechanisms.* J Immunol, 2003. **171**(11): p. 6164-72.

163. Nusrat, A., et al., *Tight junctions are membrane microdomains.* J Cell Sci, 2000. **113 (Pt 10)**: p. 1771-81.

CHAPTER II

Decoding the entry of two novel cell-penetrating peptides in HeLa cells: lipid raft-mediated endocytosis and endosomal escape.

Christina Foerg[1], Urs Ziegler[2], Jimena Fernandez-Carneado[3], Ernest Giralt[3,4], Robert Rennert[5], Annette G. Beck-Sickinger[5], Hans P. Merkle[1]

[1]Department of Chemistry and Applied Biosciences, Institute of Pharmaceutical Sciences, ETH Zurich, Switzerland

[2]Institute of Anatomy, University of Zurich, Switzerland

[3]Institut de Recerca Biomèdica de Barcelona, Parc Científic de Barcelona, Spain

[4]Departament de Química Orgànica, Universitat de Barcelona, Spain,

[5]Institute of Biochemistry, University of Leipzig, Germany

Biochemistry **44** (1): 72-81 (2005)

ABSTRACT

Cellular entry of peptide, protein and nucleic acid biopharmaceuticals is severely impeded by the cell membrane. Linkage or assembly of such agents and cell penetrating peptides (CPPs) with ability to cross cellular membranes has opened a new horizon in biomedical research. Nevertheless, the uptake mechanisms of most CPPs have been controversially discussed and are poorly understood. We present data on two recently developed oligocationic CPPs, the sweet arrow peptide SAP, a γ-zein related sequence, and a branched human calcitonin derived peptide, hCT(9-32)-br, carrying a simian virus derived nuclear localization sequence in the side chain. Uptake in HeLa cells and intracellular trafficking of N-terminally carboxyfluorescein labeled peptides was studied by confocal laser scanning microscopy and flow cytometry using biochemical markers in combination with quenching and colocalization approaches. Both peptides were readily internalized by HeLa cells through interaction with the extracellular matrix followed by lipid raft-mediated endocytosis as confirmed by reduced uptake at lower temperature, in presence of endocytosis inhibitors and through cholesterol depletion by methyl-β-cyclodextrin, supported by colocalization with markers for clathrin-independent pathways. In contrast to the oligocationic SAP and hCT(9-32)-br, interaction with the extracellular matrix, however, was no prerequisite for the observed lipid raft-mediated uptake of the weakly cationic, unbranched hCT(9-32). Transient involvement of endosomes in intracellular trafficking of SAP and hCT(9-32)-br prior to endosomal escape of both peptides was revealed by colocalization and pulse-chase studies of the peptides with the early endosome antigen 1. The results bear potential for CPPs as tools for intracellular drug delivery.

INTRODUCTION

Based on the largely enhanced discovery process towards novel pharmacologically active agents, increasing numbers of potential peptide, protein- or nucleic acid based biopharmaceuticals are considered for therapeutic application and drug development. Nevertheless, due to their large molecular size, charge and polarity, the clinical development of these biomacromolecules is likely to be problematic because of their insufficient ability to cross cellular membranes or reach intracellular targets. This explains their often poor or zero bioavailability and clinical efficacy. The discovery of various 10 to 30-mer peptides with the ability to translocate cellular membranes has, therefore, opened a new horizon in biomedical research [1]. Chemical ligation or physical assembly of these so-called cell penetrating peptides (CPPs) with biopharmaceuticals of poor cellular access is currently a main avenue in engineering delivery systems that could mediate the non-invasive import of such problematic cargoes into cells. Various oligocationic cell penetrating peptides, e.g., penetratin, the Antennapedia homeodomain derived CPP from Drosophila [2], HIV-1 derived Tat peptides [3] or oligoarginine peptides [4] have been well described in the literature. They were widely considered for the therapeutic delivery of peptides [5], proteins [6], oligonucleotides [7], plasmids [8], peptide nucleic acids (PNAs) [9] and even nanoparticles [10]. Besides these oligocationic CPPs, enhanced translocation of the cellular membrane has also been reported for weakly cationic peptides, e.g. hCT(9-32), a human calcitonin derived CPP that has been introduced by our group [11, 12]. Despite the wide-spread interest in such molecular carriers, the mechanisms underlying the cellular translocation of CPPs are yet incompletely understood and were subject to controversial discussions. For instance, the cellular translocation of penetratin and Tat peptides was initially assigned to a passive, temperature-independent process [2, 3, 13], not sensitive to endocytosis inhibitors [3, 14]. The observations were thought to be consistent with a theoretical model for a CPP induced physical perturbation of the lipid membrane leading to a direct translocation of the plasma membrane [2, 3, 15]. Recently, however, the related hypotheses involving direct translocation have been challenged following several reports on artefactual results that were caused by cell fixation prior to confocal laser scanning microscopy (CLSM) of cells incubated with fluorescence labeled CPPs. Another source of misinterpretation was found in the experimental difficulties to distinguish cell surface-associated CPPs from CPPs internalized in cytoplasmic compartments [16]. Unequivocal discrimination between associated and internalized fluorescence, however, is a prerequisite to interpret both CLSM and fluorescence-activated cell sorting (FACS) analysis with labeled CPPs. More recent work

demonstrated clearly the involvement of endocytosis in the internalization of a Tat derived peptide [16] and penetratin [17]. Prior to endocytosis, both peptides were shown to first interact electrostatically with the extracellular matrix (ECM) of the cell surface through binding to negatively charged glycosaminoglycans [18]. Endocytosis may involve several pathways. So far, most classical studies focused on the pathway via clathrin-coated pits [19, 20]. Meanwhile, however, technologies and reagents are available that can shed light on non-classical, clathrin-independent pathways such as endocytosis via lipid rafts [21-23]. Lipid rafts are membrane microdomains that are enriched in cholesterol and sphingolipids [24, 25]. The sensitivity of lipid raft-mediated endocytosis to cholesterol depletion distinguishes this pathway from non raft-dependent processes such as clathrin-mediated endocytosis [22, 23, 26, 27]. Lipid raft pathways mediate the internalization of sphingolipid binding toxins such as cholera toxin [22, 23, 26], whereas transferrin, a typical marker for clathrin-mediated endocytosis, is excluded from lipid rafts [24, 25, 28].

Here we investigate the cellular entry of two N-terminally carboxyfluorescein (CF) labeled, oligocationic CPPs representing more recent discoveries in the field. One is a branched derivative of the linear human calcitonin derived CF-hCT(9-32) [11], denoted as CF-hCT(9-32)-br [29], that carries an oligocationic, SV40 derived nuclear localisation sequence, the GPDEVKRKKKP motif, in the form of a side-branch to the main peptide chain (see Table I). The other one is the equally CF labeled linear proline-rich sweet arrow peptide CF-SAP (see Tab. I), a linear trimer of repetitive VRLPPP domains, and conceived as an amphipathic version of a polyproline sequence related to γ-zein, a storage protein of maize [30-32].As compared to other CPPs, both peptides offer practical advantages including good solubility in water, low cytotoxicity, and, in case of CF-SAP, non-viral origin [29, 31]. As a positive control we used the unbranched CPP CF-hCT(9-32) [11].

We report on their uptake into HeLa cells as assessed by CLSM and confirmed by flow cytometry. For their cellular entry we propose a non-classical, clathrin-independent pathway through lipid raft-mediated endocytosis. Having passed the cellular membrane, the two cationic compounds were found to transiently sojourn in endosomal compartments where sorting steps take place. A pulse-chase study revealed the endosomal escape of the peptides and their subsequent transfer to other cytoplasmic vesicles.

Table 1: Name, Sequence and Origin of the Cell-Penetrating Peptides (CPPs) Used[a]

Name	Sequence	Origin
hCT(9-32)	LGTYTQDFNKFHTFPQTAIGVGAP-NH_2	human calcitonin
hCT(9-32)-br	LGTYTQDFNKFHTFPQTAIGVGAP-NH_2 | AFGVGPDEVKRKKKP–NH_2	human calcitonin, simian virus 40
SAP	VRLPPP-VRLPPP-VRLPPP	modified maize zein sequence

[a] Throughout, peptides were CF-labeled at the N-terminus.

MATERIALS AND METHODS

Materials

HeLa cells were obtained from American Type Culture Collection ATTC (Rockville, MD, USA). Dulbecco's modified Eagle's medium (DMEM), XTT (2,3-Bis(2-methoxy-4-nitro-5-sulfophenyl)-2H-tetrazolium-5-carboxanilide) and saponin were purchased from Sigma-Aldrich (Taufkirchen, Germany). Trypsin-EDTA, penicillin, streptomycin, Hank's balanced salt solution (HBSS) and phosphate buffer solution (PBS, pH 7.4) without calcium and magnesium were from Life Technologies (Basel, Switzerland). Foetal calf serum (FCS) was purchased from Winiger AG (Wohlen, Switzerland). Hoechst 33342, cholera toxin subunit B (recombinant) Alexa Fluor 594 conjugate and tetramethylrhodamine-labeled transferrin were from Molecular Probes (Leiden, The Netherlands). The monoclonal first antibody rabbit anti-EEA1 was from Affinity BioReagents (Golden, CO, USA), the second antibodies donkey anti-rabbit biotin and donkey anti mouse Texas red were from Jackson Immuno Research Laboratories (West Grove, PA, USA) and streptavidin labeled with Texas red, Cy5 or FITC from Amersham Biosciences (Uppsala, Sweden). The monoclonal first antibodies mouse anti-Gal T and mouse anti P63 were a kind gift of Dr. Jack Rohrer from the Institute of Physiology, University of Zurich (Zurich, Switzerland). Dako fluorescent

mounting medium was purchased from DAKO Corporation (Carpinteria, CA, USA). 5(6)-carboxyfluorescein (CF), heparin, Trypan blue, sodium azide (NaN_3), Triton X-100, Menadione (2-Methyl-1,4-naphthoquinone) and 2-deoxy-glucose were obtained from Fluka (Buchs, Switzerland), and methyl-β-cyclodextrin (M-β-CD) as well as 2-hydroxypropyl-γ-cyclodextrin (HP-γ-CD) from Wacker-Chemie (Munich, Germany). Glass chamber slides were obtained from Nunc (Wiesbaden, Germany). Cell culturing flasks (25 cm^2) and 24-well plates were from TPP (Trasadingen, Switzerland). Coverslips and microscope slides were purchased from Knittel (Braunschweig, Germany).

Methods

Peptide synthesis. N-terminally fluorescence labeled sweet arrow peptide (CF-SAP) (see Tab. 1) was synthesised by solid-phase peptide synthesis on a 2-chlorotrityl resin following the 9-fluorenyl methoxy carbonyl/*tert*-butyl strategy prior to fluorescent labeling with 5(6)-carboxyfluorescein (CF) [31]; CF-hCT(9-32) and CF-hCT(9-32)-br (see Tab. 1) were synthesized according to the Fmoc-strategy by automated multiple solid phase peptide synthesis using a robot system (Syro, MultiSynTech, Germany). Introduction of the side chain into the branched peptide, CF-labeling and identification were performed as described previously [29].

Cell culture. HeLa cells were cultured as exponentially growing subconfluent monolayers at 37°C under 5% CO_2. Cell culture was in 25 cm^2 culture flasks in DMEM (high glucose) supplemented with 10% heat-inactivated FCS and 1% penicillin/streptomycin. Medium was exchanged 3 times per week. Exponentially growing HeLa cells were seeded at constant density of about 10^5 cells/cm^2 on chamber slides, 24-well plates or coverslips. For experiments cells were used 24 hours post seeding.

XTT cell viability assay. To check for cell proliferation and viability of HeLa cells after treatment with hCT(9-32) or hCT(9-32)-br, we measured overall activity of mitochondrial dehydrogenase by XTT assays [33]. HeLa cells were grown in 96-well plates until 70-80 % confluency and then incubated with peptide solutions in medium ranging from 30 to 100 μM at 37°C for 2 hours. As negative or positive controls, we used untreated cells or cells treated with 70% EtOH for 7 min, respectively. After discarding the peptide solutions and several washing steps, XTT solution was added for 2 hours at 37°C. Overall activity of mitochondrial dehydrogenase in each well was measured spectrophotometrically at 450 nm using a SpectraFluor Plus (Tecan, Crailsheim, Germany).

Confocal laser scanning microscopy (CLSM) of CPP uptake. For uptake, cells were equilibrated in HBSS for several minutes prior to incubation with HBSS containing either CF-SAP (50 μM), CF-hCT(9-32)-br (30 μM), CF-hCT(9-32) (30 μM) or unconjugated fluorophore (50 μM or 30 μM, respectively) for 1 hour. After 30 min, Hoechst 33342 was added to a final concentration of 1 μg/ml for nuclear staining. The study was conducted at 37°C or 4°C under horizontal mechanical shaking at 150 min^{-1}. For inhibition of endocytosis, cells were pre-treated for 1 h with NaN_3/2-deoxyglucose (0.1%/50 mM in HBSS), heparin (5 U/ml in PBS) or methyl-β-cyclodextrin (10 mM in serum free medium), prior to incubation with CPPs.

Subsequently, cells were washed three times with PBS and inspected immediately in a HBSS solution without any fixation, using a Zeiss CLSM 410 inverted microscope [34] with a 63x, 1.4 NA plan apochromatic lens (lasers: HeNe 543 nm, Ar 488 nm and Ar UV 364 nm). 3-D multichannel image processing was performed using the IMARIS software (Bitplane AG, Zurich, Switzerland) on a Silicon graphics workstation. Background fluorescence was determined by analysing non-treated cells.

Uptake and endocytosis inhibition study by FACS. HeLa cells were seeded in 24-well plates and incubated with CF-SAP (50 μM), CF-hCT(9-32) (30 μM) or CF-hCT(9-32)-br (30 μM) in HBSS for 3 hours. After incubation, cells were washed 3 times with PBS, trypsinized for 10 min, resuspended in medium and immediately put on ice. To quench potentially remaining external fluorescence, Trypan blue was added to the samples before analysis by FACS on a FacScan (Becton Dickinson, Franklin Lakes, NJ) within 2 hours after trypsinization. A total of 10,000 cells per sample was analyzed. The mean fluorescence intensity of peptide-labeled cell populations was compared to non-treated control cells and control cells incubated with 5(6)-carboxyfluorescein.

For inhibition of endocytosis, cells were pre-treated for 1 h with NaN_3/2-deoxyglucose (0.1%/50 mM in HBSS), heparin (5 U/ml in PBS) or methyl-β-cyclodextrin (10 mM in serum free medium), prior to incubation with CPPs.

Colocalization study by CLSM. HeLa cells were seeded on coverslips (12 mm) in 24-well plates as described above. After equilibration, cells were coincubated for 30 min in solutions of CF-SAP (50 μM), CF-hCT(9-32)-br or CF-hCT(9-32) (both 30 μM) with either cholera toxin (10 μg/ml) or transferrin (50 μg/ml) in HBSS. Cells were washed three times with PBS and fixed in 1% (v/v) aqueous formaldehyde solution at room temperature for 30 min. Cells were washed again with PBS and analysed using a high resolution TCS-SP2 laser

scanning confocal microscope (Leica Microsystems, Mannheim, Germany) with a 63x, 1.4 NA plan apochromatic lens using HeNe 594 nm, HeNe 543 nm, Ar 488 and Ar UV 405 nm lasers. To avoid cross talk, emission signals were collected independently. Image processing was performed using the IMARIS software (Bitplane AG, Zurich, Switzerland) on a Silicon graphics workstation. The images were deconvolved using Huygens software (Scientific Volume Imaging B.V., Hilversum, Netherlands).

Immunofluorescence labeling. Tracing early endosomes. HeLa cells seeded on coverslips were incubated with CF-SAP or CF-hCT(9-32)-br for 30 min as described, and at the same time incubated with 1 μg/ml Hoechst 33342 to stain the nuclei. To monitor the intracellular fate of the ingested CPPs, pulse-chase studies [35] were performed with a 30 min CPP incubation period, followed by several PBS washings, and with a chase period of 2.5 hours incubation in DMEM. Cells were fixed for 30 min in 1% (v/v) formaldehyde and permeabilized with 0.1% Triton X-100 in PBS for 1 min at room temperature. Cells were washed several times with PBS. Non-specific binding sites were blocked by incubating for 30 min with 1% BSA in PBS. Cells were then incubated with rabbit anti-EEA1 (1:250) in 1% BSA in PBS for 1 hour at room temperature. After another washing step, cells were incubated with donkey anti-rabbit biotin (1:200) in 1% BSA in PBS for 1 hour at room temperature. After washing 3 times with PBS, streptavidin conjugated to Texas red (1:100) in 1% BSA in PBS were added to cells incubated with donkey anti-rabbit biotin for 1 hour at room temperature. All samples were washed again three times with PBS and mounted in Dako mounting medium.

Immunofluorescence labeling. Tracing the endoplasmic reticulum and the Golgi network. HeLa cells seeded on coverslips were incubated with CF-SAP or CF-hCT(9-32)-br for 30 min as described, and simultaneously incubated with 1 μg/ml Hoechst 33342 to stain the nuclei. Cells were fixed for 30 min in 1% (v/v) formaldehyde and permeabilized with 0.1% Triton X-100 in PBS for 1 min at room temperature. Cells were washed several times with PBS. Non-specific binding sites were blocked by incubating for 30 min with 1% BSA in PBS. Cells were then incubated with mouse anti-Gal T (1:2) or mouse anti P63 (1:200) in 1% BSA in PBS for 1 hour at room temperature. After another washing step, cells were incubated with donkey anti-mouse Texas red (1:200) in 1% BSA in PBS for 1 hour at room temperature. All samples were washed again three times with PBS and mounted in Dako mounting medium.

Cells were scanned as described for colocalization studies. As control experiments, cells incubated with the secondary antibodies without primary antibody staining confirmed the high specificity of the antibodies.

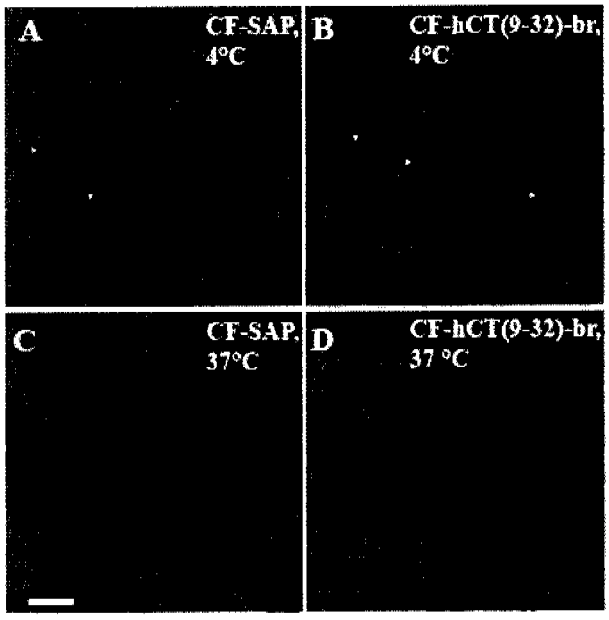

Figure 1. Cellular uptake of CF-SAP and CF-hCT(9-32)-br in HeLa cells at different incubation temperatures. HeLa cells were incubated for 1 hour with 50 μM CF-SAP (A, C) or 30 μM CF-hCT(9-32)-br (B, D). Upper panels (A, B): incubation at 4°C; lower panels (C, D): incubation at 37°C. Arrowheads indicate accumulation of CPPs on cellular membranes when incubation was performed at 4°C. The scalebar is 30 μm. 3D representation.

RESULTS

Cellular uptake in HeLa cells - As visualized by CLSM, after incubation at 37°C, HeLa cells showed marked cellular uptake when exposed to either one of the two cationic peptides, CF-SAP and CF-hCT(9-32)-br, confirming both peptides as potential cell penetrating peptides (Fig.1, C and D, respectively). The cellular uptake of CF-hCT(9-32) as control peptide was also demonstrated (data not shown). The punctuated fluorescence pattern indicated that the translocated fluorescence was localized in discrete vesicular compartments in the cytoplasm, suggestive of an endocytic pathway of internalization. This conclusion was supported by the observation that the internalization was a temperature-dependent process as cellular uptake did not take place at 4°C for both CF-SAP and CF-hCT(9-32)-br, respectively (Fig.1, A and B, respectively). Some accumulation of the peptides in the periphery of cells

was also observed (Fig. 1, arrowheads), supporting the assumption of cellular binding between the cationic peptides and the negatively charged ECM of HeLa cells prior to uptake. Non-treated cells and cells incubated with the fluorescence marker carboxyfluorescein alone were analysed as controls. No intracellular fluorescence was observed in both cases (data not shown).

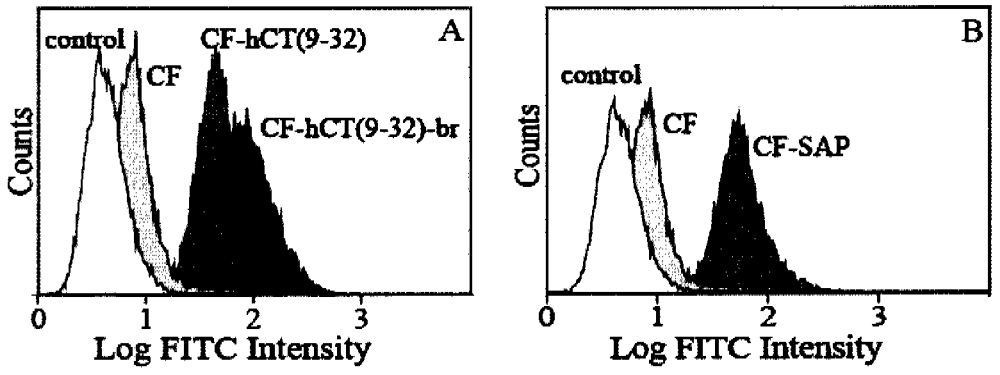

Figure 2. Uptake of CPPs as determined by FACS analysis. A, B - Frequency distributions of fluorescence intensity in HeLa cells incubated for 3 hours with 30 μM CF-hCT(9-32), 30 μM CF-hCT(9-32)-br (A) or 50 μM CF-SAP (B), at 37 °C. Open distributions represent non-treated control cells, light grey distributions stand for cells treated with the fluorescence marker 5(6)-carboxyfluorescein (CF), dark grey distributions show HeLa cells incubated with CF-SAP or CF-hCT(9-32) and the black distribution in Fig. 2B represents CF-labeled CF-hCT(9-32)-br.

Quantitative assessment of peptide internalization by FACS analysis - For confirmation of these findings we quantified the internalization of the two peptides by FACS analysis. Fig. 2 A and B show HeLa cells after incubation with CF-hCT(9-32)-br and CF-SAP, respectively, which resulted in uptake and labeling of the cells with both peptides. Non-treated cells and cells incubated with free carboxyfluorescein were used as negative controls. As positive control, the non-branched CF-hCT(9-32) was used. As shown in Fig. 2A, internalization of CF-hCT(9-32)-br was significantly more efficient than CF-hCT(9-32). It is likely that the enhancement resulted from the oligocationic NLS sequence in the side chain of CF-hCT(9-32)-br (see Table 1).

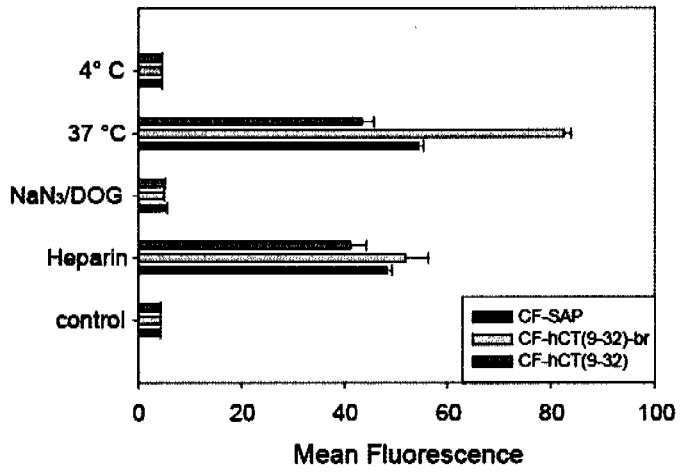

Figure 3. Uptake and endocytosis inhibition of CF-SAP, CF-hCT(9-32)-br and CF-hCT(9-32) in HeLa cells as determined by FACS analysis. HeLa cells were incubated for 3 hours at either 37°C or 4°C with 50 μM CF-SAP (black bars), 30 μM CF-hCT(9-32)-br (light grey bars) or 30 μM CF-hCT(9-32) (dark grey bars). Endocytosis inhibition was performed by pre-treating cells with 0.1% NaN_3 / 50 mM 2-deoxyglucose (NaN_3/DOG) or 5 U/ml heparin before incubation with CF-SAP, CF-hCT(9-32)-br or CF-hCT(9-32). Non-treated cells were used as control cells.

Uptake studies under endocytosis inhibition - Next we investigated the internalization of CF-SAP, CF-hCT(9-32)-br and the control peptide CF-hCT(9-32) under the influence of various endocytosis inhibiting conditions. Again, internalization was quantified by FACS analysis. As negative controls, non-treated cells and cells incubated with carboxyfluorescein alone (data not shown) were analysed. As expected, uptake of CF-SAP, CF-hCT(9-32)-br as well as CF-hCT(9-32) was largely reduced when incubation was performed at 4°C (Fig. 3). Previously, inhibition of endocytosis at 4°C was not only attributed to a blockade of active processes but also to the rigidification of the lipid membrane at this temperature [36]. Therefore, we also tested peptide internalization at 37°C after pre-incubation with NaN_3/2-deoxyglucose, which was expected to impair energy-dependent translocation by ATP depletion. As shown in Fig. 3, internalization of all three peptides was blocked through pre-treatment with NaN_3/2-deoxyglucose, again suggesting endocytic internalization as the underlying translocation mechanism.

It was previously demonstrated that the endocytic translocation of the Tat peptide is triggered by its electrostatic interaction with the negatively charged sulfated proteoglycans of the ECM, as suggested by an inhibitory effect of heparin [37]. Therefore, we examined the

possibility that ECM-based sulfated proteoglycans contribute to the endocytosis of CF-SAP and CF-hCT(9-32)-br. Again, the non-branched CF-hCT(9-32) was used as a control peptide. A marked drop in internalization by about one third was observed with CF-hCT(9-32)-br only. In contrast, the drop was minor with CF-SAP, and absent with CF-hCT(9-32). The difference is likely to result from the high charge density in the cationic NLS domain in the side chain of CF-hCT(9-32)-br versus only one cationic amino acid per VRLPPP unit for the CF-SAP trimer molecule. For the weakly cationic CPP CF-hCT(9-32) carrying one positive charge only no suppression was seen after heparin treatment. The result confirmed the role of sulfated proteoglycans in binding oligocationic CPPs to the ECM and in assisting in their internalization. Nevertheless, interaction with sulfated proteoglycans alone did not appear to be an exclusive prerequisite for the internalization of the oligocationic peptides, CF-SAP and CF-hCT(9-32)-br, since the weakly cationic CPP CF-hCT(9-32) was also internalized in Hela cells. The results indicate contrasting features of internalization between oligocationic and weakly cationic peptides. All endocytosis inhibition studies were also performed qualitatively by CLSM corroborating the above decribed results (data not shown).

No endocytosis via clathrin-coated endosomes – We investigated the endocytic pathway involved in the internalization process of both CF-SAP and CF-hCT(9-32)-br. Transferrin is a well-known marker for its internalization via clathrin-coated pits on the plasma membrane that eventually invaginate and detach from the membrane to form clathrin-coated vesicles. The cargo in those clathrin-coated vesicles undergoes further trafficking to endosomes where sorting to lysosomes may occur [35, 38]. To assess whether this scenario could be the case for the two novel peptides, we performed a colocalization study. CF-SAP, CF-hCT(9-32)-br, respectively, were each coincubated together with TRITC-labeled transferrin in HeLa cells. Fig.4 B shows CLSM micrographs of an overlay of CF-SAP and transferrin, together with related panels of the individual contributions of the peptides and transferrin alone. Predominantly distinct internalization patterns of the peptides and the marker with only minor colocalization were observed that point towards an essentially clathrin-independent endocytosis. A corresponding set of experiments was also performed with CF-hCT(9-32)-br and transferrin. Again the obtained vesicular patterns of both components were mostly distinct from each other with only few colocalized vesicles of CF-hCT(9-32)-br and transferrin (Fig. 4 D). This result excludes a major role of clathrin-mediated endocytosis for the cellular translocation of CF-SAP and CF-hCT(9-32)-br and suggests clathrin-independent uptake mechanisms for these CPPs.

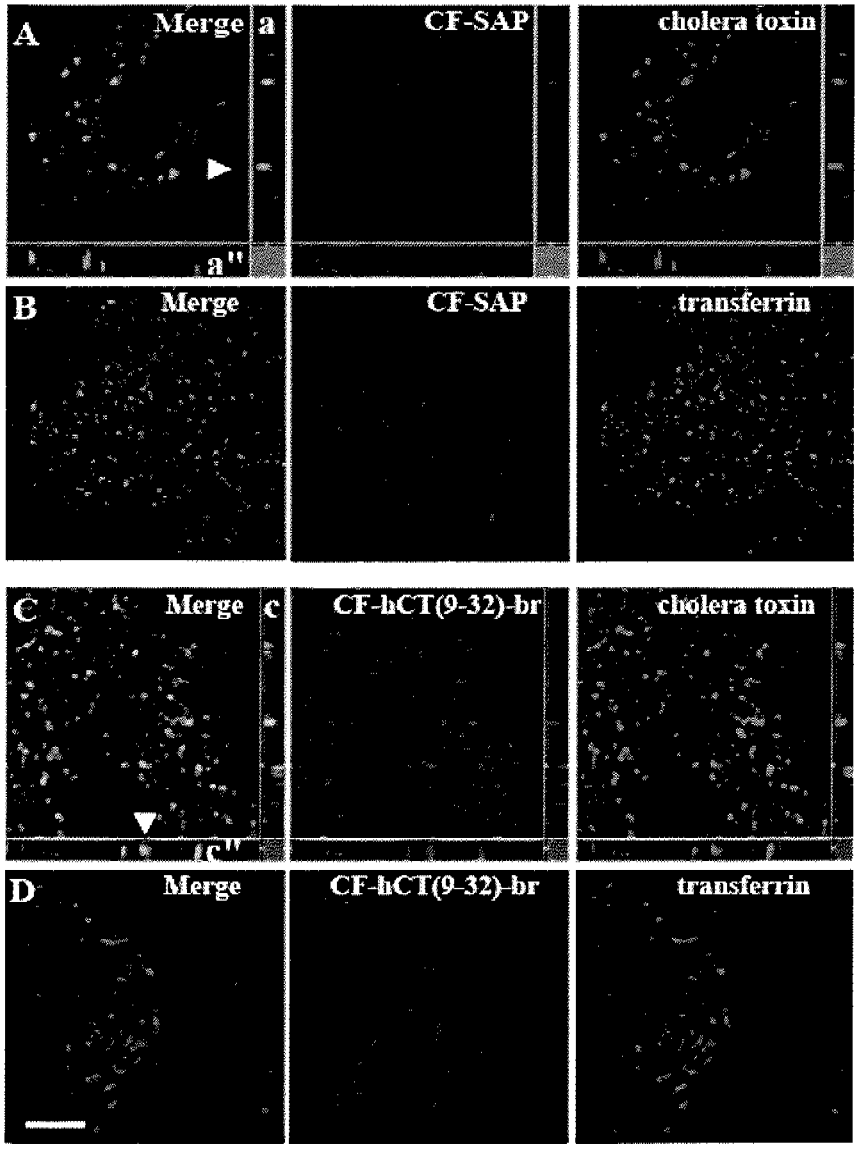

Figure 4. Colocalization study of CF-SAP and CF-hCT(9-32)-br with cholera toxin or transferrin, respectively. Colocalized vesicles in yellow, peptides (CF-SAP or CF-hCT(9-32)-br) in green and endocytosis markers (cholera toxin and transferrin) in red. Cells were incubated with 50 μM CF-SAP or 30 μM CF-hCT(9-32)-br and simultaneously stained with 10 μg/ml cholera toxin or 50 μM transferrin, repectively, for 30 min. Colocalization of both CF-SAP and CF-hCT(9-32)-br with cholera toxin suggests lipid raft-mediated endocytosis (A,C). Negative colocalization with transferrin excludes clathrin-mediated endocytosis (B,D) for both peptides. Panel A - marked colocalization of CF-SAP with cholera toxin after 30 min. Panel B - no colocalization of CF-SAP with transferrin. Panel C - good colocalization of CF-hCT(9-32)-br with cholera toxin; Panel D - no colocalization of CF-hCT(9-32)-br and transferrin. The illustrations a and c are yz-projections whereas a`` and c`` represent the respective xz-projections The scalebar is 5 μm.

Endocytosis occurs via lipid rafts - The involvement of clathrin-coated endosomes in the internalization process of CF-SAP and CF-hCT(9-32)-br was further ruled out by the assessment that both peptides colocalize with cholera toxin. Similar to other microbial toxins, the active fraction of cholera toxin is internalized by a clathrin-independent endocytosis involving lipid rafts [22, 23, 26]. Lipid rafts are cell membrane microdomains enriched in cholesterol and sphingolipids. For this assessment, we tested the colocalization of CF-SAP and CF-hCT(9-32)-br with the labeled B-subunit of cholera toxin. As shown in Fig. 4 A, the predominant fraction of endosomal vesicles proved positive for both CF-SAP and cholera toxin. Further support for the concurrent localization of peptide and marker is also documented in the respective yz- and the xz-sections. For CF-hCT(9-32)-br colocalization with cholera toxin is demonstrated in Fig 4 C. A large fraction of the vesicles proved positive for both the peptide and the marker. Consequently, the data points towards an involvement of lipid raft-mediated endocytosis.

Lipid rafts are defined by their cholesterol enrichment. Methyl-β-cyclodextrin (M-β-CD) extracts cholesterol from cell membranes and, therefore, disrupts lipid rafts whereas it does not disturb clathrin-dependent endocytosis [22, 23, 26, 27]. Thus, to further corroborate our hypothesis of a lipid raft dependent internalization of extracellular CF-SAP and CF-hCT(9-32)-br, we pre-treated HeLa cells with M-β-CD prior to incubation with the peptides. For control CF-hCT(9-32) was also looked at. As shown in Fig. 5A, the intracellular fluorescence was significantly reduced when HeLa cells were pre-treated with M-β-CD. Taken together, our results indicate in a consistent fashion that CF-SAP and CF-hCT(9-32)-br are internalized via clathrin-independent endocytosis involving lipid rafts rather than via a clathrin-mediated pathway. Surprisingly, pretreatment with M-β-CD also reduced the internalization of the weakly cationic control peptide CF-hCT(9-32). To further confirm this outcome, we performed colocalization studies of CF-hCT(9-32) with both cholera toxin and transferrin (Fig. 5B and C). Clearly, colocalization was predominant with cholera toxin, but negligible with transferrin. Prior to colocalization studies with fixed cells, preliminary experiments were performed in unfixed, living cells. The two experimental protocols led to identical vesicular distributions of the two CPPs as well as to identical colocalization patterns with cholera toxin (data not shown). Therefore, we followed a mild fixation protocol with 1% PFA in order to exactly terminate the experiment after 30 min and for better handling.

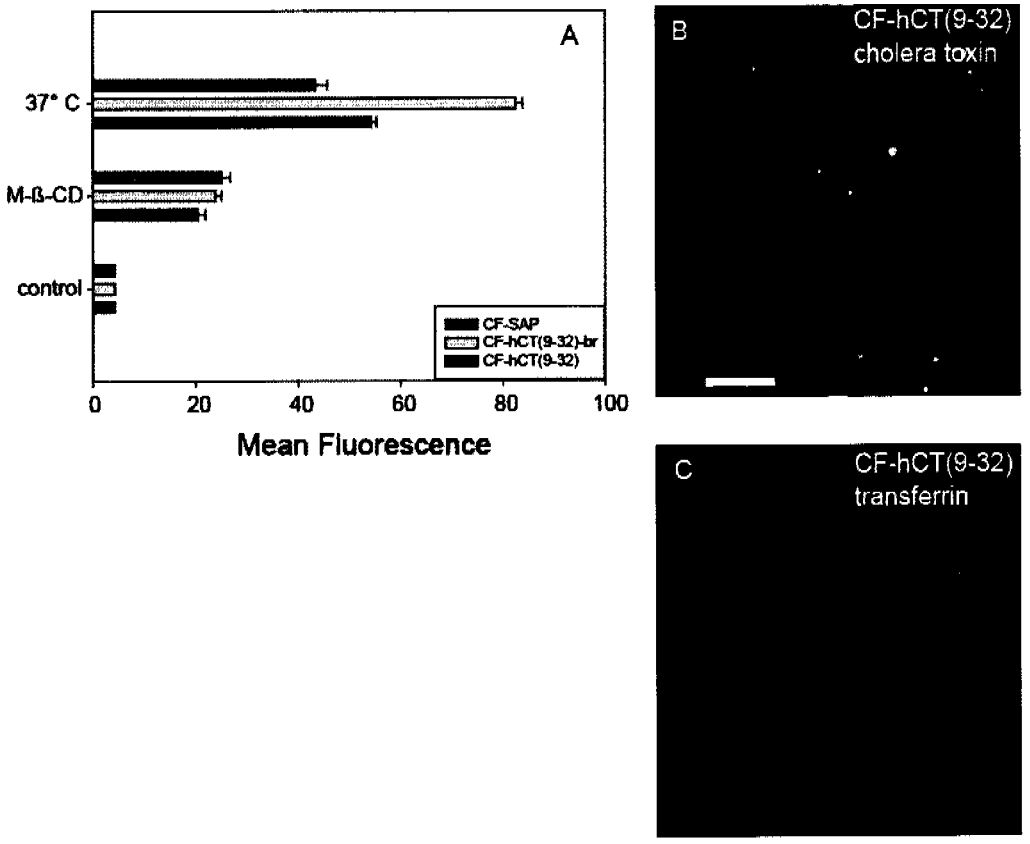

Figure 5. Panel A. Inhibition of lipid raft-mediated endocytosis of CF-SAP, CF-hCT(9-32)-br and CF-hCT(9-32) in HeLa cells as determined by FACS analysis. HeLa cells were incubated for 3 hours at 37°C with 50 μM CF-SAP (black bars), CF-hCT(9-32)-br (light grey bars) or CF-hCT(9-32) (dark grey bars) (both 30 μM). Inhibition of lipid raft-mediated endocytosis was performed by pre-treating cells with 10 mM methyl-β-cyclodextrin (M-β-CD) before incubation with the peptide solutions. Non-treated cells were used as control cells. **Panels B, C. Colocalization of CF-hCT(9-32) with cholera toxin (B) or transferrin (C), respectively.** Colocalized vesicles in yellow, CF-hCT(9-32) in green, and endocytosis markers (cholera toxin and transferrin) in red. Cells were incubated with 30 μM CF-hCT(9-32) and simultaneously stained with 10 μg/ml cholera toxin or 50 μM transferrin, repectively, for 30 min. Panel B - marked colocalization of CF-hCT(9-32) with cholera toxin after 30 min. Panel C - no colocalization of CF-hCT(9-32) with transferrin. The scalebar is 5 μm.

Involvement of early endosomes in the intracellular trafficking pathways of CF-SAP and CF-hCT(9-32)-br - Subsequent to endocytic internalization, vesicles move from the surface of the cell to intracellular compartments within the cytosol where they often undergo complex trafficking and sorting events [35]. To determine whether our peptides were sorted into endosomes before they move to other vesicles, we examined the colocalization of both peptides with the early endosomal antigen 1 (EEA1), a protein associated with early endosomes [39]. The overlay micrographs in Fig. 6 clearly demonstrate the partial colocalization of CF-SAP (Fig. 6A) or CF-hCT(9-32)-br (Fig. 6B), respectively, with EEA1. Therefore, endosomal compartments are concluded to be involved in the uptake and intracellular trafficking of these cationic peptides.

We further carried out a pulse-chase experiment. The pulse referred to a brief peptide incubation period which was then followed by the chase intervall where the cells were exposed to peptide-free medium. Such experiments have been suggested to allow identification of cellular trafficking pathways [35]. After incubating the cells with the appropriate peptide solutions for 30 min, they were washed with PBS and transferred into medium. After a 2.5-hour chase period, we checked for the peptides and performed immunostaining for the presence of EEA1. The overlay (Fig. 6C, D) demonstrated that only few vesicles were still positive for CF-SAP or CF-hCT(9-32)-br, respectively, and EEA1. These leads to the conclusion that after a 3 hours incubation time, major fractions of the two investigated cationic peptides did no longer remain in the early endosome compartments, but may have moved to other compartments within the cytosol.

Subsequently we tested the hypothesis that the peptides may have entered the endoplasmic reticulum or the Golgi network, using a colocalization technique. None of the related experiments yielded unequivocal results, neither in favor nor against this hypothesis (data not shown).

Cell proliferation and viability. As measured by XTT assays, proliferation and cellular viability of HeLa cells were not affected by incubation with hCT(9-32) or hCT(9-32)-br. We tested concentrations up to three times higher than the concentrations used in this study. No relevant reduction of cell viability could be detected (data not shown).

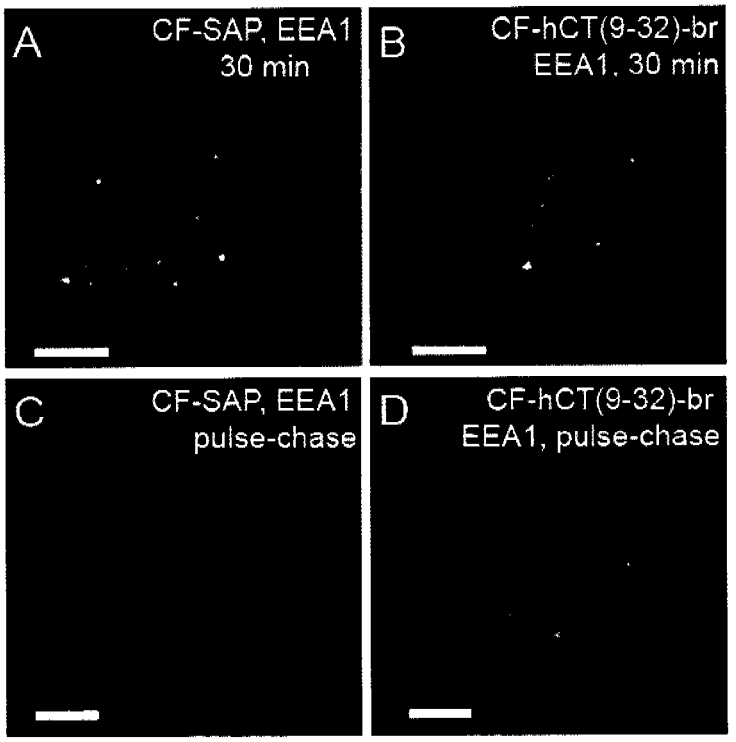

Figure 6. Colocalization of CF-SAP and CF-hCT(9-32)-br with EEA1. Colocalized vesicles are visible in yellow, whereas peptides (CF-SAP or CF-hCT(9-32)-br) are visible in green and endocytosis marker (EEA1) in red. Panel A shows colocalization of CF-SAP (50 μM) with the endosomal endocytosis marker EEA1 (10 μg/ml). Panel B: Merge of 30 μM CF-hCT(9-32)-br and EEA1 (10 μg/ml). Incubation time with peptides was 30 min. Panel C and D represent pulse chase studies of EEA1 and CF-SAP (C) or CF-hCT(9-32)-br (D) with an incubation time with peptides of 30 min followed by a chase period of 2.5 hours. The scalebar is 5 μm.

DISCUSSION

The cell membrane poses a substantial hurdle to the use of pharmacologically active biomacromolecules that are not *per se* actively translocated into cells. To overcome this limitation, a variety of CPPs has been developed [2-4] and evaluated for their ability to deliver therapeutics into cells that otherwise cannot translocate cellular membranes. Because of their highly cationic nature, concerns have been raised as to their cytotoxicity in cell culture experiments [31, 40], in light of a theoretical extrapolation to a clinical scenario.

In recent years, the translocation mechanisms of major CPPs have been controversially discussed, and are not yet fully understood. An early assumption that oligocationic CPPs such as Tat peptides and penetratin translocate via a direct, energy-independent mechanism [2, 3, 15] has been widely questioned and concluded to result from fixation artefacts and other experimental shortcomings. The recent re-evaluation of the involved mechanisms is about to converge into the opposite: an energy-dependent, endocytic uptake mechanism, as demonstrated for Tat and penetratin [16, 17]. More recent studies dissected the endocytic uptake of the Tat peptide in greater detail [41, 42].

To preclude any artefacts through cell fixation in our study, we abstained from fixation of CLSM and FACS samples and performed our experiments in living cells without fixation, except for the colocalization studies where a mild fixation protocol was performed to stop the experiment after an exact time point of 30 min and for better handling conditions. With this protocol, we saw no differences between fixed and unfixed samples as previously also observed by Pichon et al. [43]. Clear distinction between intracellular and membrane bound fluorescence in our FACS experiments was achieved in a twofold way: we (i) digested eventually adsorbed CPPs by trypsinization with trypsin-EDTA [16] and (ii) quenched remaining extracellular fluorescence by Trypan blue [44, 45].

We analysed the uptake mechanism of two novel oligocationic CPPs, CF-SAP [30] [31] [32] and CF-hCT(9-32)-br [29]. Compared with other CPPs, CF-SAP and CF-hCT(9-32)-br may offer several advantages including their good solubility in water, the documented lack of cytotoxicity, and in case of CF-SAP, its nonviral origin [29, 31]. In previous studies, truncated linear sequences of human calcitonin could translocate plasma membranes and demonstrated punctuated vesicular-type, cytoplasmic distribution after incubation [11]. The translocation efficiency of its branched derivative, CF-hCT(9-32)-br, turned out to be superior to the corresponding linear peptide CF-hCT(9-32), used as control peptide in this study. Most probably, the enhancement resulted from the oligocationic NLS sequence in the side chain of CF-hCT(9-32)-br, representing a well known import sequence [46].

For both peptides, CF-SAP and CF-hCT(9-32)-br, we observed marked cellular uptake in HeLa cells with the vesicular distribution pattern in the cytoplasm typical for an endocytic translocation mechanism [47]. Consistent with this finding, translocation occurred through a temperature- and energy-dependent pathway. Uptake occurred at 37°C, but was strongly reduced at 4°C in coincidence with an accumulation of peptide on the cell surfaces forming small patches, presumably membrane-associated aggregates. Consistent with this

observation is that ATP depletion impaired the translocation of both CF-SAP and CF-hCT(9-32)-br in HeLa cells.

Addition of heparin reduced the translocation rate in a way that correlated with their content of cationic amino acids, in that inhibition was much more efficient with CF-hCT(9-32)-br than with the less cationic CF-SAP. This supports the assumption that the primary interaction of the two peptides with the cell surface occurred via sulfated proteoglycans of the negatively charged ECM through electrostatic binding. Our observation is in agreement with findings for other oligocationic CPPs [14]. Consistently, the weakly cationic control peptide CF-hCT(9-32) was unaffected by heparin, indicating absence of significant interaction with the ECM.

There are several endocytic pathways for CPPs possible through which trafficking into cytoplasmic compartments may proceed including endocytosis via clathrin-coated pits [19, 20] and endocytosis via lipid rafts [24, 25]. In the present study, we could reveal that the two investigated oligocationic CPPs, CF-SAP and CF-hCT(9-32)-br, were internalized by clathrin-independent endocytosis via lipid rafts. The rationale of our experiments was based on the following considerations: (i) transferrin is a marker for clathrin-mediated endocytosis and is excluded from lipid rafts [24, 25], (ii) the function and organization of lipid rafts is perturbed by depletion of cholesterol from membranes, providing a tool to discriminate between raft- and non raft–dependent processes [22, 23, 27], and (iii) cholera toxin subunit B follows a clathrin-independent pathway from the plasma membrane to the Golgi [22, 23, 26]. Colocalization studies with transferrin gave no indication for an internalization pathway of CF-SAP or CF-hCT(9-32)-br via clathrin-coated pits. Instead we detected marked colocalization of both CF-SAP and CF-hCT(9-32)-br with cholera toxin. This confirms the existence of a clathrin-independent internalization pathway of the two peptides. Further, depletion of cholesterol by methyl-β-cyclodextrin (M-β-CD) [48] drastically reduced the amount of intracellular fluorescence suggesting an involvement of lipid rafts. Taken together, our findings led us to the proposition of both CF-SAP and CF-hCT(9-32)-br being internalized via a clathrin-independent mechanism that originates from plasma membrane lipid rafts. Our findings corroborate with recent observations of other groups on already established cationic peptides revealing comparable clathrin-independent mechanisms to originate from plasma membrane lipid rafts as the underlying translocation mechanisms, namely for Tat fusion proteins [49] and the equally oligocationic antimicrobial peptide LL-37 [50]. Nevertheless, as shown for the unbranched CF-hCT(9-32) control peptide, the lipid raft-mediated pathway is not exclusive for oligocationic peptides. As demonstrated by the

outcome of the M-β-CD inhibition study in combination with cholera toxin colocalization, lipid rafts represent the preferred pathway of uptake even for the weakly cationic CF-hCT(9-32). Remarkably, even with one positive charge only and not subject to significant interaction with the ECM, the cellular access of CF-hCT(9-32) occured via the lipid raft-mediated pathway. This is in disagreement with recent proposals of a mandatory combination of proteoglycan interaction and lipid raft dependent uptake, as proposed for Tat fusion proteins [49] and the human antimicrobial peptide LL-37 [50]. Our results suggest that irrespective of charge and interaction with the ECM, the lipid raft-mediated pathway represents the preferred port of entry for various classes of CPPs and is not exclusive for oligocationic peptides.

On its way into the cell cholera toxin starts by binding the ganglioside GM1 that associates with lipid rafts on the cell surface [24, 51]. Following endocytic internalization, cholera toxin exploits the retrograde pathway and can be found in early and recycling endosomes, the Golgi apparatus and in the endoplasmic reticulum [52-54]. To get insight into the intracellular trafficking pathways of CF-SAP and CF-hCT(9-32)-br and to determine whether these peptides are sorted in endosomes before they move to other vesicles, we performed colocalization studies with the early endosomal antigen 1 (EEA1), a protein associated with early endosomes. The overlay revealed that early endosomes are involved in the uptake and initial intracellular trafficking of the two oligocationic peptides. Additionally, from the result of a pulse-chase study, we conclude that after an incubation time of three hours, most of the internalized CF-SAP or CF-hCT(9-32)-br was no longer present in early endosomes but moved to other compartments within the cytosol or was metabolically degraded. Studies on the metabolic stability of the two peptides revealed pronounced stability of CF-SAP excluding metabolic degradation as an explanation of poor endosomal retention (C. Foerg, unpublished data). Equipped with an endosomal cleavage site in the side chain, CF-hCT(9-32)-br revealed a significantly lower metabolic stability (C. Foerg, unpublished data). Therefore, as an alternative, high susceptibility to intracellular proteases in combination with endosomal escape of the generated fragments may explain the loss of endosomal fluorescence observed with CF-hCT(9-32)-br.

Fischer et al. hypothesized about the involvement of a retrograde pathway in cellular trafficking of cationic CPPs [41] via the Golgi apparatus to the cytosol. In the current study, however, we could not visualize CF-SAP or CF-hCT(9-32)-br beyond endosomal vesicles, such as in the Golgi or in the endoplasmic reticulum. This could possibly indicate that translocation occurs with a minor fraction of the internalized molecules only, as it was also

the case for ricin [55]. For the further development of efficient CPPs it will be of crucial importance to dissect the intracellular trafficking pathways further and to determine the final cellular target compartment(s) of each CPP. Preliminary data from our group (C. Foerg, unpublished data) suggest that cellular translocation is highly cell type specific, and that the stage of proliferation has an important impact on CPP translocation rates and mechanisms. In parallel to the tightening of the paracellular barrier formed by the tight-junctional complex, confluency and cellular differentiation appear to evoke tighter plasma membrane barriers against CPPs, and result in lower translocation rates. This phenomenon is subject to further studies in our laboratories at the moment.

ACKNOWLEDGEMENTS

The authors acknowledge the following contributions: Professor Heidi Wunderli-Allenspach (ETH Zurich) for the opportunity to use the confocal laser scanning microscope; Dr. Annette Koch for help and advice with the cell studies and Dr. Jack Rohrer for providing antibodies.

REFERENCES

1. Kueltzo, L.A. and C.R. Middaugh, *Potential use of non-classical pathways for the transport of macromolecular drugs.* Expert Opin Investig Drugs, 2000. **9**(9): p. 2039-50.
2. Derossi, D., et al., *The third helix of the Antennapedia homeodomain translocates through biological membranes.* J Biol Chem, 1994. **269**(14): p. 10444-50.
3. Vives, E., P. Brodin, and B. Lebleu, *A truncated HIV-1 Tat protein basic domain rapidly translocates through the plasma membrane and accumulates in the cell nucleus.* J Biol Chem, 1997. **272**(25): p. 16010-7.
4. Futaki, S., *Arginine-rich peptides: potential for intracellular delivery of macromolecules and the mystery of the translocation mechanisms.* Int J Pharm, 2002. **245**(1-2): p. 1-7.
5. Prochiantz, A., *Getting hydrophilic compounds into cells: lessons from homeopeptides.* Curr Opin Neurobiol, 1996. **6**(5): p. 629-34.
6. Schwarze, S.R., et al., *In vivo protein transduction: delivery of a biologically active protein into the mouse.* Science, 1999. **285**(5433): p. 1569-72.
7. Astriab-Fisher, A., et al., *Conjugates of antisense oligonucleotides with the Tat and antennapedia cell-penetrating peptides: effects on cellular uptake, binding to target sequences, and biologic actions.* Pharm Res, 2002. **19**(6): p. 744-54.

8. Singh, D., et al., *Peptide-based intracellular shuttle able to facilitate gene transfer in mammalian cells.* Bioconjug Chem, 1999. **10**(5): p. 745-54.
9. Pooga, M., et al., *Cell penetrating PNA constructs regulate galanin receptor levels and modify pain transmission in vivo.* Nat Biotechnol, 1998. **16**(9): p. 857-61.
10. Lewin, M., et al., *Tat peptide-derivatized magnetic nanoparticles allow in vivo tracking and recovery of progenitor cells.* Nat Biotechnol, 2000. **18**(4): p. 410-4.
11. Trehin, R., et al., *Cellular internalization of human calcitonin derived peptides in MDCK monolayers: a comparative study with Tat(47-57) and penetratin(43-58).* Pharm Res, 2004. **21**(1): p. 33-42.
12. Trehin, R.K., U.; Beck-Sickinger, A.; Merkle, H.P.; Moerck Nielsen, H., *Cellular Uptake but low Permeation of Human Calcitonin Derived Cell Penetrating Peptides and Tat(47-57) through Well-Differentiated Epithelial Models.* Pharm Res, 2004.
13. Futaki, S., et al., *Arginine-rich peptides. An abundant source of membrane-permeable peptides having potential as carriers for intracellular protein delivery.* J Biol Chem, 2001. **276**(8): p. 5836-40.
14. Suzuki, T., et al., *Possible existence of common internalization mechanisms among arginine-rich peptides.* J Biol Chem, 2002. **277**(4): p. 2437-43.
15. Derossi, D., et al., *Cell internalization of the third helix of the Antennapedia homeodomain is receptor-independent.* J Biol Chem, 1996. **271**(30): p. 18188-93.
16. Richard, J.P., et al., *Cell-penetrating peptides. A reevaluation of the mechanism of cellular uptake.* J Biol Chem, 2003. **278**(1): p. 585-90.
17. Drin, G., et al., *Studies on the internalization mechanism of cationic cell-penetrating peptides.* J Biol Chem, 2003. **278**(33): p. 31192-201.
18. Console, S., et al., *Antennapedia and HIV transactivator of transcription (TAT) "protein transduction domains" promote endocytosis of high molecular weight cargo upon binding to cell surface glycosaminoglycans.* J Biol Chem, 2003. **278**(37): p. 35109-14.
19. Vendeville, A., et al., *HIV-1 Tat enters T cells using coated pits before translocating from acidified endosomes and eliciting biological responses.* Mol Biol Cell, 2004. **15**(5): p. 2347-60.
20. Schmid, S.L., *Clathrin-coated vesicle formation and protein sorting: an integrated process.* Annu Rev Biochem, 1997. **66**: p. 511-48.

21. Pelkmans, L., J. Kartenbeck, and A. Helenius, *Caveolar endocytosis of simian virus 40 reveals a new two-step vesicular-transport pathway to the ER.* Nat Cell Biol, 2001. **3**(5): p. 473-83.

22. Puri, V., et al., *Clathrin-dependent and -independent internalization of plasma membrane sphingolipids initiates two Golgi targeting pathways.* J Cell Biol, 2001. **154**(3): p. 535-47.

23. Nichols, B.J., et al., *Rapid cycling of lipid raft markers between the cell surface and Golgi complex.* J Cell Biol, 2001. **153**(3): p. 529-41.

24. Simons, K. and E. Ikonen, *Functional rafts in cell membranes.* Nature, 1997. **387**(6633): p. 569-72.

25. Brown, D.A. and E. London, *Functions of lipid rafts in biological membranes.* Annu Rev Cell Dev Biol, 1998. **14**: p. 111-36.

26. Orlandi, P.A. and P.H. Fishman, *Filipin-dependent inhibition of cholera toxin: evidence for toxin internalization and activation through caveolae-like domains.* J Cell Biol, 1998. **141**(4): p. 905-15.

27. Lamaze, C., et al., *Interleukin 2 receptors and detergent-resistant membrane domains define a clathrin-independent endocytic pathway.* Mol Cell, 2001. **7**(3): p. 661-71.

28. Simons, K. and D. Toomre, *Lipid rafts and signal transduction.* Nat Rev Mol Cell Biol, 2000. **1**(1): p. 31-9.

29. Krauss, U., et al., *In vitro gene delivery by a novel human calcitonin (hCT)-derived carrier peptide.* Bioorg Med Chem Lett, 2004. **14**(1): p. 51-4.

30. Crespo, L., et al., *Peptide dendrimers based on polyproline helices.* J Am Chem Soc, 2002. **124**(30): p. 8876-83.

31. Fernandez-Carneado, J., et al., *Potential Peptide Carriers: Amphipathic Proline-Rich Peptides Derived from the N-Terminal Domain of gamma-Zein.* Angew Chem Int Ed Engl, 2004. **43**(14): p. 1811-1814.

32. Fernandez-Carneado, J., et al., *Amphipathic peptides and drug delivery.* Biopolymers, 2004. **76**(2): p. 196-203.

33. Roehm, N.W., et al., *An improved colorimetric assay for cell proliferation and viability utilizing the tetrazolium salt XTT.* J Immunol Methods, 1991. **142**(2): p. 257-65.

34. Rothen-Rutishauser, B., et al., *MDCK cell cultures as an epithelial in vitro model: cytoskeleton and tight junctions as indicators for the definition of age-related stages by confocal microscopy.* Pharm Res, 1998. **15**(7): p. 964-71.

35. Karp, G., *Cell and Molecular Biology*. 2nd ed. 1999: John Wiley & Sons, Inc. 292-325.

36. Letoha, T., et al., *Membrane translocation of penetratin and its derivatives in different cell lines.* J Mol Recognit, 2003. **16**(5): p. 272-9.

37. Tyagi, M., et al., *Internalization of HIV-1 tat requires cell surface heparan sulfate proteoglycans.* J Biol Chem, 2001. **276**(5): p. 3254-61.

38. Pelkmans, L. and A. Helenius, *Endocytosis via caveolae.* Traffic, 2002. **3**(5): p. 311-20.

39. Mu, F.T., et al., *EEA1, an early endosome-associated protein. EEA1 is a conserved alpha-helical peripheral membrane protein flanked by cysteine "fingers" and contains a calmodulin-binding IQ motif.* J Biol Chem, 1995. **270**(22): p. 13503-11.

40. M. Pooga, A.E., Ü. Langel, *Cell-penetratin peptides, Processes and applications.* 2002, Boca Raton, FL: CRC Press. 245-261.

41. Fischer, R., et al., *A stepwise dissection of the intracellular fate of cationic cell-penetrating peptides.* J Biol Chem, 2004. **279**(13): p. 12625-35.

42. Wadia, J.S., R.V. Stan, and S.F. Dowdy, *Transducible TAT-HA fusogenic peptide enhances escape of TAT-fusion proteins after lipid raft macropinocytosis.* Nat Med, 2004. **10**(3): p. 310-5.

43. Pichon, C., M. Monsigny, and A.C. Roche, *Intracellular localization of oligonucleotides: influence of fixative protocols.* Antisense Nucleic Acid Drug Dev, 1999. **9**(1): p. 89-93.

44. Innes, N.P. and G.R. Ogden, *A technique for the study of endocytosis in human oral epithelial cells.* Arch Oral Biol, 1999. **44**(6): p. 519-23.

45. Hed, J., et al., *The use of fluorescence quenching in flow cytofluorometry to measure the attachment and ingestion phases in phagocytosis in peripheral blood without prior cell separation.* J Immunol Methods, 1987. **101**(1): p. 119-25.

46. Ragin, A.D., R.A. Morgan, and J. Chmielewski, *Cellular import mediated by nuclear localization signal Peptide sequences.* Chem Biol, 2002. **9**(8): p. 943-8.

47. Mann, D.A. and A.D. Frankel, *Endocytosis and targeting of exogenous HIV-1 Tat protein.* Embo J, 1991. **10**(7): p. 1733-9.

48. Ikonen, E., *Roles of lipid rafts in membrane transport.* Curr Opin Cell Biol, 2001. **13**(4): p. 470-7.

49. Fittipaldi, A., et al., *Cell membrane lipid rafts mediate caveolar endocytosis of HIV-1 Tat fusion proteins.* J Biol Chem, 2003. **278**(36): p. 34141-9.

50. Sandgren, S., et al., *The human antimicrobial peptide LL-37 transfers extracellular DNA plasmid to the nuclear compartment of mammalian cells via lipid rafts and proteoglycan-dependent endocytosis.* J Biol Chem, 2004. **279**(17): p. 17951-6.

51. Spangler, B.D., *Structure and function of cholera toxin and the related Escherichia coli heat-labile enterotoxin.* Microbiol Rev, 1992. **56**(4): p. 622-47.

52. Richards, A.A., et al., *Inhibitors of COP-mediated transport and cholera toxin action inhibit simian virus 40 infection.* Mol Biol Cell, 2002. **13**(5): p. 1750-64.

53. Majoul, I., et al., *Fluorescence resonance energy transfer analysis of protein-protein interactions in single living cells by multifocal multiphoton microscopy.* J Biotechnol, 2002. **82**(3): p. 267-77.

54. Majoul, I., et al., *KDEL receptor (Erd2p)-mediated retrograde transport of the cholera toxin A subunit from the Golgi involves COPI, p23, and the COOH terminus of Erd2p.* J Cell Biol, 1998. **143**(3): p. 601-12.

55. Rapak, A., P.O. Falnes, and S. Olsnes, *Retrograde transport of mutant ricin to the endoplasmic reticulum with subsequent translocation to cytosol.* Proc Natl Acad Sci U S A, 1997. **94**(8): p. 3783-8.

CHAPTER III

Metabolic cleavage and translocation efficiency of selected cell penetrating peptides: a comparative study with epithelial cell cultures

Christina Foerg[1†], Kathrin M. Weller[1†], Helene Rechsteiner[2], Hanne M. Nielsen[3], Jimena Fernández-Carneado[4], René Brunisholz[2], Ernest Giralt[4,5], Hans P. Merkle[1]

[1]Department of Chemistry and Applied Biosciences, Institute of Pharmaceutical Sciences, ETH Zurich, Switzerland,

[2]Institute of Molecular Biology and Biophysics, ETH Zurich, Switzerland,

[3]Department of Pharmaceutics and Analytical Chemistry, The Danish University of Pharmaceutical Sciences, Copenhagen, Denmark,

[4]Institut de Recerca Biomèdica de Barcelona, Parc Científic de Barcelona, Spain,

[5]Departament de Química Orgànica, Universitat de Barcelona, Spain

[†] Both authors contributed equally to the present work.

ABSTRACT

We investigated the metabolic stability of four cell penetrating peptides (CPPs), namely SAP, hCT(9-32)-br, [Pα] and [Pβ], when in contact with three epithelial cell cultures, consisting of either subconfluent HeLa or confluent MDCK or Calu-3 cells. Additionally, through analysis of their cellular translocation, we were interested in revealing possible relations between metabolic stability and translocation efficiency. Metabolic degradation kinetics of the CPPs was assessed using RP-HPLC, and their metabolites were identified by MALDI-TOF mass spectrometry. Translocation efficiencies were determined using fluorescence-activated cell sorting (FACS) and confocal laser scanning microscopy (CLSM) based on ligated fluorescence markers (CF and IAF). Between HeLa, MDCK and Calu-3 we found the levels of proteolytic activities to be highly variable. However, for each peptide, the individual patterns of metabolic degradation were quite similar. The metabolic stability of the investigated CPPs was in the order of CF-SAP = CF-hCT(9-32)-br > [Pβ]–IAF > [Pα]. We were further able to identify specific cleavage sites for each of the four peptides. For all investigated CPPs, we observed higher translocation efficiencies into HeLa cells as compared to MDCK and Calu-3, corresponding to the lower state of differentiation of HeLa cell cultures. For the four CPPs, there was no direct relation between metabolic stability and translocation efficiency. These results indicate that metabolic stability is not a main limiting factor for efficient cellular translocation. Nevertheless, translocation of individual CPPs may be improved by structural modifications aiming at increased metabolic stability.

INTRODUCTION

The appealing prospects of peptide, protein and nucleic acid therapeutics has made the delivery of large and hydrophilic molecules across the plasma membrane into the cytoplasm and to cellular organelles a vital issue for current and future drug development. Owing to the barrier properties of the plasma membrane, the cellular uptake of such biopolymers is inherently poor, necessitating the development of efficient delivery vectors. Hence, chemical ligation or physical assembly of biopolymers of poor cellular accessibility with so-called cell penetrating peptides (CPPs) has turned into a prime topic in the biomedical engineering of delivery systems that are hoped to mediate the non-invasive import of such therapeutics into cells [1-8].

A major obstacle to CPP mediated drug delivery consists in the often rapid metabolic clearance of the peptides when in contact or passing the enzymatic barriers of epithelia and endothelia [9]. Prior to release of the cargo at its destination, cell penetrating peptides should be sufficiently stable when carrying the chemically ligated or physically complexed cargo across the barrier. Nevertheless, to date information on the momentous subjects of enzymatic stability and degradation of CPPs is rare [10-14]. For instance, the stability of pVEC, a CPP derived from murine vascular endothelial cadherin, was previously assessed by Langel and coworkers [10, 11]. pVEC was rapidly degraded when incubated with human aorta endothelial cells and murine A9 fibroblasts. By contrast, when replacing the L-amino-acid residues of its sequence by their non-natural D-counterparts, pVEC was no longer susceptible to degradation, without losing its translocating properties [10]. Another related study focused on the metabolic stability of transportan, the transportan analogue transportan 1, and penetratin, revealing transportan as the most stable and penetratin as the least metabolically stable peptide among the three CPPs [13]. Moreover, we analyzed the metabolic degradation kinetics and the cleavage patterns of selected CPPs, namely human calcitonin (hCT) derived peptides, Tat(47-57) and penetratin(43-58) by incubation with three epithelial models, MDCK, Calu-3 and TR 146 cell layers [14]. The proteolytic activities among the different epithelial models and the CPPs were highly variable. Yet the individual patterns between the three models for the metabolic degradation of each peptide were quite similar.

In the present study, we envisaged to explore a potential relation between the metabolic stability of CPPs and their translocation capacity. To this end we focused on (i) metabolic degradation kinetics and cleavage patterns of four oligocationic CPPs when in contact with epithelial cell cultures, and on (ii) their cellular uptake. We used cultures from three epithelial cell lines, HeLa [15], MDCK [16] and Calu-3 cells [17]. All four investigated CPPs represent

more recent discoveries in the field. Their sequences are listed in Table 1: The first one is the carboxyfluorescein (CF) labeled linear proline-rich sweet arrow peptide CF-SAP, a linear trimer of repetitive VRLPPP domains, and designed as an amphipathic version of a polyproline sequence related to γ-zein, a storage protein of maize [18-20]. Another one is a branched modification of the previously reported linear human calcitonin (hCT) derived, equally CF labeled CPP; namely CF-hCT(9-32) [21], denoted as CF-hCT(9-32)-br [22], that carries the oligocationic, SV40 large T antigen in the form of a side-branch to the main peptide chain. Previous studies revealed that both CF-SAP and CF-hCT(9-32)-br , non-toxic peptides even in higher concentrations, were readily translocated into HeLa cells as triggered by interaction with the negatively charged extracellular matrix and followed by lipid raft-mediated endocytosis [23]. Next, [Pβ]-IAF, carrying the C-terminal iodoacetamido-fluorescein (IAF) fluorescence marker, combines the hydrophobic fusion peptide of HIV-1 gp41 and the oligocationic sequence of SV40 large T antigen. It was originally synthesized by Vidal et al. [24] and has been previously demonstrated to deliver oligonucleotides into cultured cells [25]. To directly monitor its cellular uptake, the peptide was C-terminally labeled with IAF. Finally, [Pα], has been developed through amino acid modifications of [Pβ] in five positions, aiming at an α-helical structure [20, 26]. Deshayes et al [27] previously reported about its high affinity for membranes and its secondary structure required for uptake. The near negligible toxicity of [Pα] and [Pβ] has been reported by Fernandez et al. [19].

CF-SAP and CF-hCT(9-32)-br demonstrated marked metabolic stability under all experimental conditions, whereas, in contrast, [Pα] and [Pβ]-IAF showed drastic enzymatic degradation, and decomposed quickly even when incubated in serum free medium. Moreover, we were able to identify specific cleavage sites for each of the four peptides. Emphasizing the relevance of the chosen cellular models, we found the uptake efficiencies of all four CPPs to be strongly cell line dependent. Interestingly, despite their high enzymatic stability, CF-SAP and CF-hCT(9-32)-br showed only low translocation rates into well differentiated cell layers. This excludes enzymatic degradation to represent a main factor that limits cellular translocation. Nevertheless, with respect to [Pα] and [Pβ]-IAF, improved stability through structure modification cannot be excluded to enhance their performance as CPPs.

Table 1

Amino acid sequences and molecular weights of the investigated CF and IAF modified CPPs.

Name	Sequence[a]	MW[b] (Da)
CF-SAP	CF-V**R**LPPP-V**R**LPPP-V**R**LPPP	2356
CF-hCT(9-32)-br	CF-LGTYTQDFNKFHTFPQTAIGVGAP-NH_2 | AFGVGPDEV**KRKKK**P-NH_2	4606
[Pα]	Ac-GALFLAFLAAALSLMGL-WSQ-P**KKKRK**V-Cya	3047
[Pα]-IAF	Ac-GALFLAFLAAALSLMGL-WSQ-P**KKKRK**V-Cya-IAF	3434
[Pβ]-IAF	Ac-GALFLGFLGAAGSTMGA-WSQ-P**KKKRK**V-Cya-IAF	3296

[a]basic aa are indicated in bold

[b]calculated molecular weight of the peptides

MATERIALS AND METHODS

Materials.

HeLa and Calu-3 cells were obtained from American Type Culture Collection ATCC (Rockville, MD, USA). The MDCK cell line (low resistance, type II) was a gift from the Biopharmacy group of ETH Zurich (Switzerland) [28]. Cell culture media, trypsin-EDTA, penicillin, streptomycin and Hanks Balanced Salt Solution (HBSS) were from Gibco (Paisley, USA). Fetal calf serum (FCS) was either obtained from HyClone (Logan, Utah, USA) or from Fisher Scientific (Wohlen; Switzerland) and Hoechst 33342 from Molecular Probes (Leiden, Netherlands). Cell culturing flasks 25 cm^2 were from TPP (Trasadingen, Switzerland). Cell culture inserts (polyethylene terephthalate (PET), 0.4 μm pore size, 1.6 x 10^6 pores/cm^2, 0.9 cm^2 growth area), companion 12 well plates, 24 well plates and 5 ml polypropylene round-bottom tubes (FACS tubes) were purchased from Falcon (Becton Dickinson Labware, Franklin Lakes, NJ, USA). 96 well plates and 8 well glass chamber slides were obtained from Nunc (Roskilde, Denmark). Aqueous 0.4% Trypan blue solution with 0.81% sodium chloride and 0.06% potassium phosphate, DMSO and 5(6)-carboxyfluorescein (CF) were purchased

from Fluka (Buchs, Switzerland), and Bradford reagent from Sigma (St. Louis, MO, USA). α-cyano-4-hydroxy-cinnamic acid was obtained from Agilent Technologies (Burnsville, Minnesota, USA), ZipTip from Millipore (Bedford, MA, USA).

Peptides. The investigated CPPs are listed in Table 1. N-terminally CF-labeled sweet arrow peptide, CF-SAP, was synthesised by solid-phase peptide synthesis on a 2-chlorotrityl resin following the 9-fluorenyl methoxy carbonyl/*tert*-butyl strategy prior to labeling with 5(6)-carboxyfluorescein [19]. The branched human calcitonin (hCT) derived CPP, N-terminally labeled with 5(6)-carboxyfluorescein (CF), CF-hCT(9-32)-br, was synthesized by the peptide synthesis unit of the University of Barcelona (Spain). CF-hCT(9-32)-br derives from the linear hCT(9-32) CPP [14, 21] and was equipped with the oligocationic SV40 large T antigen in the side chain of K_{18} [22]. [Pα] and C-terminally 5-(iodoacetamido)-fluorescein (IAF) labeled [Pα], [Pα]–IAF, as well as C-terminally IAF labeled [Pβ], [Pβ]-IAF , were obtained from NMI TT GmbH (Reutlingen, Germany). Common structural elements of [Pα], [Pα]-IAF and [Pβ]-IAF are a non-polar HIV derived sequence, HIV-1 gp41, and the polar, oligocationic sequence of SV40 large T antigen, KKKRKV, connected via a self-fluorescent WSQP spacer [20, 25, 34, 35]. Owing to the poor aqueous solubility of the IAF-labeled [Pα]-IAF, we analyzed its metabolism kinetics with unlabeled [Pα] which was sufficiently soluble. However, for FACS and CLSM, which required more sensitive fluorescence detection, we used [Pα]-IAF expecting translocation to occur with dissolved peptide only.

Cell culture. Cells were cultured under standard conditions in 25 cm^2 culture flasks at 37°C and 5% CO_2. HeLa and Calu-3 cells were maintained in Dulbecco's modified Eagle medium (DMEM), MDCK cells in minimum essential medium with Earl's salts (MEM). Media contained 10% heat-inactivated FCS and 1% penicillin/streptomycin. Each cell line was used within a range of 10 consecutive passage numbers (HeLa: 9-15; MDCK: 225–235; Calu-3: 36–42).

Confocal laser scanning microscopy (CLSM) of cellular uptake. We investigated the cellular uptake of fluorescently labeled CPPs by CLSM. HeLa cells were seeded onto 8 well glass chamber slides at a density of 40'000 cells/cm^2 and were used one day after seeding as exponentially growing, subconfluent cells. MDCK and Calu-3 cells were seeded at a constant density of 20'000 or 50'000 cells/cm^2, respectively and were used at day 10 or 16, respectively, as fully confluent monolayers. For uptake experiments, cells were incubated in

150 µl serum free medium containing fluorescently labeled CPPs or unconjugated fluorophore at a concentration of 20 µM for 2 hours under standard cell culture conditions. We used 2 mM stock solutions of CPPs or unconjugated fluorophore, respectively, in DMSO that were further diluted with serum free medium to obtain a final concentration of 20 µM. For the last 30 minutes of incubation, Hoechst 33342 was added for nuclear staining at a final concentration of 1 µg/ml. Prior to microscopy, cells were rinsed 3 times with HBSS buffer and overlaid with HBSS buffer. To avoid fixation artefacts, we abstained from any fixation of the samples [36]. Additionally, to avoid misinterpretation due to extracellular fluorescence bound to cell membranes or working materials, half of the volume was replaced with aqueous 0.4% Trypan blue solution. Trypan blue is unable to translocate intact cell membranes which makes it a selective quencher for extracellularly bound fluorescence [37-39]. Cells were then scanned using a Zeiss CLSM 410 inverted microscope. Image processing was performed with Imaris, a 3D multi-channel image processing software for confocal microscope images (Bitplane, Zurich, Switzerland).

Quantification of CPP translocation by fluorescence activated cell sorting (FACS). We used FACS analysis to quantify the translocation of fluorescently labeled CPPs. As with CLSM, HeLa cells were seeded onto 24 well plates at a density of 40'000 cells/cm^2 and were used one day after seeding as exponentially growing cells. MDCK and Calu-3 cells were seeded at a constant density of 20'000 or 50'000 cells/cm^2, respectively and were used at day 10 or 16, respectively, as fully confluent monolayers. For uptake experiments, cells were incubated in 250 µl serum free medium containing fluorescently labeled CPPs or unconjugated fluorophore at a concentration of 20 µM for 2 hours under standard cell culture conditions. Prior to dilution with serum free medium, 2 mM stock solutions of the respective CPP or unconjugated dye in DMSO were prepared. After incubation, all cells were extensively washed with PBS buffer. To cleave adhering CPPs from the cell membranes and to detach the cells from the well plates, HeLa cells were trypsinized for 5 minutes, MDCK and Calu-3 cells for 15 minutes, as adapted from the literature [36, 40]. Cells were then transferred into FACS tubes and washed once with PBS prior to further analysis. Half of the volume was replaced with aqueous 0.4% Trypan blue solution to quench extracellular CPPs [41, 42]. Cells were analyzed by FACS on a FacsCalibur (BectonDickinson, Franklin Lakes, NJ) within one hour after trypsinization. A total of 8'000 gated cells per sample was counted. Data were analyzed using Cytomation Summit software (Cytomation Inc., Fort Collins, USA).

CPP stability in serum free medium. We used 2 mM stock solutions of CPPs or unconjugated fluorophore, respectively, in DMSO that were further diluted with serum free medium to a final concentration of 20 µM. Tightly closed and protected against light, the tubes were incubated for 21 days at 37°C under mechanical shaking (150 min^{-1}). Every second or third day, a sample of 50 µl was withdrawn from each tube and analyzed by RP-HPLC and MALDI-TOF MS.

Metabolism kinetics of CPPs in contact with cell cultures - RP-HPLC. HeLa and MDCK cells were seeded and cultivated as described above for FACS studies. Calu-3 cells were plated onto filter supports at a constant density of 100'000 cells/cm^2. After the cells had attached to the filter overnight, the medium was removed from the apical compartment to allow the monolayer to grow at the air interface. Prior to metabolic degradation, Calu-3 cells were equilibrated for 30 min at 37°C with serum free medium in order to adjust the apical side to the experimental conditions. 20 µM of each of the investigated CPPs were dissolved in the respective medium and added to the apical side. Mechanical shaking at 150 min^{-1} was applied to minimize the thickness of the aqueous boundary layer. Samples of 50 µl were taken from the apical compartment after 1 and 30 min, and 1, 2, 3, 4, 6 and 8 h incubation for HeLa and MDCK cells, and after 1, 15, 30 and 45 min, and 1, 2, 3, and 8 h incubation for Calu-3 monolayers. As controls, HeLa, MDCK or Calu-3 cells were incubated with peptide-free medium and samples were taken as described above. Immediately after taking the samples, 2.5 µl acetic acid (3.7 M) was added in order to stop enzyme activity [43]. Determination of the respective half-lives was by RP-HPLC. Throughout, we used a Merck-Hitachi RP-HPLC (VWR International, Dietikon, Switzerland). In order to improve analytical sensitivity, degradation of CF-SAP, CF-hCT(9-32)-br and [Pβ]-IAF was monitored by fluorescence detection of the labels. Accordingly, detection was limited to intact fluorescently labeled peptides and their N- or C-terminal metabolites carrying the N- or C-terminally ligated fluorophore, respectively. Fluorescence was excitated at 492 nm and detected at 517 nm. Due to the insufficient solubility of labeled [Pα]–IAF, unlabeled [Pα] was used for analysis of metabolism kinetics as the experimental setting did not necessarily require IAF fluorescence detection. Therefore, we performed UV detection at 216 nm, and fluorescence detection of tryptophane at 283 nm for excitation and 350 nm for emission.

RP-HPLC of CPPs was performed as follows: For CF-SAP we used a linear gradient mobile phase starting at 25% solvent A consisting of AcCN:TFA, 99.9:0.1 (v/v) to 25% solvent B

(water:TFA, 99.9:0.1) over 40 min. For CF-hCT(9-32)-br the linear gradient mobile phase was 30% solvent A to 20% solvent B over 20 min. In case of [Pα] the linear gradient mobile phase was 50% solvent A to 0% solvent B over 25 min, and for [Pβ]-IAF 20% solvent A to 20% solvent B over 40 min. An analytical RP-18 column with 250 mm x 4.6 mm, particle size 5 µm, pore diameter 300 Å from Vydac (Hesparia, CA, USA) was applied. The flow rate was 1 ml/min. Peptide concentrations were calculated from the area under the curve. The data were evaluated according to pseudo first-order kinetics. The half-lives of the CPPs, $t_{1/2}$, were calculated according to:

$$t_{1/2} = \frac{\ln 2}{\left[\frac{d(\log C)}{dt}\right]}$$

To account for the difference in the cross sectional area of the cell culture inserts – 2 cm^2 with HeLa and MDCK cells versus 0.9 cm^2 with Calu-3 cells – the experimental half-life values were normalized to 1 cm^2. This approximation was strictly limited to the assumption of linear kinetics for the full concentration range and excluded any enzyme saturation. Also all effects of diffusion kinetics were neglected. All experiments were run in triplicate.

Analysis of cell line specific protein content and cell density. The content of protein per well was assessed for each cell line. For this purpose, seeding conditions of all cell models like density and time of growth were kept as described for the FACS experiments. As described by the manufacturer, cells were lysed and analyzed using a Bradford assay in a 96 well plate by measuring the absorption at 595 nm with a ThermoMax microplate reader (Molecular Device, Sunnyvale, CA, USA). Standard curves were established using BSA dissolved in HBSS. Results were normalized to mg protein per cm^2 cell culture surface.
In order to determine the cell density of each cell line, seeding conditions were kept as described for the FACS experiments. Cells were counted using a haemocytometer (Assistent, Sondheim/Rhön, Germany), and the results were converted into number of cells per cm^2 cell culture surface. All experiments were performed in triplicate.

Identification of metabolites using MALDI-TOF MS. Metabolites emerging from the degradation of the investigated CPPs in contact with the cell cultures were identified by matrix assisted laser desorption ionization time of flight mass spectroscopy (MALDI-TOF

MS) analysis. Samples were directly taken from cell culture incubates. For this purpose, 1 µl samples containing CPPs and/or metabolites were mixed with 2 µl of a saturated matrix solution of α-cyano-4-hydroxy-cinnamic acid. 0.7 µl of this solution was applied to the target plate, allowed to crystallize, and dedusted. CF-SAP, [Pα], and [Pβ]-IAF were analyzed in reflectron mode, CF-hCT(9-32)-br in linear mode. Acquisition mass ranged from 750 to 6000 Da. External calibration was performed with a peptide mix ranging between 900 and 1700 Dalton. All experiments were performed in triplicate. For each of the CPPs in contact with either one of the cell models, one sample per time point was pre-treated in order to desalt the sample and increase the detection limit and accuracy using ZipTip according to the manufacturer's instructions. Analysis was performed on a MALDI-TOF mass spectrometer 4700 Proteomics analyzer type AB347000084 Applied Biosystems (Foster City, USA).

RESULTS

Cell line dependent translocation. To investigate a potential relation between metabolic stability and translocation efficiency of the CPPs in three epithelial cell lines, we determined their rates of translocation. HeLa, MDCK and Calu-3 cell cultures were exposed to either one of the four cationic CPPs: CF-SAP, CF-hCT(9-32)-br, [Pα]-IAF and [Pβ]-IAF. Owing to their strong cationic charge, the CPPs closely sticked to cell membranes rendering direct interpretation of CLSM data difficult (Fig. 1B). As shown in Fig. 1C, Trypan blue efficiently quenched extracellular fluorescence. Therefore, all CLSM studies were strictly performed under Trypan blue quenching.

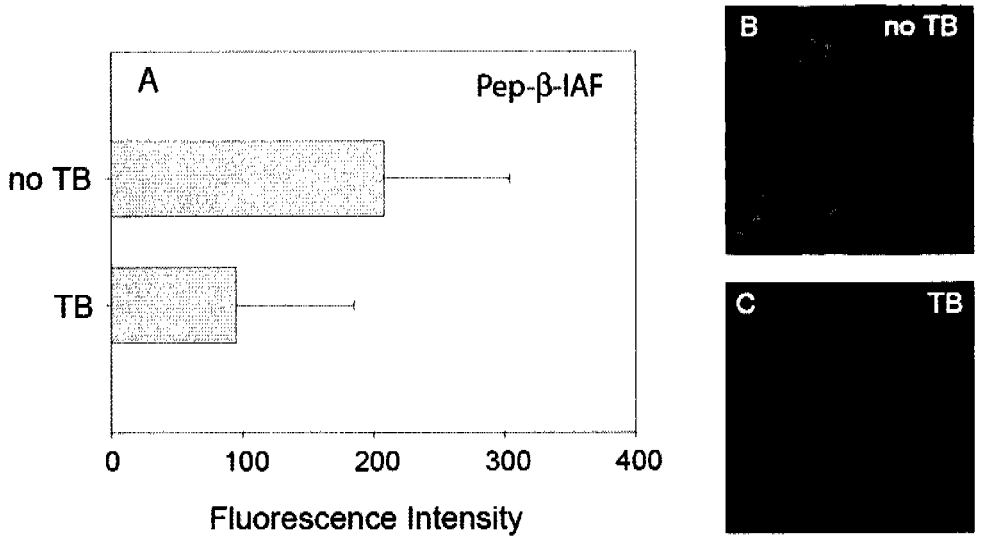

Figure 1

Quenching effect through the addition of Trypan blue. MDCK cells were incubated with [Pβ]-IAF in the absence or in the presence of Trypan blue and analyzed by FACS (A) and CLSM in the absence (B) or in the presence (C) of Trypan blue. Cell nuclei (in blue) were stained with Hoechst 33342. CPPs are displayed in green. Bar = 50 μm.

After incubation for 2 hours at 37°C, there was ready cellular uptake of all four CPPs in non-confluent, proliferating HeLa cells (Fig. 2). As shown in Fig. 2, a significantly lower amount of each of the four CPPs was taken up by the confluent MDCK layers. CF-SAP and CF-hCT(9-32)-br mainly accumulated in the paracellular space between the cells. Obviously, paracellular fluorescence was not accessible to Trypan blue quenching. In the confluent Calu-3 model, none of the four investigated CPPs showed any relevant translocation or accumulated in the paracellular space. Throughout, non-treated cells and cells incubated with the fluorescence marker carboxyfluorescein alone did not show significant intracellular or paracellular fluorescence (data not shown).

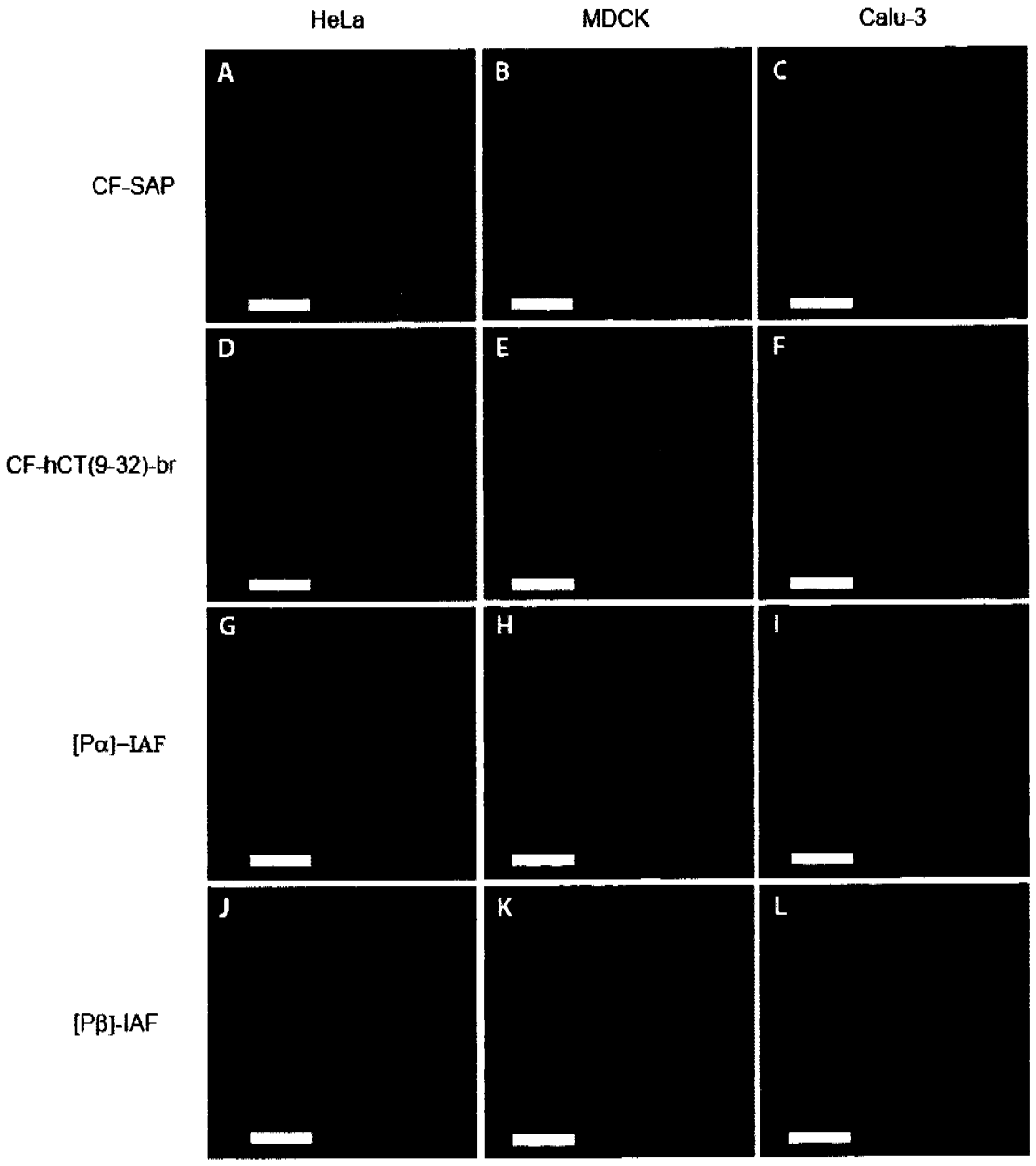

Figure 2

Translocation of CPPs in epithelial cell models. Each of the cell models, HeLa (A, D, G, J), MDCK (B, E, H, K) and Calu-3 (C, F, I, L), was incubated for 2 hours with the investigated CPPs: CF-SAP (A, B, C), CF-hCT(9-32)-br (D, E, F), [Pα]-IAF (G, H, I) or [Pβ]-IAF (J, K, L) and cells were observed by CLSM. Cell nuclei (displayed in blue) were stained with Hoechst 33342. Bar = 50 μm.

Quantification of CPP translocation by FACS analysis. For confirmation and quantification of our CLSM findings, we also tested the rates of translocation by FACS analysis (Fig. 3). Fig. 3A compares the uptake of CF-SAP in the three different cell models. Similar to CLSM data, confluent Calu-3 cells showed rather low rates of translocation. Higher rates were found in confluent MDCK layers, and highest in non-confluent, proliferating HeLa cells. The cell model dependent drop in translocation was the same for all investigated CPPs (Fig. 2A-D). Throughout, HeLa cells featured the highest rates of translocation, whereas the well differentiated and polarized MDCK and Calu-3 layers showed lower or no relevant uptake. Cells incubated with free fluorophore were used as negative controls. There was no uptake whatsoever of the fluorophore alone. Throughout, we used Trypan blue quenching to exclude adherent extracellular fluorescence. As shown in Fig. 1A, a drastic drop in fluorescence intensity ocurred when Trypan blue was added to the cell suspension prior to FACS analysis.

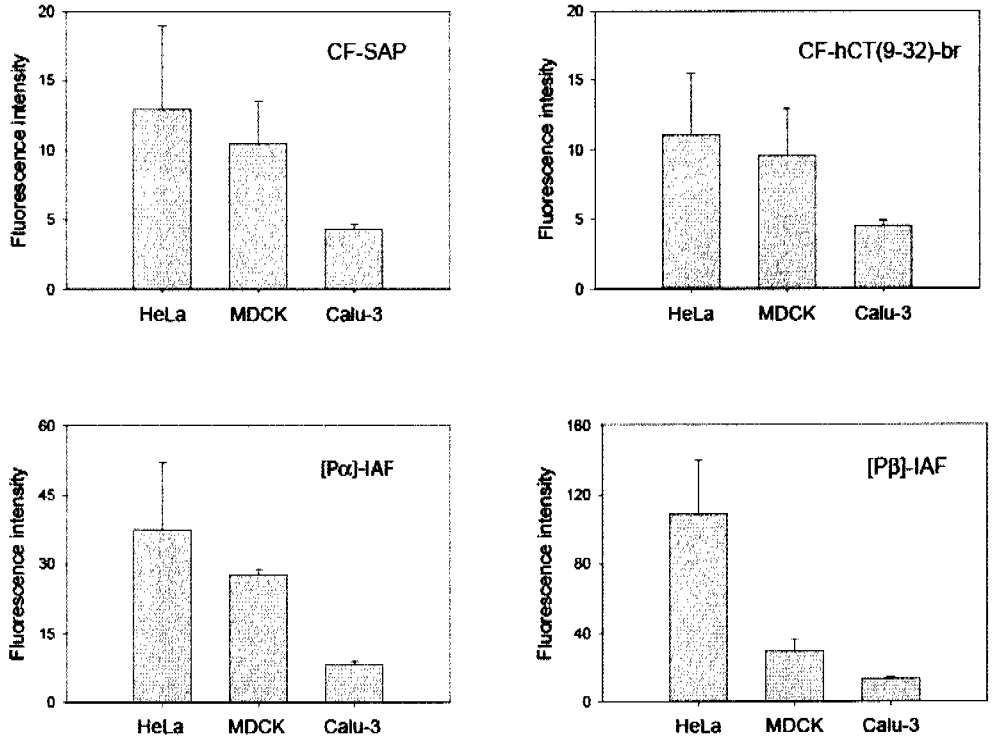

Figure 3

Quantification of translocated CPPs in cell models. Each cell model, HeLa, MDCK and Calu-3, was incubated for 2 hours with the investigated CPPs: CF-SAP, CF-hCT(9-32)-br, [Pα]-IAF or [Pβ]-IAF and analyzed by FACS. Mean cell fluorescence ± SD (n=3).

Peptide stability in serum free medium. To explore the chemical stability of the four CPPs over the duration of the translocation experiments, we performed exploratory chemical stability studies of all investigated CPPs in the respective medium without serum. CF-SAP and CF-hCT(9-32)-br showed good stability over 7 days in serum free medium. After the same period of time, however, only 70% of [Pβ]-IAF and strikingly low 18% of [Pα] were detected (data not shown). Thus, with the exception of [Pα], all compounds demonstrated reasonable or good chemical stability for metabolism studies of up to 8 hours.

Protein content and cell density of cell models. As shown in Table 2, the protein contents of the employed cell models ranged from 1.55 ± 0.13 mg/cm^2 for HeLa cells to 6.17 ± 2.2 mg/cm^2 for Calu-3 cells. The cell number per cm^2 was found to be highest for MDCK cells with a cell density of 520'000 cells/cm^2 and lowest for HeLa cells with a cell density of 47'083 cells/cm^2.

Table 2

Protein contents and cell densities in HeLa, MDCK and Calu-3 cell models. Measurements performed on cells seeded and cultured as described for use in FACS and CLSM experiments. Mean values ± SD (n=3) are given.

Cell line	Protein content (mg/cm^2)	Cell number per cm^2
HeLa	1.55 ± 0.13	47'083 ± 6'166
MDCK	3.03 ± 0.64	520'000 ± 36'055
Calu-3	6.17 ± 2.20	353'333 ± 32'145

Kinetics of metabolic degradation of CPPs in contact with epithelial cell cultures. To analyze the susceptibility of the four CPPs to metabolic degradation as well as to evaluate contrasts in metabolism kinetics between the investigated cell lines, we determined the metabolic degradation of CF-SAP, CF-hCT(9-32)-br, [Pα] and [Pβ]-IAF upon incubation with HeLa cells, and MDCK and Calu-3 cell layers. The obtained degradation profiles of the CPPs were evaluated according to pseudo first-order degradation kinetics, with the semilogarithmic ln c versus t diagrams showing a linear dependence. The results were

based on three experiments utilizing cells of the same passage for each combination of peptide and cell line. The half lives are given in Table 3. During the investigated time interval of 8 hours, CF-SAP and CF-hCT(9-32)-br were essentially stable in all cell models. Much shorter half-lives were observed for [Pα] and [Pβ]-IAF. For [Pβ]-IAF, cleavage was fastest in the presence of Calu-3, showing a normalized half-life of about 1 h only; in the presence of both HeLa and MDCK cells the half-lives were around 5 h. [Pα] showed the fastest degradation rate, featuring a normalized $t_{1/2}$ value of only 1 h with HeLa and MDCK cells, and 0.5 h with Calu-3 cells.

Table 3

Metabolic degradation of CF-SAP, CF-hCT(9-32)-br, [Pα] and [Pß]-IAF on different cell models represented as normalized half-lives. Mean ± SD (n=3).

Peptides	Half-life (h)		
	HeLa	MDCK	Calu-3
CF-SAP	stable	stable	stable
CF-hCT(9-32)-br	stable	stable	stable
[Pα]	0.94 ± 0.28	0.98 ± 0.08	0.43 ± 0.05
[Pβ]-IAF	5.12 ± 0.56	5.52 ± 0.38	0.99 ± 0.65

Identification of metabolites emerging from CPP degradation. To identify the typical cleavage sites of the four investigated CPPs, we analyzed the occurrence of metabolites and identified the resulting fragments of CF-SAP, CF-hCT(9-32)-br, [Pα] and [Pβ]-IAF upon incubation with HeLa, MDCK or Calu-3 cells. Reversed-phase high performance liquid chromatography (RP-HPLC) and matrix assisted laser desorption ionization time of flight mass spectrometry (MALDI-TOF MS) were used for analysis of the samples. Whereas RP-HPLC revealed the remaining amount of CPP and the level of metabolites, MALDI-TOF MS allowed us to uncover the identity of N- and C-terminal metabolites (Fig. 4). Using RP-HPLC, only fluorophore-carrying fragments labeled with either N-terminal CF or C-terminal IAF, respectively, were detectable. Because of the insufficient solubility of [Pα]-IAF, [Pα] was exclusively used in its better soluble, unlabeled form and monitored through Trp based intrinsic fluorescence and UV. The observed m/z values of the MALDI-TOF mass spectra

represent $[M+H]^+$. For control, we analyzed cells incubated with pure medium solution instead of peptide solution. High salt concentrations led to low detection limits and high background noise in MALDI-TOF MS measurements. Introduction of an additional desalting step using ZipTips markedly improved the detection sensitivity. Fig. 4 shows two typical MALDI-TOF MS and RP-HPLC spectra, each after 1 and 120 min, and demonstrates that detection of metabolites by MALDI-TOF MS and RP-HPLC was consistent.

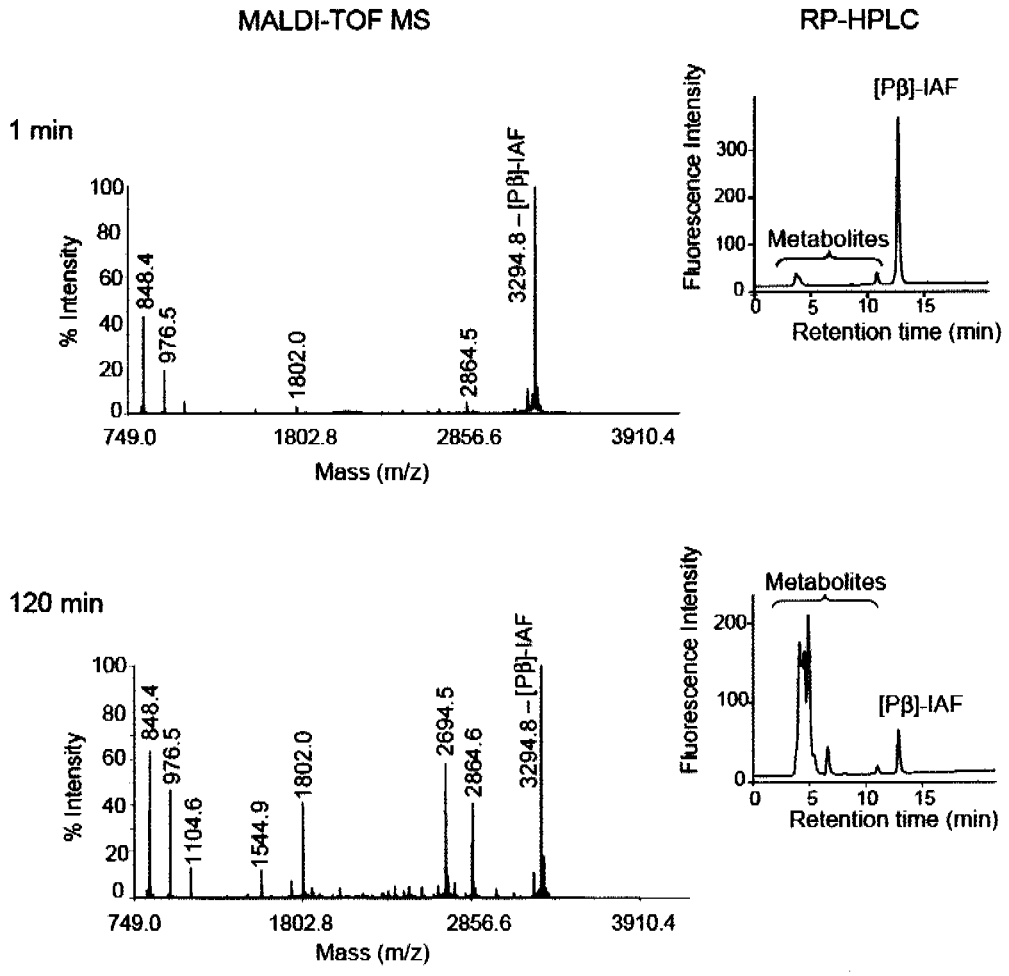

Figure 4

Typical MALDI-TOF MS and RP-HPLC profiles of metabolites upon metabolic degradation of [Pβ]-IAF in contact with MDCK layers. After 1 min, [Pβ]-IAF was practically fully intact and represented by the main peak corresponding to the original CPP in the RP-HPLC diagram as well as in the MALDI-TOF MS spectrum. After 2 hours of incubation with MDCK cells, the increase in number of metabolite peaks as obtained by RP-HPLC was consistent with that in the MALDI-TOF MS spectra.

There was a clear time dependence of degradation. Only few small metabolite peaks emerged after 1 min incubation, whereas several distinct metabolite peaks were observed after 120 min. When incubated with the HeLa, MDCK and Calu-3 cell cultures, each of the four investigated CPPs degraded into between three and ten identifiable metabolites. As shown in Fig.5, all three cell cultures yielded mostly identical metabolite patterns. Due to the high background noise up to 750 Da only fragments above this mass range were considered. A summary of expected and measured molecular weights corresponding to the proposed metabolites is given in Table 4. Throughout, we considered only frequently occurring peptide fragments. These are listed in Table 4, with the main fragments indicated in bold.

Fig. 6 schematically illustrates the suggested cleavage patterns of CF-SAP, CF-hCT(9-32)-br, [Pα] and [Pβ]-IAF in contact with either one of the cell cultures. For all peptides, each amino acid (aa) was numbered, including the side chain of CF-hCT(9-32)-br (aa S1-S15).

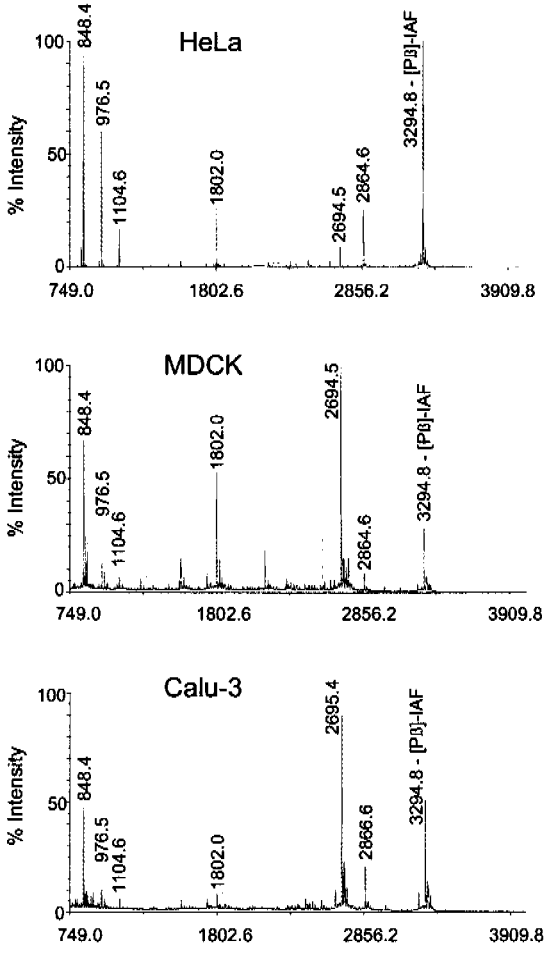

Figure 5

Identical metabolite patterns of [Pß]-IAF in all three cell models. MALDI-TOF MS spectra of [Pß]-IAF after incubation with HeLa, MDCK or Calu-3 cell models, respectively, demonstrate identical metabolite patterns as shown by selected MALDI spectra within the first hour after incubation.

Table 4

Measured versus expected molecular weights of metabolite fragments detected by MALDI-TOF MS. Measured and expected MW values represent $[M+H]^+$. Metabolites found in all three cell models after approximately 1 to 90% degradation of the CPPs. Most frequently occurring metabolites are indicated in bold. S indicates the side chain of CF-hCT(9-32)-br. For all peptides, each amino acid was numbered, including the side chain S1-S15 of CF-hCT(9-32)-br.

Peptide	Fragment	Measured MW	Calculated MW
CF-SAP	CF-18	2356.3	2356.9
	4-18	**1630.1**	**1630.3**
	3-13	**1182.7**	**1182.7**
CF-hCT(9-32)-br	11-32	3977.0	3976.2
	16-25; S14	2807.6	2808.8
	17-32	3322.3	3322.1
	18-20; S11	1587.0	1586.0
	18-22;S5	1110.4	1111.0
[Pα]	**10-27**	**1655.1**	**1659.2**
	3-14	**1250.5**	**1250.7**
	4-23	2190.2	2193.9
	6-20	1577.6	1580.1
	5-20	1691.4	1693.2
[Pβ]-IAF	1-IAF	3294.8	3298.2
	5-IAF	2864.6	2867.7
	7-IAF	**2694.5**	**2697.4**
	17-IAF	**1802.0**	**1804.3**
	23-IAF	1104.6	1106.4
	24-IAF	976.5	978.2
	25-IAF	**848.4**	**850.0**

CF-SAP. Throughout we observed only minor metabolism of CF-SAP, in terms of both numbers and peak intensities of the metabolites, corresponding to high stability in contact with HeLa, MDCK and Calu-3 cell cultures over a time interval of 8 hours (Table 3). Nevertheless, some distinct fragments could be revealed, e.g. with cleavage sites within the first trimer between Arg_2 and Leu_3, together with an additional site in the third trimer between

Val_{13} and Arg_{14} resulting in the fragment Leu_3-Val_{13} (Table 4 and Fig. 6). For this fragment the resulting counterpart, fragment Arg_{14}-Pro_{18}, was also found. A frequently occurring fragment, Pro_4-Pro_{18}, was found to result also from cleavage in the first trimer between Leu_3 and Pro_4.

CF-hCT(9-32)-br. Due to its branched character, the cleavage pattern of CF-hCT(9-32)-br was inherently complex to evaluate. Clear assignments of distinct fragments were difficult and made unequivocal identification problematic. Even more so, the marked stability of this peptide led to a weak intensity of metabolite peaks. Hence, for further evaluation we only considered a subset of selected and clearly identifiable fragments. Within the hCT derived backbone of CF-hCT(9-32)-br, the main cleavage sites were between Gly_{10} and Thr_{11}, Asp_{15} and Phe_{16}, and Asn_{17} and Lys_{18}. In the side branch, an important cleavage site was found between Gly_{S5} and Pro_{S6} (Table 4 and Fig. 6).

[Pα]. As suggested by its short half-life, [Pα] was subject to fast stepwise cleavage of single amino acids from both the C- as well as the N-terminus. Two fragments were observed consistently, namely fragments Ala_{10}-Val_{27} and Leu_3-Leu_{14} indicating distinct cleavage sites between amino acids Leu_3 and Phe_4, Ala_9 and Ala_{10}, and Leu_{14} and Met_{15}. Also we observed cleavage sites in the cationic domain of the molecule at position Lys_{23}-Lys_{24} as well as Lys_{24}–Arg_{25}.

[Pβ]-IAF. Corresponding to their analogous sequences, the degradation patterns of [Pβ]-IAF and [Pα] were similar. Important cleavage sites were between Gly_6 and Phe_7 as well as between Gly_{16} and Ala_{17} and led to the fragments Phe_7-IAF and Leu_{17}-IAF. As similarly observed for [Pα], one of the peptide's most frequent fragments, Arg_{25}-IAF, was the result of a break in the cationic section between position Lys_{24} and Arg_{25}, suggesting high susceptibility to enzymatic degradation in this domain.

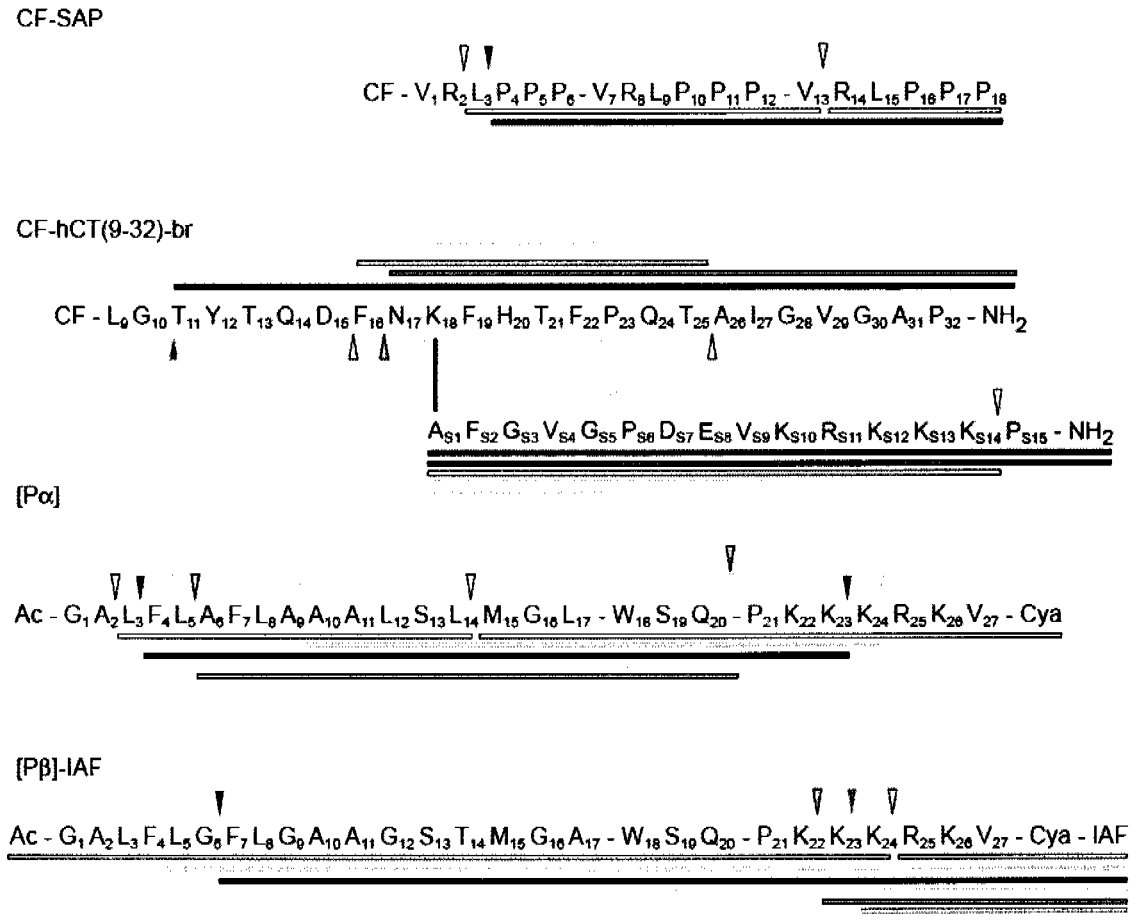

Figure 6

Scheme of suggested metabolic cleavage sites of CPPs upon incubation with the three cell models. Individually shaded arrowheads correspond to the corresponding cleavage sites between the respective amino acids. The resulting metabolites are indicated through equally shaded bars as identified by MALDI-TOF MS.

DISCUSSION

The aim of the present study was to investigate the metabolic fate of four CPPs, namely CF-SAP, CF-hCT(9-32)-br, [Pα], and [Pβ]-IAF, when in contact with three selected epithelial cell lines. As yet, information on the important subjects of enzymatic stability and degradation of CPPs is rare [10-14]. Additionally, we studied the cellular translocation efficiency of the four peptides into three epithelial cell cultures. To our knowledge, our study is the first to aim towards a relation between metabolic stability and translocation efficiency of CPPs.

The metabolic clearance of CPPs has several aspects: on the one hand, CPPs should be stable enough to deliver a cargo to its destination prior to be metabolically cleared [10]. On the other hand, metabolic clearance of CPPs after delivery to its target is desired in order to release the cargo or a biologically active unit thereof, and avoid systemic toxicity.

We investigated the metabolic stability of CF-SAP, CF-hCT(9-32)-br, [Pα], and [Pβ]-IAF in three epithelial cell cultures with different phenotypes and enzymatic activities, namely HeLa, MDCK and Calu-3. On surfaces, HeLa cells grow as proliferating, subconfluent layers with no tight junctional network. By contrast, MDCK cells develop confluent monolayers forming a continuous sheet of cells joined by tight junctions [28]. Similarly, the airway epithelial cell line Calu-3 forms polarized and well differentiated monolayers with tight-junctional networks [29] and, different from MDCK, generates extracellular mucus [30, 31].

Among the four investigated CPPs, CF-SAP and CF-hCT(9-32)-br were the most stable ones, allowing only minor rates of metabolic cleavage. Even in contact with Calu-3 cells, CF-SAP and CF-hCT(9-32)-br were rather stable whereas the normalized half-lives of intact [Pα] and [Pβ]-IAF were much shorter. We observed higher protein levels per cm^2 for Calu-3 cells as compared to HeLa and MDCK cells. Assuming that protein and enzyme activity levels correlate, we conclude that the increased protein levels in Calu-3 layers contribute to the enhanced metabolism of the four CPPs in this model.

In a former study, we investigated the half-life of the unbranched CF-hCT(9-32) [14]. For this linear peptide, a half-life of several hours was found when in contact with MDCK monolayers and less than one hour with Calu-3 cells. Through side chain modification of CF-hCT(9-32), resulting in the branched CF-hCT(9-32)-br, we achieved not only an increase in cellular translocation [23] but also improved metabolic stability as shown in the present work. Its improved metabolic stability is concluded to result from efficient steric hindrance through the introduction of the side chain reaching out from K_{18} (Table 1). Metabolites of CF-hCT(9-32)-br occurred in only minor quantities as indicated by small peaks in the MALDI-TOF MS spectra. Theoretically, metabolic degradation of the branched CF-hCT(9-32)-br may allow concurrent cleavage in all three segments of the peptide which implies a more complex pattern of theoretically possible fragments as compared to its linear derivative.

Contrasting to the pronounced stability of CF-SAP and CF-hCT(9-32)-br, cleavage of [Pβ]-IAF was rather quick with relatively short half-lives ranging from about one hour in the presence of Calu-3 cells to about two hours in the presence of HeLa and MDCK cells. Among the four investigated CPPs, [Pα] had the shortest half-life of around 30 min only. Even in

medium alone, i.e. in the absence of any cellular enzyme activity, [Pα] was subject to fast degradation. Possible explanations for its non-enzymatic degradation might be (i) hydrolytic cleavage. Further on, (ii) adhesion to cell surfaces and/or working material [32] and (iii) exclusion from analytical detection by insufficient solubility and aggregation may occur. In fact, we observed high affinity of [Pα]-IAF to membrane surfaces. The insufficient solubility of [Pα]-IAF and [Pβ]-IAF has to be taken into account for the interpretation of results from uptake and metabolism studies. Therefore, to avoid misinterpretations, we focus on the individual relationship of uptake efficiency and metabolism of each peptide in cultures of the three cell lines, rather than comparing between the peptides. Structural differences between [Pβ]-IAF and [Pα] through amino acid modifications of Gly_6, Gly_9, Gly_{12}, Thr_{14} and Ala_{17} versus Ala_6, Ala_9, Leu_{12}, Leu_{14} and Leu_{17}, respectively, were of no significant impact on the net chemical stability of the peptides as indicated by the occurrence of the cleavage sites Gly_6-Phe_7 and Gly_{16}-Ala_{17} for [Pβ]-IAF, versus Ala_9-Ala_{10} and Leu_{14}-Met_{15} for [Pα]. Furthermore, there was no reduction in the number of cleavage sites through these modifications. Equally, the sequence modifications did not have any significant effect on the efficiency of translocation of these two CPPs in the investigated cell lines. Altogether, inspite of large differences in the rates, there was no major difference in the cleavage patterns between the three cell lines for each of the investigated CPPs. This finding is in agreement with a former study of our group where we described similar cleavage patterns for hCT derived CPPs irrespective of the applied epithelial cell model [14].

In order to assess the impact of metabolic cleavage on the efficiency of translocation, we studied the translocation of CF-SAP, CF-hCT(9-32)-br, [Pα]-IAF and [Pβ]-IAF. For all investigated CPPs, we observed efficient uptake in HeLa cells by CLSM and FACS. Corresponding to its higher state of cellular differentiation, uptake in the MDCK model was significantly reduced for each of the four CPPs, and none of the CPPs was observed to translocate efficiently into confluent Calu-3 cells. Hallbrink et al. [33] recently suggested that the uptake of cell-penetrating peptides is dependent on the peptide-to-cell ratio. As a consideration of the lack of uptake in MDCK and Calu cells, there is a relatively much higher number of cells in these experiments as compared with the uptake in HeLa.

In this study, we used two types of [Pα], namely unlabeled [Pα] and fluorescence labelled [Pα]-IAF. For analytical reasons, due to the poor aqueous solubility of the IAF-labeled [Pα]-IAF, we analyzed the metabolism kinetics with the sufficiently soluble unlabeled [Pα], even though, consequently, the obtained results were not directly comparable with the fluorescently

labelled peptides. However, for FACS and CLSM, which required more sensitive fluorescence detection, we used [Pα]-IAF throughout.

To conclude, we demonstrate here that CPP stability and translocation capacity were strongly cell line dependent, whereas their cleavage patterns were quite similar in the three cell cultures. When comparing all four CPPs, there was no direct relation between metabolic stability and translocation efficiency. In fact, [Pα] featuring the shortest $t_{1/2}$ was efficiently taken up into HeLa cells. Although CF-SAP was stable on Calu-3 cells, no translocation was found. These results indicate that stability is not a main limiting factor in cellular translocation, at least in the investigated cell cultures. However, in the context of individual CPPs, stabilization against chemical as well as enzymatic degradation may further improve their translocation efficiency. For this purpose, enhanced metabolic CPP stability might be achieved through replacement of L-amino acids by their non-physiologic D-counterparts, through N-methylation or exchange of certain amino acids.

ACKNOWLEDGEMENTS

The authors acknowledge the following contributions: Professor Heidi Wunderli-Allenspach and Dr. Gabor Csúcs (ETH Zurich) for the opportunity to use the confocal laser scanning microscopes. Moreover, the technical support of the Functional Genomics Center Zurich is gratefully acknowledged.

REFERENCES

1. Kueltzo, L.A. and C.R. Middaugh, *Potential use of non-classical pathways for the transport of macromolecular drugs.* Expert Opin Investig Drugs, 2000. **9**(9): p. 2039-50.
2. Derossi, D., et al., *The third helix of the Antennapedia homeodomain translocates through biological membranes.* J Biol Chem, 1994. **269**(14): p. 10444-50.
3. Vives, E., P. Brodin, and B. Lebleu, *A truncated HIV-1 Tat protein basic domain rapidly translocates through the plasma membrane and accumulates in the cell nucleus.* J Biol Chem, 1997. **272**(25): p. 16010-7.
4. Prochiantz, A., *Getting hydrophilic compounds into cells: lessons from homeopeptides.* Curr Opin Neurobiol, 1996. **6**(5): p. 629-34.

5. Schwarze, S.R., et al., *In vivo protein transduction: delivery of a biologically active protein into the mouse.* Science, 1999. **285**(5433): p. 1569-72.
6. Singh, D., et al., *Peptide-based intracellular shuttle able to facilitate gene transfer in mammalian cells.* Bioconjug Chem, 1999. **10**(5): p. 745-54.
7. Lewin, M., et al., *Tat peptide-derivatized magnetic nanoparticles allow in vivo tracking and recovery of progenitor cells.* Nat Biotechnol, 2000. **18**(4): p. 410-4.
8. Astriab-Fisher, A., et al., *Conjugates of antisense oligonucleotides with the Tat and antennapedia cell-penetrating peptides: effects on cellular uptake, binding to target sequences, and biologic actions.* Pharm Res, 2002. **19**(6): p. 744-54.
9. Fix, J.A., *Oral controlled release technology for peptides: status and future prospects.* Pharm Res, 1996. **13**(12): p. 1760-4.
10. Elmquist, A. and U. Langel, *In vitro uptake and stability study of pVEC and its all-D analog.* Biol Chem, 2003. **384**(3): p. 387-93.
11. Elmquist, A., et al., *VE-cadherin-derived cell-penetrating peptide, pVEC, with carrier functions.* Exp Cell Res, 2001. **269**(2): p. 237-44.
12. Fischer, R., et al., *A stepwise dissection of the intracellular fate of cationic cell-penetrating peptides.* J Biol Chem, 2004. **279**(13): p. 12625-35.
13. Lindgren, M.E., et al., *Passage of cell-penetrating peptides across a human epithelial cell layer in vitro.* Biochem J, 2004. **377**(Pt 1): p. 69-76.
14. Trehin, R., et al., *Metabolic cleavage of cell-penetrating peptides in contact with epithelial models: human calcitonin (hCT)-derived peptides, Tat(47-57) and penetratin(43-58).* Biochem J, 2004. **382**(Pt 3): p. 945-56.
15. Karp, G., *Cell and Molecular Biology.* 2nd ed. 1999: John Wiley & Sons, Inc. 292-325.
16. Simons, K. and S.D. Fuller, *Cell surface polarity in epithelia.* Annu Rev Cell Biol, 1985. **1**: p. 243-88.
17. Florea, B.I., et al., *Drug transport and metabolism characteristics of the human airway epithelial cell line Calu-3.* J Control Release, 2003. **87**(1-3): p. 131-8.
18. Crespo, L., et al., *Peptide dendrimers based on polyproline helices.* J Am Chem Soc, 2002. **124**(30): p. 8876-83.
19. Fernandez-Carneado, J., et al., *Potential Peptide Carriers: Amphipathic Proline-Rich Peptides Derived from the N-Terminal Domain of gamma-Zein.* Angew Chem Int Ed Engl, 2004. **43**(14): p. 1811-1814.

20. Fernandez-Carneado, J., et al., *Amphipathic peptides and drug delivery.* Biopolymers, 2004. **76**(2): p. 196-203.

21. Trehin, R., et al., *Cellular internalization of human calcitonin derived peptides in MDCK monolayers: a comparative study with Tat(47-57) and penetratin(43-58).* Pharm Res, 2004. **21**(1): p. 33-42.

22. Krauss, U., et al., *In vitro gene delivery by a novel human calcitonin (hCT)-derived carrier peptide.* Bioorg Med Chem Lett, 2004. **14**(1): p. 51-4.

23. Foerg, C., et al., *Decoding the Entry of Two Novel Cell-Penetrating Peptides in HeLa Cells: Lipid Raft-Mediated Endocytosis and Endosomal Escape.* Biochemistry, 2005. **44**(1): p. 72-81.

24. Vidal, P., et al., *Solid-phase synthesis and cellular localization of a C- and/or N-terminal labelled peptide.* J Pept Sci, 1996. **2**(2): p. 125-33.

25. Morris, M.C., et al., *A new peptide vector for efficient delivery of oligonucleotides into mammalian cells.* Nucleic Acids Res, 1997. **25**(14): p. 2730-6.

26. Deshayes, S., et al., *Primary amphipathic cell-penetrating peptides: structural requirements and interactions with model membranes.* Biochemistry, 2004. **43**(24): p. 7698-706.

27. Deshayes, S., et al., *On the mechanism of non-endosomial peptide-mediated cellular delivery of nucleic acids.* Biochim Biophys Acta, 2004. **1667**(2): p. 141-7.

28. Rothen-Rutishauser, B., et al., *MDCK cell cultures as an epithelial in vitro model: cytoskeleton and tight junctions as indicators for the definition of age-related stages by confocal microscopy.* Pharm Res, 1998. **15**(7): p. 964-71.

29. Shen, B.Q., et al., *Calu-3: a human airway epithelial cell line that shows cAMP-dependent Cl- secretion.* Am J Physiol, 1994. **266**(5 Pt 1): p. L493-501.

30. Forbes, I.I., *Human airway epithelial cell lines for in vitro drug transport and metabolism studies.* 2000. **3**(1): p. 18-27.

31. Mathia, N.R., et al., *Permeability characteristics of calu-3 human bronchial epithelial cells: in vitro-in vivo correlation to predict lung absorption in rats.* J Drug Target, 2002. **10**(1): p. 31-40.

32. Chico, D.E., R.L. Given, and B.T. Miller, *Binding of cationic cell-permeable peptides to plastic and glass.* Peptides, 2003. **24**(1): p. 3-9.

33. Hallbrink, M., et al., *Uptake of cell-penetrating peptides is dependent on peptide-to-cell ratio rather than on peptide concentration.* Biochim Biophys Acta, 2004. **1667**(2): p. 222-8.

34. Morris, M.C., et al., *A new potent HIV-1 reverse transcriptase inhibitor. A synthetic peptide derived from the interface subunit domains.* J Biol Chem, 1999. **274**(35): p. 24941-6.

35. Vidal, P., et al., *Conformations of a synthetic peptide which facilitates the cellular delivery of nucleic acids.* Letters in Peptide Science, 1997. **4**(4-6): p. 227-230.

36. Richard, J.P., et al., *Cell-penetrating peptides. A reevaluation of the mechanism of cellular uptake.* J Biol Chem, 2003. **278**(1): p. 585-90.

37. Sahlin, S., J. Hed, and I. Rundquist, *Differentiation between Attached and Ingested Immune-Complexes by a Fluorescence Quenching Cytofluorometric Assay.* Journal of Immunological Methods, 1983. **60**(1-2): p. 115-124.

38. Ma, Z.S. and L.Y. Lim, *Uptake of chitosan and associated insulin in Caco-2 cell monolayers: A comparison between chitosan molecules and chitosan nanoparticles.* Pharmaceutical Research, 2003. **20**(11): p. 1812-1819.

39. Wan, C.P., C.S. Park, and B.H.S. Lau, *A Rapid and Simple Microfluorometric Phagocytosis Assay.* Journal of Immunological Methods, 1993. **162**(1): p. 1-7.

40. Tseng, W.C., et al., *Cationic liposomal delivery of plasmid to endothelial cells measured by quantitative flow cytometry.* Biotechnology and Bioengineering, 1996. **50**(5): p. 548-554.

41. Hed, J., et al., *The use of fluorescence quenching in flow cytofluorometry to measure the attachment and ingestion phases in phagocytosis in peripheral blood without prior cell separation.* J Immunol Methods, 1987. **101**(1): p. 119-25.

42. Innes, N.P. and G.R. Ogden, *A technique for the study of endocytosis in human oral epithelial cells.* Arch Oral Biol, 1999. **44**(6): p. 519-23.

43. Kang, H.C., Y.H. Park, and S.J. Go, *Growth inhibition of a phytopathogenic fungus, Colletotrichum species by acetic acid.* Microbiol Res, 2003. **158**(4): p. 321-6.

CHAPTER IV

Endocytosis of cell-penetrating peptides is differentiation restricted

Christina Foerg[1], Urs Ziegler[2], Jimena Fernandez-Carneado[3], Ernest Giralt[3,4], Hans P. Merkle[1]

[1] Department of Chemistry and Applied Biosciences, Institute of Pharmaceutical Sciences, ETH Zurich, Switzerland

[2]Institute of Anatomy, University of Zurich, Switzerland

[3]Institut de Recerca Biomèdica de Barcelona, Parc Científic de Barcelona, Spain

[4]Departament de Química Orgànica, Universitat de Barcelona, Spain

ABSTRACT

Cellular entry of biomacromolecules is restricted by the barrier function of cell membranes. Tethering such molecules to cell penetrating peptides (CPPs) that can translocate cell membranes has opened new horizons in biomedical research. Here, we investigate the translocation of the CPPs hCT(9-32)-br, a human calcitonin derived peptide and SAP, a γ-zein related sequence. We observed marked endocytic uptake of the two peptides into proliferating MDCK by a mechanism involving lipid rafts and clathrin-coated pits. In confluent MDCK, however, we noted a massive slow-down of compound-unspecific endocytosis. The underlying mechanism is the down-regulation of endocytosis by Rho-GTPases, previously identified to be intimately involved in endocytic traffic. We found a correlation between endocytic translocation and active Rho-A, as well as a correlation between cell density, cellular differentiation and endocytic slow-down on the one hand, and active Rac-1 on the other. To our knowledge, this is the first study to cast light on the mechanism for the differentiation restricted translocation of CPPs into epithelial cell models. Our findings were further elaborated using an inflammatory IFN-γ/TNF-α induced MDCK model mimicking inflammatory epithelial diseases. CPP translocation in this model was enhanced in a cytokine concentration dependent way resulting in maximum enhancement rates of up to 90 %. Interestingly, our observations suggest cytokine induced redistribution of lipid rafts in confluent MDCK to be involved in the observed enhancement of CPP translocation. Altogether, our findings emphasize the importance of differentiated cell models to study CPP translocation and point towards inflammatory epithelia as potential niche for CPPapplication.

INTRODUCTION

The plasma membrane of mammalian cells widely restricts the passage of large, charged and hydrophilic compounds into cells, preventing most peptide, protein and nucleic acid biopharmaceuticals to reach intracellular targets which frequently results in low or zero biological efficacy. Cell penetrating peptides (CPPs) constitute a collection of various families of short peptide sequences that have been shown to translocate the plasma membrane. The prospects of chemical ligations or physical assemblies between CPPs and therapeutic cargoes has, therefore, attracted considerable interest, and created widespread hopes to exploit the CPP approach for drug delivery purposes, gene therapy and vaccine development [1, 2]. Various oligocationic cell penetrating peptides, e.g., HIV-1 derived Tat peptides, penetratin (pAntp), oligoarginine peptides or the weakly cationic, human calcitonin derived CPPs and others, have been described in the literature in broad detail [3-7]. They were commonly considered for the therapeutic delivery of peptides, proteins, oligonucleotides, plasmids, peptide nucleic acids (PNAs) and even nanoparticles [8-13].

In this study, we investigate the cellular entry of two recently developed, N-terminally carboxyfluorescein (CF) labeled, oligocationic CPPs. One is a branched derivative of the linear human calcitonin derived CF-hCT(9-32) [7], denoted as CF-hCT(9-32)-br, that carries an oligocationic, SV40 derived nuclear localisation sequence, the GPDEVKRKKKP motif, in the form of a side-branch to the main peptide chain (see Table I) [14]. The other one is the proline-rich sweet arrow peptide CF-SAP (see Tab. I), a linear trimer of repetitive VRLPPP domains, and conceived as an amphipathic version of a polyproline sequence related to γ-zein, a storage protein of maize [15-17]. The translocation of both CPPs into HeLa cells was recently found to follow the pathway of lipid raft-mediated endocytosis prior to endosomal escape [18]. The diversity of mammalian cell lines that have been applied to study the translocation of CPPs across the plasma membrane is large. In the majority of cases, "leaky" cell lines, such as HeLa, KB 3-1, Bowes Human Melanoma or MC57 fibrosarcoma cells, have been used for CPP translocation [19-23]. Such cell lines lack the ability to form tight junctions and, therefore, are considered as permeable, although they may grow to monolayers [24]. Despite the clear biological relevance of these cell lines, tissue-like cellular models involving junctional complexes may be more justified under therapeutic considerations, namely the penetration or permeation of CPP-cargo constructs into and through tissues. Therefore, our research in this area has been particularly concentrated on translocation studies in epithelial like models with fully developed tight junctions [7]. One of the best characterized epithelial cell models derives from the Madine-Darby canine kidney (MDCK)

cell line. When grown to confluence, MDCK cells feature all elements of well-differentiated, polarized epithelia, such as apical–basolateral polarization and tight junctions. Thus, MDCK monolayers represent a well-established *in vitro* model for various absorptive and respiratory epithelia [25, 26]. The plasma membranes of polarized epithelial cells are divided into an apical domain, facing the external milieu of the organism, and the basolateral domain which is in contact with the internal domain and faces the mesenchymal space and the bloody supply [27, 28]. Epithelial cells are connected by a junctional complex encircling the apex of each cell. Tight junctions are the most apical structure of the junctional complex which also includes adherens junctions, desmosomes and gap junctions. Tight junctions constitute a barrier to the paracellular diffusion of solutes from the lumen to the tissue parenchyma (gate function) and restrict the lateral exchange of lipids and proteins between the apical and basolateral plasma membrane domains (fence function) [29-33]. Cell line dependence of CPP translocation has been suggested by different research groups [7, 23, 24]. Previously, Hallbrink et al.[34] hypothesized about a cell density dependent translocation of CPPs. In the present study, we demonstrate a differentiation state dependence of the mechanism and efficiency of translocation. We observed marked endocytic translocation of two CPPs into proliferating MDCK cells by a mechanism involving both lipid rafts and chlathrin-coated pits. In well-differentiated, confluent MDCK monolayers, however, we noted a massive slow-down of compound unspecific endocytosis and no detectable contribution of lipid raft-mediated endocytosis. The Rho family of small GTPases, comprising Rho, Rac and Cdc42, are ubiquitously expressed across eukaryotes where they act as molecular switches, cycling between an active GTP-bound state and an inactive GDP-bound state [35, 36]. In the active state, they interact with various downstream effectors and regulate a variety of cellular events such as actin polymerization, cell morphology and polarity, cell growth control, transcription and membrane trafficking events such as endocytosis [37-42]. There is evidence to date suggesting that Rho GTPases are ideally placed to mediate the signalling interface between endocytic traffic and the actin cytoskeleton [43, 44]. Considering the close apposition between the perijunctional F-actin ring and the epithelial tight junction complex, it is also conceivable that Rho-GTPases, through cytoskeletal modification, could affect epithelial barrier function [45]. In fact, in the present study in MDCK cells, we found a correlation between endocytic translocation and active form Rho-A, as well as a correlation between cell density, cellular differentiation and endocytic slow-down on the one hand, and active form Rac-1 on the other. To our knowledge, this is the first study that casts light on the role of Rho GTPases for the differentiation restricted endocytosis of CPPs into an epithelial cell model.

The observed relationship between endocytic slow-down and cellular differentiation was further elaborated using an inflammatory epithelial, IFN-γ/TNF-α induced model mimicking inflammatory epithelial diseases. Inflammatory epithelial diseases such as inflammatory bowel diseases, e.g. Crohn's disease and ulcerative colitis [46-50], or inflammatory airway diseases associated with cystic fibrosis [51] or asthma bronchiale [52], typically show increased cytokine production, and significant barrier dysfunction. CPP translocation efficiency in the inflammatory model was enhanced in a cytokine concentration dependent way resulting in maximum enhancement rates of up to 90 %. Interestingly, our data suggest cytokine induced redistribution of lipid rafts in confluent MDCK layers to be involved in the observed enhancement of CPP translocation.

Altogether, our findings emphasize the importance of appropriate cell models to study CPP translocation and point towards inflamed epithelia as an interesting niche for CPP application in drug delivery.

Table 1: Name, sequence, and origin of the cell-penetrating peptides (CPPs) used[a]

Name	Sequence	Origin
hCT(9-32)-br	LGTYTQDFNKFHTFPQTAIGVGAP-NH_2 | AFGVGPDEVKRKKKP–NH_2	human calcitonin, simian virus 40
SAP	VRLPPP-VRLPPP-VRLPPP	modified maize
Tat(FITC)	GRKKRRQRRRGYK(FITC)C-NH_2	HIV-1

[a] hCT(9-32)-br and SAP were CF-labeled at the N-terminus

MATERIALS AND METHODS

Materials

MDCK (low resistance, type II) was a kind gift from the Biopharmacy group (ETH Zurich, Switzerland). Cell culture media, trypsin-EDTA, penicillin, streptomycin and Hank's Balanced Salt Solution (HBSS) were from Gibco (Paisley, USA). Phosphate buffer solution (PBS, pH 7.4) without calcium and magnesium were from Life Technologies (Basel, Switzerland). Foetal calf serum (FCS) was purchased from Winiger AG (Wohlen, Switzerland). Hoechst 33342, cholera toxin subunit B (recombinant), Alexa Fluor 594 conjugate and tetramethylrhodamine-labeled transferrin were from Molecular Probes (Leiden, The Netherlands). 5(6)-carboxyfluorescein (CF), Trypan blue, sodium azide (NaN_3), Triton X-100, 2-deoxy-glucose, Tris(hydroxymethyl)-aminomethane hydrochloride, Tween 20 and bovine serum albumin (BSA) were obtained from Fluka (Buchs, Switzerland), and methyl-β-cyclodextrin (M-ß-CD) from Wacker-Chemie (Munich, Germany). EZ-Detect Rho and Rac1 activation kits as well as Halt Protease Inhibitor Cocktail (EDTA free) were from Perbio Science (Lausanne, Switzerland). The polyclonal first antibody rabbit Anti-ZO-1 was from Zymed Laboratories (South San Francisco, CA), the second antibodies goat anti-rabbit Texas red and goat anti-mouse conjugated with horseradish peroxidase were from Jackson ImmunoResearch Laboratories (West Grove, PA). *E. coli* derived recombinant canine interferon-gamma (IFN-γ) and tumor necrosis factor-alpha (TNF-α) were obtained from R&D Systems (Minneapolis, MN). Filter inserts (polyethylene terephthalate (PET), 0.4 μm pore size), companion 12 well plates, 24 well plates and 5 ml polypropylene round-bottom tubes (FACS tubes) were purchased from Falcon (Becton Dickinson Lab ware, Franklin Lakes, NJ). 96 well plates and glass chamber slides were obtained from Nunc (Roskilde, Denmark). MTT (3-[4,5-dimethylthiazol-2-yl]-2,5-diphenyltetrazolium bromide), Fluorescein isothiocyanate-dextran (FITC-dextran, MW 4400), mouse anti-actin, sodium dodecyl sulphate (SDS) and Bradford reagent were from Sigma (St. Louis, MO, USA). Cell culturing flasks (25 and 75 cm^2) were from TPP (Trasadingen, Switzerland). Centricon centrifugal filter devices were obtained from Millipore (Billerica, MA). ECL Plus Western Blotting Detection Reagent was from Amersham Biosciences (Uppsala, Sweden). [^{3}H]-mannitol (19.7 Ci/mmol) was from Perkin Elmer (Boston, MA). Coverslips and microscope slides were purchased from Knittel (Braunschweig, Germany).

Methods

Peptide synthesis. Investigated CPPs are listed in Table I. The branched human calcitonin (hCT) derived CPP (hCT(9-32)-br was synthesized by the peptide synthesis unit of the University of Barcelona (Barcelona, Spain). This peptide is derived from the human calcitonin fragment hCT(9-32) and is equipped with the nuclear localization sequence (NLS) of simian virus 40 large T antigen in the side chain of K18 [14]. N-terminally fluorescence labeled sweet arrow peptide (CF-SAP) was synthesised by solid-phase peptide synthesis on a 2-chlorotrityl resin following the 9-fluorenyl methoxy carbonyl/*tert*-butyl (Fmoc/*t*Bu) strategy prior to fluorescent labeling with 5(6)-carboxyfluorescein (CF) [16]. Finally, a FITC labeled Tat peptide with the sequence GRKKRRQRRRGYK(FITC)C-NH_2 (MW 2237) was synthesized and purified as described previously [53].

Cell culture. MDCK cells were cultured under standard conditions in minimum essential medium with Earl's salts (MEM) containing 10% heat-inactivated FCS and 1% penicillin/streptomycin. For translocation experiments, if not otherwise indicated, cells were seeded at a constant density of 2 x 10^4 cells/cm^2 on Transwell filters in 12 or 24-well plates or on chamber glasses and incubation was at 37°C. Cells were used in both proliferating and confluent states, starting from 12 hours post seeding until 10 days post seeding. For detection of filter grown cells, filters were cut out, put upside down on coverslips and mounted in Dako mounting medium. Cell numbers were determined with a haemocytometer (Assistent, Sondheim/Rhön, Germany).

Confocal laser scanning microscopy (CLSM) of CPP translocation. MDCK cells were incubated with serum free MDCK medium containing either CF-SAP (50 μM), CF-hCT(9-32)-br (30 μM) or unconjugated fluorophore (50 μM or 30 μM, respectively) for 1 hour under horizontal mechanical shaking at 150 min^{-1}. After 30 min, Hoechst 33342 was added to a final concentration of 1 μg/ml for nuclear staining.

To inhibit endocytosis, one or 10 days old cells were pre-treated for 1 h with NaN_3/2-deoxyglucose (0.1%/50 mM in HBSS) prior to incubation with CPPs. To study the temperature-dependency of translocation, studies were carried out at 4 and 37°C. For colocalization studies, cells were co-incubated apically for 30 min in solutions of CF-SAP (50 μM) or CF-hCT(9-32)-br (30 μM) with either cholera toxin (10 μg/ml) or transferrin (50 μg/ml) in serum free MDCK medium. Subsequently, all samples were washed with phosphate buffered saline (PBS), fixed in 1% (w/v) aqueous paraformaldehyde (PFA) solution for 30 min and washed again. To exclude artefacts owing to cell fixation, preliminary experiments were also performed in unfixed, living cells. Both protocols led to

identical vesicular distributions of the two CPPs as well as to identical colocalization patterns with transferrin and cholera toxin. Therefore, we followed a mild fixation protocol with 1% PFA for better handling and to more exactly terminate the experiments. Cellular uptake was visualized using a TCS-SP2 laser scanning confocal microscope (Leica Microsystems, Mannheim, Germany) with a 63x, 1.4 NA, plan-apochromatic lens using HeNe 594 nm, HeNe 543 nm, Ar 488 and diode 405 nm lasers. To avoid cross talk, emission signals were collected independently. 3-D multichannel image processing was performed using the IMARIS software (Bitplane AG, Zurich, Switzerland) on a Silicon graphics workstation. Background fluorescence was determined by analysing unlabeled cells. The images were deconvolved using Huygens software (Scientific Volume Imaging B.V., Hilversum, Netherlands). Colocalization images were obtained by the colocalization program of IMARIS software (Bitplane AG, Zurich, Switzerland).

Translocation and endocytosis inhibition study by FACS. Individual MDCK cultures were used for experiments after 12 hours, 1 day and then every 24 hours until 10 days post seeding. Cells were incubated from either the apical or the basolateral side with CF-SAP (50 μM), hCT(9-32)-br (30 μM) or unconjugated fluorophore (50 μM or 30 μM, respectively) in serum free MDCK medium for 3 hours. Additional experiments were performed, incubating MDCK cells with 30 μM FITC-dextran, 5 μM Tat peptide, and 30 μM hCT(9-32), respectively, from the apical side or 30 μM transferrin from the basolateral side for 3 hours. After incubation, cells were washed, trypsinized for 10 min, re-suspended in medium and immediately put on ice. To quench potentially remaining external fluorescence, Trypan blue was added to the samples prior analysis by FACS on a FacScan (Becton Dickinson, Franklin Lakes, NJ) or a FACSCalibur (Becton Dickinson, Franklin Lakes, NJ) within 2 hours after trypsinization. A total of 10,000 cells per sample was analyzed. The mean fluorescence intensity of peptide-labeled cell populations was normalized to unlabeled control cells and compared to control cells labeled with 5(6)-carboxyfluorescein. To study the effects of seeding and cell culture density in MDCK layers, FACS studies were performed comparing half or one day old cells with a low seeding density of 2×10^4 cells/cm^2, half or one day old cells having a high seeding density of 5×10^5 cells/cm^2, and, finally, 10 days old cells with a low initial seeding density of 2×10^4 cells/cm^2 but a high final cell culture density of 5×10^5 cells/cm^2, after 10 days. Cells were incubated from the apical side with CF-SAP (50 μM), hCT(9-32)-br (30 μM) or unconjugated fluorophore (50 μM or 30 μM, respectively) in serum free MDCK medium for 3 hours. Quantification was performed as described above.For inhibition of endocytosis, one or 10 days old cells were pre-treated for 1 h with NaN_3/2-

deoxyglucose (0.1%/50 mM in HBSS) or M- β -CD (10 mM in serum free MDCK medium) prior to incubation with CPPs. Statistical significance of translocation was evaluated by pairwise t-tests (n=3). Furthermore, temperature-dependent translocation was studied at 4 and 37°C.

ZO-1 staining monitored by CLSM. MDCK cells seeded on filter inserts in 12-well plates were incubated with 1 μg/ml Hoechst 33342 to stain the nuclei. After several washing steps, cells were fixed for 30 min in 1% (v/v) PFA and permeabilized with 0.1% Triton X-100 in PBS for 1 min. Non-specific binding sites were blocked by incubating for 30 min with 1% BSA in PBS. Cells were then incubated for 1 hour with the polyclonal antibody rabbit anti-ZO-1 (1:200) in 1% BSA in PBS. After another washing step, cells were incubated with goat anti-rabbit Texas red (1:200) in 1% BSA in PBS for 1 hour and washed again. Cells were scanned as described for colocalization studies. As control experiments, cells incubated with the secondary antibodies without primary antibody staining confirmed the high specificity of the antibodies. To investigate the ZO-1 distribution in an inflammatory epithelial model, 10 days old MDCK cells were treated for 24 hours with a combination of 100 ng/ml IFN-γ and 1 ng/ml TNF-α in the apical and basolateral compartments, prior to ZO-1 antibody staining as described above and CLSM analysis. For graphical representation of ZO-1 distribution we used the maximum intensity projection as provided by IMARIS software (Bitplane AG, Zurich, Switzerland).

TEER measurement. MDCK cells were cultured as described above. Transepithelial electrical resistance (TEER) was measured in an Endohm tissue resistance measurement chamber (World Precision Instruments, Inc., Sarasota, USA.) and monitored with a Millicell-ERS meter (Millipore/Continental Water Systems, Bedford, USA.) as previously described [54]. To obtain values independent of the membrane area, TEER measurements were multiplied by the effective membrane area and reported as Ω cm^2. All measurements were reported as net TEER (total minus the mean TEER of two cell-free inserts).We also performed TEER measurement in an inflammatory IFN-γ/TNF-α epithelial model. 10 days old MDCK cells were treated for 24 hours with combinations of 10 - 1000 ng/ml IFN-γ and 0.1 - 1000 ng/ml TNF-α in the apical and basolateral compartments, prior to TEER measurement as described above. After a cytokine treatment for 2 days, IFN-γ and TNF-α were removed, cells washed with PBS and TEER recovery was measured.

Measurement of active form Rho-A and Rac-1 (pull-down assay and Western blot analysis). Active-form Rho-A or Rac-1, respectively, were measured in 0.5, 1 or 10 day old MDCK cell cultures with cell seeding densities as described for density experiments. MDCK

cells grown in 75 cm^2 flasks were lysed in lysis buffer plus protease inhibitor (25 mM Tris x HCl, pH 7.5, 1% NP-40, 150 mM NaCl, 5 mM MgCl2, 1 mM DTT, 5 % glycerol, 1 μg/ml each of aprotinin and leupeptin, and 1 mM PMSF) and clarified by centrifugation at 16 000 x g at 4°C for 15 min. Cell lysates were incubated with GST-Rhotekin-RBD or GST-human Pak1-PBD to pull down active Rho-A or Rac-1 in the presence of Swell Gel immobilized Glutathione at 4°C for 1 hour. After incubation, the mixture was centrifuged at 8 000 x g to remove unbound proteins. The resins were washed several times with lysis buffer and the sample was eluted by adding 50 μl of SDS sample buffer (5% β-mercaptoethanol, 125 mM Tris x HCl, pH 6.8, 2% glycerol, 4% SDS (w/v) and 0.05% bromophenol blue) and boiling at 95°C for 5 min. 20 μl of the sample volume were analyzed by SDS page and transferred to a nitrocellulose membrane. Unfractionated cell lysates were included for protein quantification and to verify that the Western blot analysis functioned properly. The active Rho-A and Rac-1 were detected by using a specific mouse monoclonal anti-Rho (1:500) or anti-Rac1 (1:1000) antibody. Goat anti-mouse antibody conjugated with horseradish peroxidase (1:5000) was used as the secondary antibody. To ensure equal protein content of the samples, actin was quantified by a specific mouse monoclonal anti-actin antibody (1:5000). Detection was performed with Chemiluminiscent Substrate followed by exposure to X-ray film (average exposure time was 10 sec to 5 min).

Bradford test. To obtain the same protein content for all samples of active form Rho-A or Rac-1 analyses, we determined protein contents by performing Bradford tests as described by the manufacturer. Absorption was measured at 570 nm using a ThermoMax microplate reader (Molecular Device, Sunnyvale, CA).

CPP translocation in an inflammatory IFN-γ/TNF-α model as studied by FACS. Filter grown 10 day old MDCK cells were treated with MDCK medium containing 10-1000 ng/ml IFN-γ and 0.1-1000 ng/ml TNF-α for 24 hours. Cytokines were present in both the apical and the basolateral media. After washing, cells were incubated from the apical side with CF-SAP (50 μM), hCT(9-32)-br (30 μM), Tat peptide (5 μM) or unconjugated fluorophore (50 μM or 30 μM, respectively) in serum free MDCK medium for 3 hours. FACS analysis was performed as described previously. Pairwise t-tests were performed to reveal the significance of an increase in translocation between untreated and cytokine treated cells (1000 ng/ml IFN-γ / 10 ng/ml TNF- α) (n=3).

Influence of cholesterol depletion in the inflammatory model was studied by pre-treating cells for 1 h with M-β-CD (10 mM in serum free MDCK medium) prior to

incubation with CPPs. Pairwise t-tests were performed to reveal the significance of a decrease in translocation between untreated and M-β-CD treated cells (n=5).

Cytotoxicity assay. An MTT assay was performed to measure cell viability in the described inflammatory model. 10 day old MDCK cells seeded in 96-well plates were treated with cytokine solutions of 10 - 1000 ng/ml IFN-γ and 0.1 - 1000 ng/ml TNF-α, for 24 hours, with 70 % EtOH for 7 min or left untreated as control cells. All wells were washed three times with medium and loaded with 100 µl medium. 10 µl MTT reagent (5 mg MTT powder in 1 ml PBS) were added to all wells. After 2 hours, the medium was removed and replaced with 100 µl detergent reagent (81 % isopropanol, 15 % SDS (20%) and 4% 1 M HCl. After additional 4 hours, absorbance was measured at 570 nm in a ThermoMax microplate reader (Molecular Device, Sunnyvale, CA).

Transepithelial permeability. 10 days old MDCK cells seeded on filters in 12-well plates were either treated with combinations of 10 - 1000 ng/ml IFN-γ and 0.1 - 1000 ng/ml TNF-α for 24 hours or used as untreated control cells. Prior to permeability measurements, all monolayers were checked for TEER as described above. Confluent MDCK monolayers were equilibrated for 30 min in HBSS, pH 7.4. Monolayers were loaded apically with 0.5 ml HBSS solutions containing 30 µM CF or [^{3}H]-mannitol (4 µCi/ml), respectively and 1.8 ml of HBSS was added to the basolateral side. Blank wells were used as controls. Samples of 100 µl were withdrawn from the basolateral receiver compartment and immediately replaced with the same volume of HBSS at t = 0, 1 h, 2 h and 4 h. Effective permeability coefficients of 5(6)-carboxyfluorescein (CF) were determined by direct fluorescence spectrometry (λ_{ex} 492 nm, λ_{em} 517 nm; Varian CARY Eclipse, Zug, Switzerland). CF concentrations transported into the basolateral compartment were extrapolated from a standard curve and expressed as µM cm^{-2} h^{-1} for compound transported. For [^{3}H]-mannitol permeability studies, the samples were mixed with 2 ml scintillation cocktail (Ultima Gold, PerkinElmer Life Sciences, Beltsville, MD) and radioactivity was counted using a liquid scintillation spectrometer from Beckman (Model LS 6500, Fullerton, CA).

RESULTS

CPP translocation in MDCK cells – As demonstrated by CLSM, proliferating MDCK cells one day post seeding showed marked cellular translocation when exposed to either one of the two cationic CPPs, CF-SAP or CF-hCT(9-32)-br (Fig.1A or 1B, left inserts, respectively). At this time point the internalized fluorescence featured a punctuated pattern

indicating localization in discrete vesicular compartments in the cytoplasm typical for endocytosis [55]. In contrast, confluent monolayers, 10 days post seeding with well-established cell-to-cell contacts, enabled significantly less translocation (Fig.1A or 1B, right insets). The measure of punctuated fluorescence in the cytoplasm was markedly reduced, and the CPPs accumulated mainly in the junctional complex. Unlabeled cells and cells incubated with the fluorescence marker carboxyfluorescein alone were analysed as controls. No cellular fluorescence was observed in both cases (data not shown).

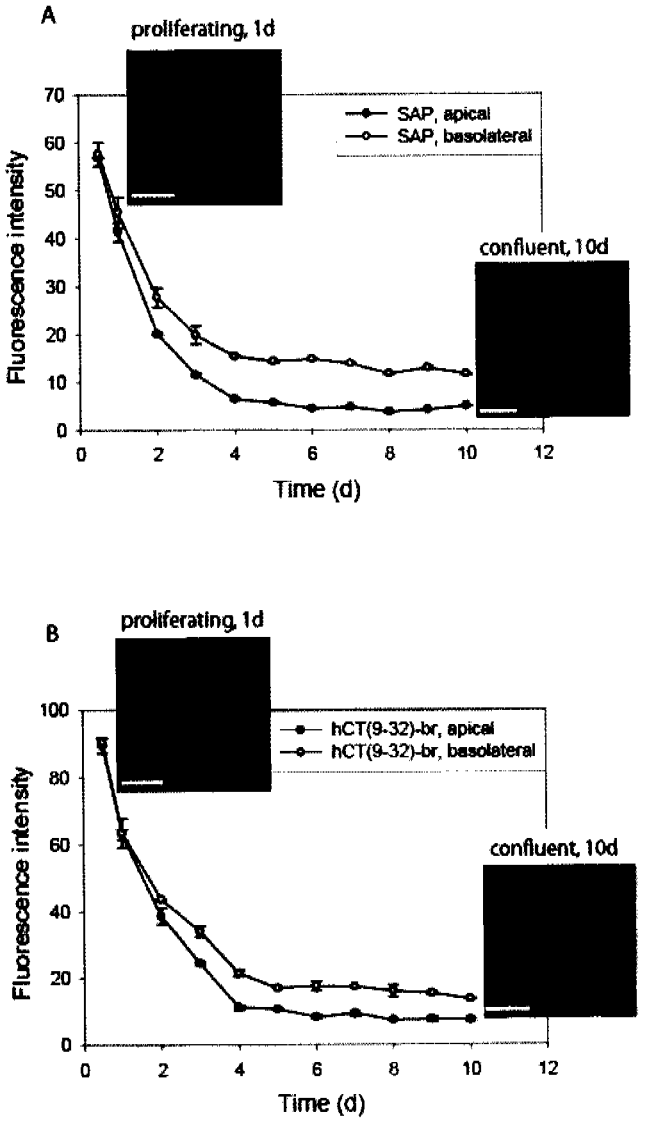

Figure 1. Translocation of CF-SAP and CF-hCT(9-32)-br in MDCK cells varying in differentiation states. (FACS and CLSM). MDCK cells ranging from 12 hours to 10 days post seeding were incubated for 3 hour with 50 μM CF-SAP (A) or 30 μM CF-hCT(9-32)-br (B) (FACS). Fluorescence intensities were normalized to control cells of the same age. Inserted CLSM pictures show incubation of 1 or 10 day old MDCK cells with CF-SAP (1A, left or right picture, respectively) or CF-hCT(9-32)-br (1B, left picture or right picture, respectively) for 1 hour.
The scalebar is 10 μm.

FACS analysis of CPP translocation – To confirm the contrasts in translocation in proliferating versus confluent MDCK cells, we quantified the translocation of CF-SAP and CF-hCT(9-32)-br, respectively, by FACS analysis. As shown in Fig. 1A and 1B, translocation in proliferating MDCK was marked for both CPPs, and similar whether treated from the apical or the basolateral side. With increasing culture time, however, the degree of translocation from both the apical and the basolateral sides decreased strikingly. At confluence, i.e. after a growth period of 4 days, apical translocation reached a baseline level of around one tenth of the initial value and stayed constant for the rest of the growth period. Translocation rates from the basolateral side followed a similar trend but were around twice as high than those from the apical side, probably resulting from the higher surface area of the basolateral membrane. Fluorescence intensities were normalized to untreated control cultures of the same age.

Endocytic translocation into proliferating and confluent MDCK layers – To further identify the translocation mechanisms of CF-SAP and CF-hCT(9-32)-br in proliferating and confluent MDCK cells, we analysed by FACS the translocation under conditions which inhibited endocytosis. Non-treated cells and cells incubated with carboxyfluorescein alone (data not shown) were used as negative controls. At 4°C, translocation of CF-SAP and CF-hCT(9-32)-br, respectively, was strongly reduced in both proliferating and confluent MDCK cells (Fig. 2A and 2B). Previously, inhibition of endocytosis at 4°C was not only attributed to a blockade of active processes but also to rigidification of lipid membranes at this temperature [56]. Therefore, we also tested CPP translocation at 37°C after pre-incubation with NaN_3/2-deoxyglucose, which was expected to impair energy-dependent translocation by ATP depletion. As shown in Fig. 2A and 2B, translocation of both peptides in proliferating as well as confluent MDCK cells was blocked through pre-treatment with NaN_3/2-deoxyglucose, supporting endocytosis as the underlying translocation mechanism in proliferating as well as confluent MDCK cells.

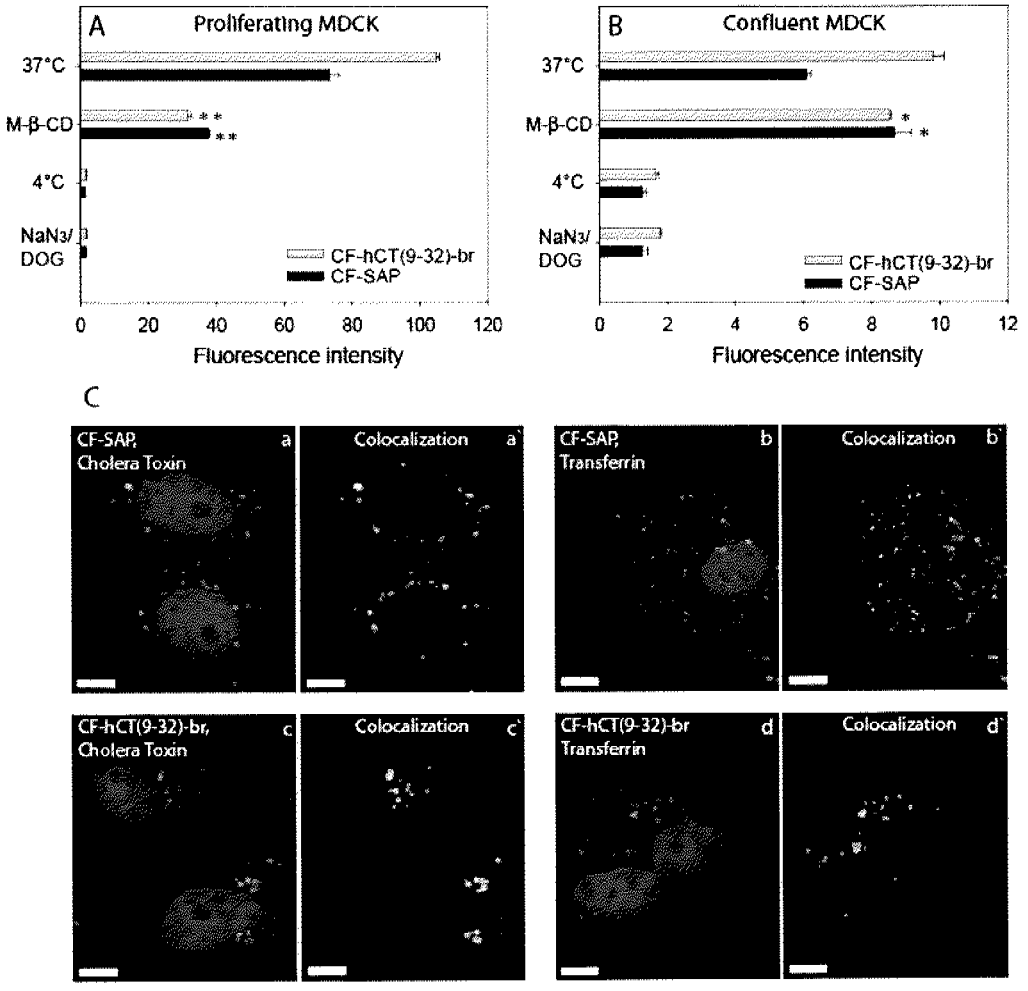

Figure 2. Translocation of CF-SAP or CF-hCT(9-32)-br into MDCK cells. A and B. Translocation and endocytosis inhibition (FACS). Proliferating MDCK cells (Fig. 2A) and confluent MDCK cell (Fig. 2B) were incubated for 3 hours at either 37 or 4°C with 50 μM CF-SAP (black bars) or 30 μM CF-hCT(9-32)-br (grey bars). Endocytosis inhibition was performed by pre-treating cells with 10 mM M-β-CD or 0.1% NaN_3 /50 mM 2-deoxyglucose (NaN_3/DOG) before incubation with CPPs. Fluorescence intensities are normalized to control cells. Significant and highly significant results are indicated as * or ** (t-test, n=3). **C. Colocalization study with cholera toxin or transferrin in proliferating MDCK cells.** Colocalized vesicles in yellow, CPPs in green and endocytosis markers (cholera toxin and transferrin) in red. Cells were incubated with 50 μM CF-SAP or 30 μM CF-hCT(9-32)-br and simultaneously stained with 10 μg/ml cholera toxin or 50 μM transferring for 30 min. Colocalization of both CPPs with cholera toxin suggests lipid raft-mediated endocytosis (a,c). Colocalization with transferrin suggests clathrin-mediated endocytosis (b,d) for both CPPs. Panel a –CF-SAP and cholera toxin. Panel B – CF-SAP and transferrin. Panel C - CF-hCT(9-32)-br and cholera toxin; Panel D - CF-hCT(9-32)-br and transferrin. Panels a`, b`, c` and d` represent related overlay micrographs showing colocalized vesicles in white. The scalebar is 7 μm.

Endocytosis in proliferating MDCK cells involves both lipid rafts and clathrin-coated pits – Lipid rafts are defined by their cholesterol enrichment. M-β-CD extracts cholesterol from cell membranes and, therefore, disrupts lipid rafts whereas it does not disturb clathrin-dependent endocytosis [57-60]. Hence, to investigate involvement of lipid raft dependent translocation of extracellular CF-SAP and CF-hCT(9-32)-br, we pre-treated proliferating MDCK cells with M-β-CD prior to incubation with the CPPs. As shown in Fig. 2A, reduction of intracellular fluorescence was highly significant in proliferating MDCK cells, suggesting lipid raft involvement in the endocytic translocation process. Fluorescence intensities were normalized to untreated control cells. To confirm this observation, we performed colocalization studies of CF-SAP and CF-hCT(9-32)-br with transferrin and cholera toxin by CLSM. Transferrin is a well-known marker for endocytic translocation via clathrin-coated pits [61, 62], whereas cholera toxin exploits clathrin-independent, lipid raft-mediated endocytosis [58-60]. To assess whether the two CPPs were internalized via one of these endocytic pathways, CF-SAP and CF-hCT(9-32)-br were each mixed with TRITC-labeled transferrin or Alexa Fluor 594-labeled cholera toxin, respectively, and the binary mixture incubated with proliferating MDCK cells (Fig.2C). Related colocalization micrographs demonstrate colocalized vesicles of CPPs and transferrin or cholera toxin, respectively (Fig. 2C a', b', c', d'). In detail, Figure 2C a and a' shows a corresponding set of experiments with CF-SAP and cholera toxin, Fig. 2C b and b` with CF-SAP and transferrin, Fig2C c and c` with CF-hCT(9-32)-br and cholera toxin, and finally Fig 2C d and d` with CF-hCT(9-32)-br and transferrin. CF-SAP and CF-hCT(9-32)-br showed partial colocalization with both cholera toxin and transferrin, suggesting an involvement of lipid rafts as well as clathrin-dependent endocytosis in the translocation of CF-SAP and CF-hCT(9-32)-br into proliferating MDCK cells. In fact, we calculated colocalization rates of the two peptides with either one of the two endocytosis markers of about 35-54 % (data not shown). Taken together, our results indicate in a consistent fashion that CF-SAP and CF-hCT(9-32)-br are internalized by proliferating MDCK cells via endocytosis involving both lipid rafts and clathrin-coated pits. For the rest of this work we concentrated exclusively on the lipid raft mediated pathway. *Endocytic pathway in confluent MDCK cells* - To further investigate the involvement of lipid rafts in the endocytosis of CF-SAP and CF-hCT(9-32)-br by confluent MDCK, we pre-treated cell layers with M-β-CD prior to incubation with the peptides. Fluorescence intensities were normalized to untreated control cells. As shown in Fig. 2B, reduction in intracellular fluorescence was only marginal in the case of CF-hCT(9-32)-br and absent for CF-SAP (Fig. 2B). As there was only low translocation of CF-SAP and

CF-hCT(9-32)-br into confluent MDCK cells, colocalization experiments with endocytosis markers did not yield unequivocal results, neither in favour nor against involvement of lipid rafts (data not shown).

Compound unspecific endocytic slow-down - We next addressed the question whether the observed endocytic slow-down in CPP translocation was a distinct phenomenon for CF-SAP and CF-hCT(9-32)-br, or an unspecific feature of endocytosis in confluent MDCK cells. FITC-dextran and TRITC-labeled transferrin are well known markers of endocytosis, whereas CF-hCT(9-32) and FITC-labeled Tat have been previously reported to be taken up by endocytosis [7, 62-64]. Filter grown MDCK cell cultures ranging from 12 hours to 10 days post seeding were incubated with solutions of FITC-dextran, TRITC-labeled transferrin, CF-hCT(9-32) and FITC-labeled Tat, respectively. Fluorescence intensities were normalized to untreated control cells of the same age. Fig. 3 shows all compounds to be readily taken up in proliferating MDCK cells whereas the degree of translocation decreased markedly with increasing culture time. These findings suggest a compound unspecific slow-down of endocytosis in confluent MDCK cells.

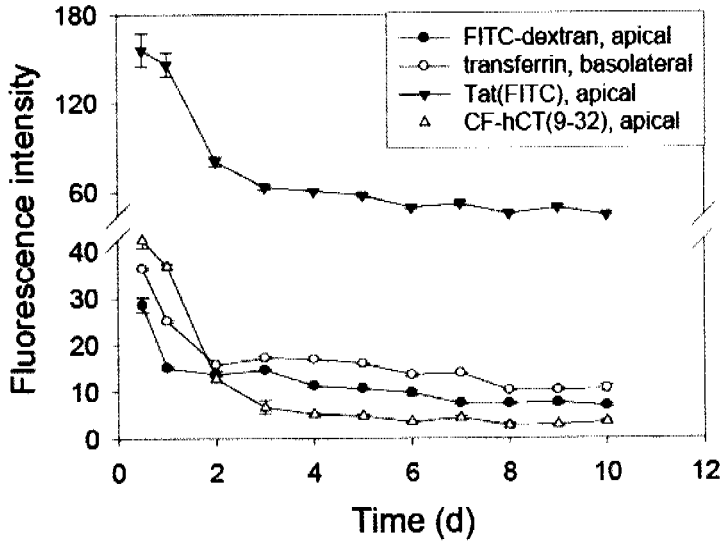

Figure 3. Endocytic translocation into MDCK cells varying in differentiation states. (FACS). MDCK cells ranging from 12 hours to 10 days post seeding were incubated for 3 hour with 30 μM FITC-dextran, 5 μM Tat(FITC) or 30 μM CF-hCT(9-32)-br from the apical side and with 30 μM transferrin from the basolateral side. Fluorescence intensities were normalized to untreated control cells of the same age.

Correlation of endocytic slow-down with increasing cell density and formation of tight junctions. Effects of seeding and cell culture density - To evaluate whether seeding and cell culture density had an impact on CPP translocation efficiency in MDCK cells, we compared translocation rates of CF-SAP and CF-hCT(9-32)-br, respectively, in half or one day old MDCK cells of low or high seeding density, as well as in 10 day old, well-differentiated cell cultures with low seeding density but high final cell culture density. As shown in Table 2, translocation in cells with high initial seeding density is much lower than in that of low seeding density of the same age (~84% less translocation) indicating the great impact of cell seeding density on the translocation efficiency. Still, half or one day old cells with high seeding density feature slightly higher translocation rates than 10 day old MDCK cells with a low seeding density but a high final cell culture density (~92% less translocation). Fluorescence intensity of 0.5 day old, low density cells was set as 100%.

Table 2. Fluorescence intensities (%) of CF-SAP and CF-hCT(9-32)-br in MDCK cells varying in growing period and seeding density. Fluorescence intensities are normalized to control cells of the same age.

	Fluorescence intensity (%)	
Growing period (Seeding density)	CF-SAP	CF-hCT(9-32)-br
0.5 days (2×10^4 cells/cm^2)	100 ± 9.16	100 ± 2.49
1 day (2×10^4 cells/cm^2)	65.61 ± 3.12	64.91 ± 4.47
10 days (2×10^4 cells/cm^2)	7.42 ± 0.14	7.56 ± 0.43
0.5 days (5×10^5 cells/cm^2)	14.94 ± 0.21	18.01 ± 0.78
1 day (5×10^5 cells/cm^2)	8.1 ± 0.08	8.72 ± 0.08

TEER measurements – To demonstrate the development of the tight junctional network in MDCK cultures we monitored their TEER values during the growing period of 10 days. As shown in Fig. 4A, TEERs increased initially and then dropped to a stable value of around 130 Ω cm^2 after 4 or 5 days.

ZO-1 staining - To determine whether the above described endocytic slow-down correlated with the formation of tight junctions, we performed ZO-1 staining in MDCK cell cultures from day 1 until day 10 post seeding. As shown in Fig. 4B, soon after seeding cells begin to form small cell clusters and establish first cell-to-cell contacts. Formation of tight junctions immediately started where cells came into contact, particularly at the corners between the cells. Day after day, with increasing cell cluster size, more cell-to-cell contacts were established and after day 4 post seeding a coherent tight junctional network was formed. At that time point, CPP translocation had yet reached a rather low level and stayed constant for the rest of the growth period (see Fig. 1A and B). Until day 10 post seeding, cell culture density increased constantly, resulting in a fully organized and polarized tightly packed monolayer. Taken together, the observed endocytic slow-down correlates directly with cell density and the formation of a coherent tight junctional network.

Monitoring active form Rho-A and Rac-1 – Rho-family GTPases have been recognized to be intimately involved in the regulation of endocytic traffic and cellular differentiation [36, 65]. To elucidate a potential correlation between cellular differentiation and endocytic activity, respectively, and Rho-GTPase activation, we investigated the contents of GTP-bound, active form Rho-A and Rac-1, respectively, in one-day old MDCK cells with low or high seeding density as well as in 10 day old, well-differentiated MDCK cells having a high cell culture density. As shown in Fig. 5A and C, the contents of total Rho-A and Rac-1, respectively, in all three samples were alike, confirming the equal protein content of all samples measured by a Bradford test (data not shown). One-day old, low density cells showed the highest contents of active form Rho-A, whereas active Rho-A was strongly reduced in one-day old, but high density cells, and almost abolished in 10-day old MDCK cells (Fig. 5A). For Rac-1, inverse activities were observed: almost no active Rac-1 was found in one-day old, low density cells, slightly higher contents in one-day old, high density cells, and high contents in 10 day old MDCK cells (Fig. 5C). Figure 5B and D show densitometric quantifications of active form Rho-A and Rac-1 when normalized to control values of total Rho-A or Rac-1, respectively. Our data indicate a direct correlation between endocytic activity and active form Rho-A, as well as between cell density, cellular differentiation and endocytic slow-down, respectively, and active form Rac-1. These findings

suggest the involvement of Rho-A and Rac-1 in the regulation of endocytosis in the context of cellular differentiation.

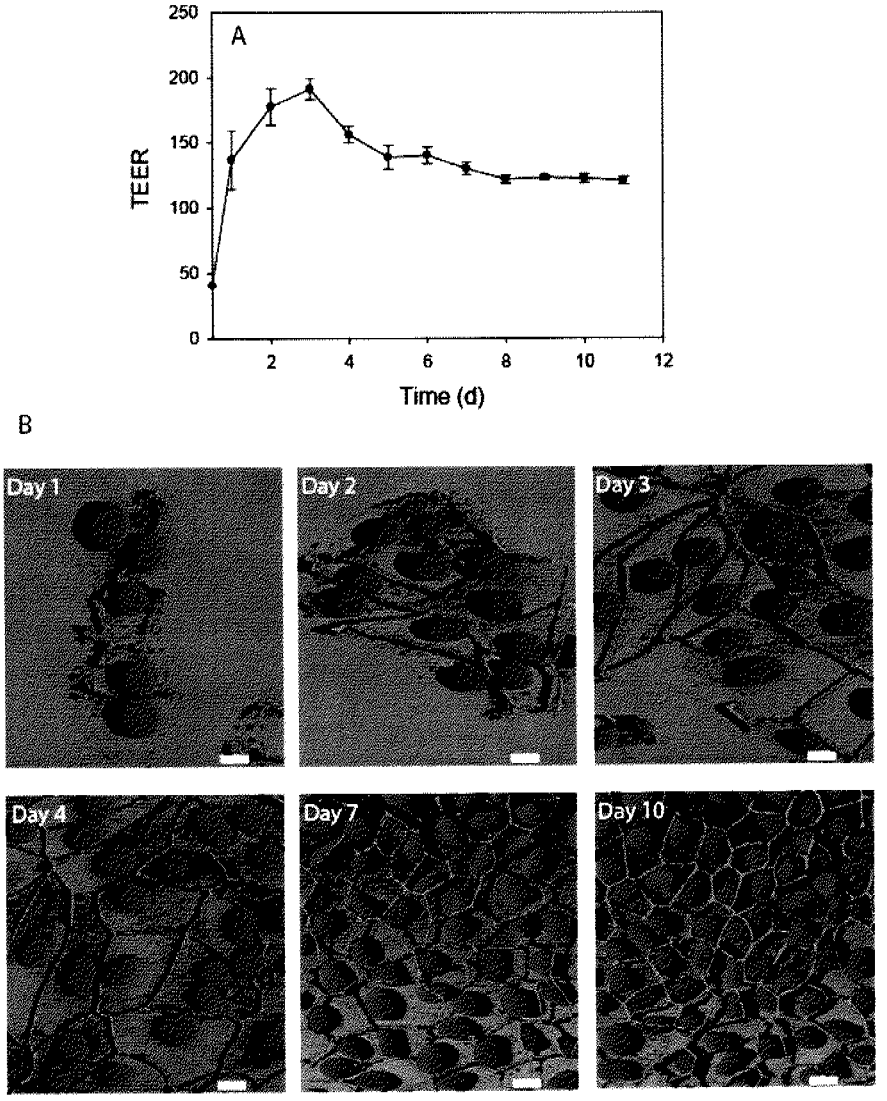

Figure 4. Tight junction formation in MDCK cells. A. TEER measurement. Transepithelial electrical resistance (TEER) was measured in MDCK cells ranging from 12 hours to 10 days post seeding. To obtain values independent of the membrane area, TEER measurements were multiplied by the effective membrane area and reported as Ω x cm^2. All measurements are reported as net TEER (total minus the mean TEER of two cell-free inserts).

B. ZO-1 staining. ZO-1 staining was performed in MDCK cells ranging from 12 hours to 10 days post seeding. The Scalebar is 20 μM.

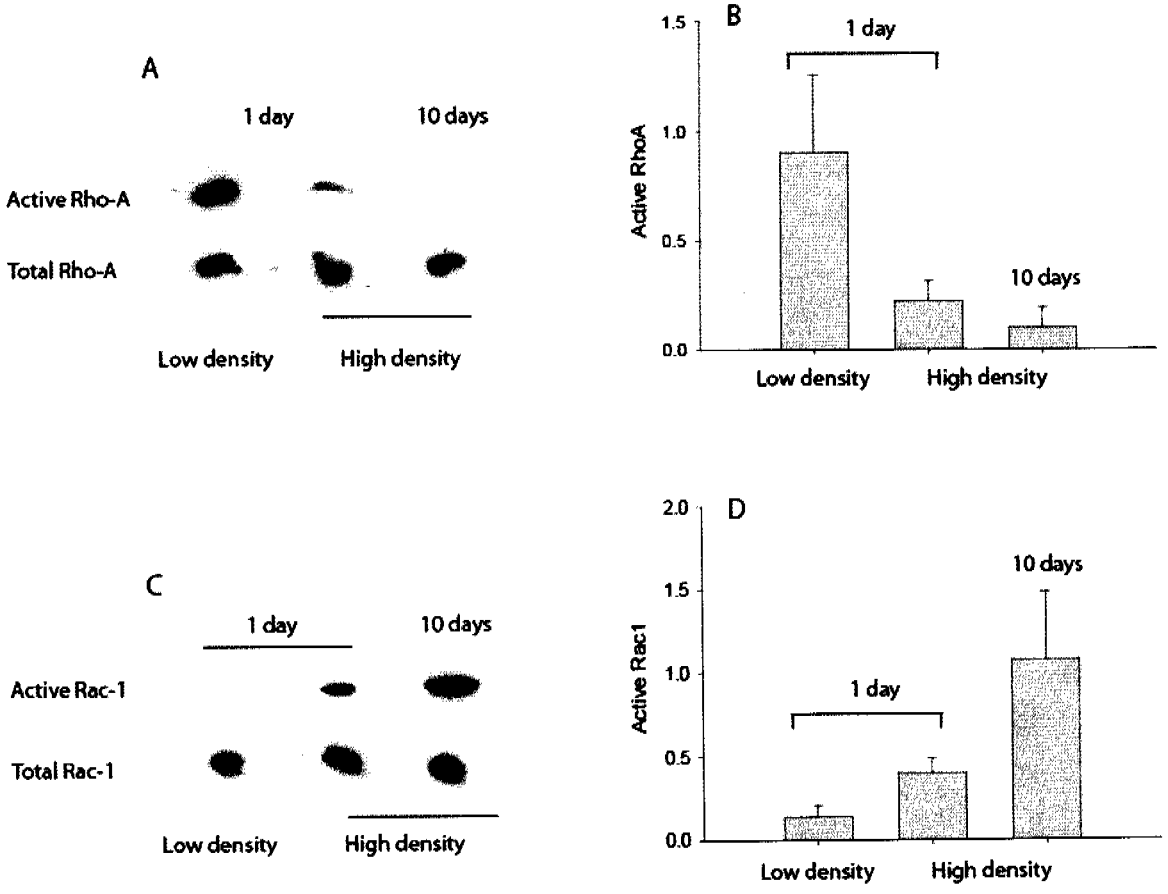

Figure 5. Active form Rho-GTPases. Contents of GTP-bound, active form Rho-A (Fig. 5A) and Rac-1 (Fig. 5C), respectively, were measured in one-day old cells with low or high seeding density as well as in 10 day old, well-differentiated MDCK cells with low seeding density but high final cell culture density and compared to total Rho-GTPase contents. Figure 5B and D show quantification of active form Rho-A and Rac-1 when normalized to control values of total Rho-A or Rac-1, respectively.

CPP translocation in an inflammatory IFN-γ/TNF-α model - To further elaborate our findings towards the correlation between endocytic slow-down and cellular differentiation, we studied CPP translocation in MDCK monolayers of compromised tight junctional organization. Therefore, prior to incubation with CPPs, fully organized MDCK monolayers were treated with MDCK medium containing IFN-γ and TNF-α at stepwise increased concentrations. As shown in Fig. 6, CPP translocation was significantly enhanced upon such inflammatory pre-treatment. A combination of IFN-γ and TNF-α provided synergistic effects on epithelial barrier function [66, 67], whereas IFN-γ or TNF-α alone were less effective.

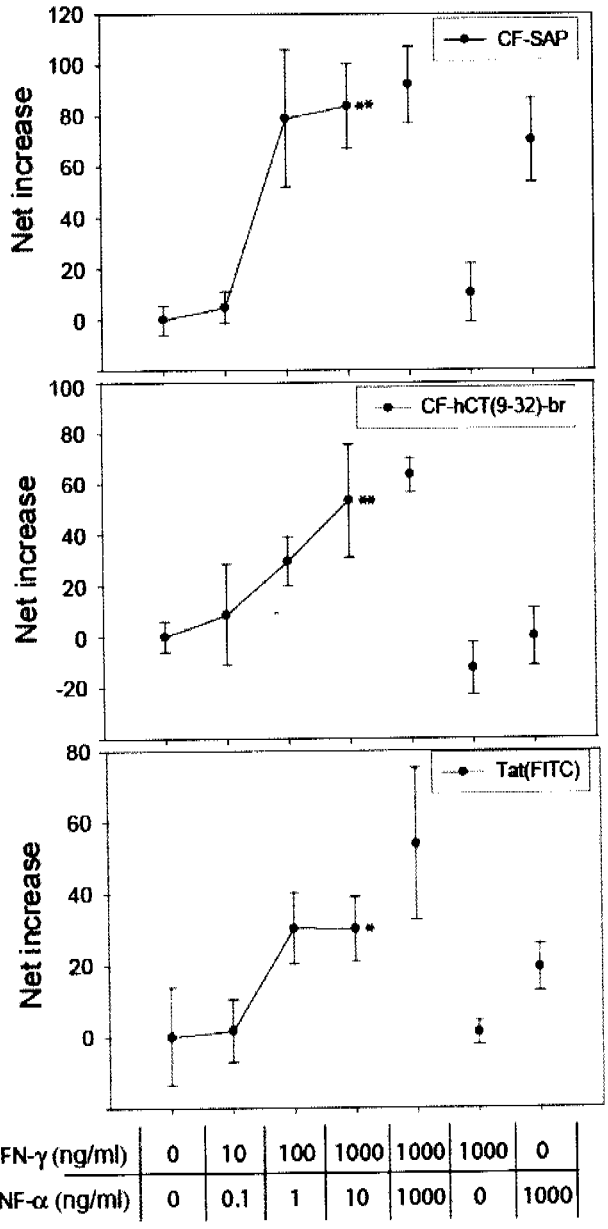

Figure 6. Net increase of CPP translocation into an inflammatory IFN-γ/TNF-α model by FACS. Fully organized MDCK monolayers were treated with MDCK medium containing IFN-γ and TNF-α in concentrations ranging from 0-1000 ng/ml, prior to incubation with 50 μM CF-SAP, 30 μM CF-hCT(9-32)-br or 5 μM Tat(FITC) for 3 hours. Fluorescence intensities are normalized to control cells.
Significant and highly significant results are indicated as * or ** (t-test, n=3).

Transepithelial permeability and cytotoxicity in an inflammatory IFN-γ/TNF-α model- To further evaluate the effects resulting from inflammatory cytokine pre-treatments, we determined the transepithelial permeability of CF and [^{3}H]-mannitol in confluent MDCK monolayers with and without prior cytokine pre-treatment. Cell culture inserts featured TEER values of 120 ± 12 Ω cm^2 for untreated MDCK layers. When MDCK monolayers were treated with a IFN-γ/TNF-α mix of 1:100 ng/ml within 24 hours, TEER values decreased significantly (36 ± 9 Ω cm^2) and stayed at low values within the investigated time interval of

48 hours. Removal of the cytokine mix led to a complete recovery to normal TEER values within 72 hours (data not shown).

As demonstrated in Fig. 7A, pre-treatments with IFN-γ/TNF-α increased the permeability of [^{3}H]-mannitol in a time and concentration dependent fashion. This was confirmed by a concomitant increase in CF flux in the same time and concentration dependent manner (Fig. 7B). Cytokine concentrations and application periods correlated directly with disintegrations per minute (DPM) and permeability coefficients, respectively.

To investigate cell viability after cytokine pre-treatment, we performed a series of MTT toxicity assays. Even at the highest cytokine concentration, i.e. 1000 ng/ml for each IFN-γ and TNF-α, cell viability was reasonably preserved at 80 % as compared to untreated control cells and EtOH treated cells. Viabilities were even better at lower concentrations.

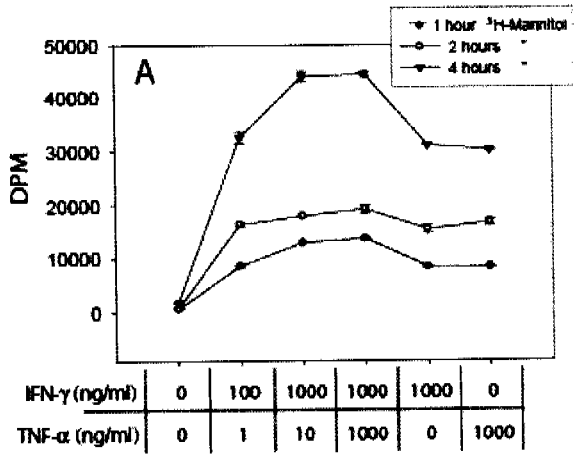

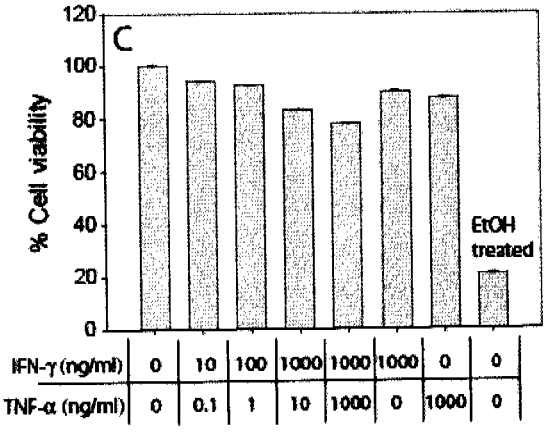

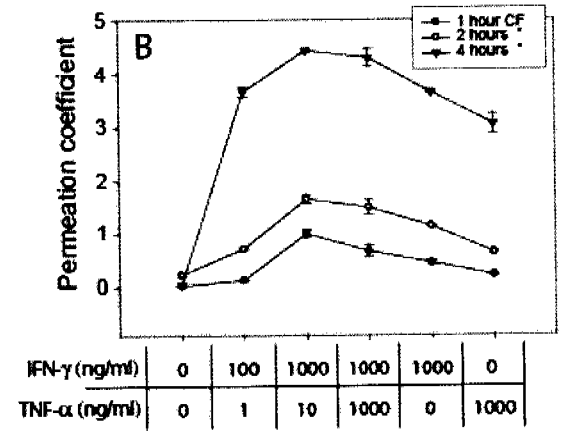

Figure 7. Transepithelial permeability and cytotoxicity in an inflammatory IFN-γ/TNF-α model. Transepithelial permeability of [^{3}H]-mannitol (Fig. 7A) and CF (Fig. 7B) was measured in confluent MDCK monolayers with or without prior cytokine pre-treatment (IFN-γ and TNF-α in concentrations ranging from 0-1000 ng/ml). CF concentrations transported into the basolateral compartment were expressed as μM cm^{-2} h^{-1} for compound transported. Figure 7C shows an MTT assay in confluent MDCK monolayers pre-treated with IFN-γ and TNF-α in concentrations ranging from 0-1000 ng/ml. Untreated control cells and cells treated with EtOH as a positive control were included.

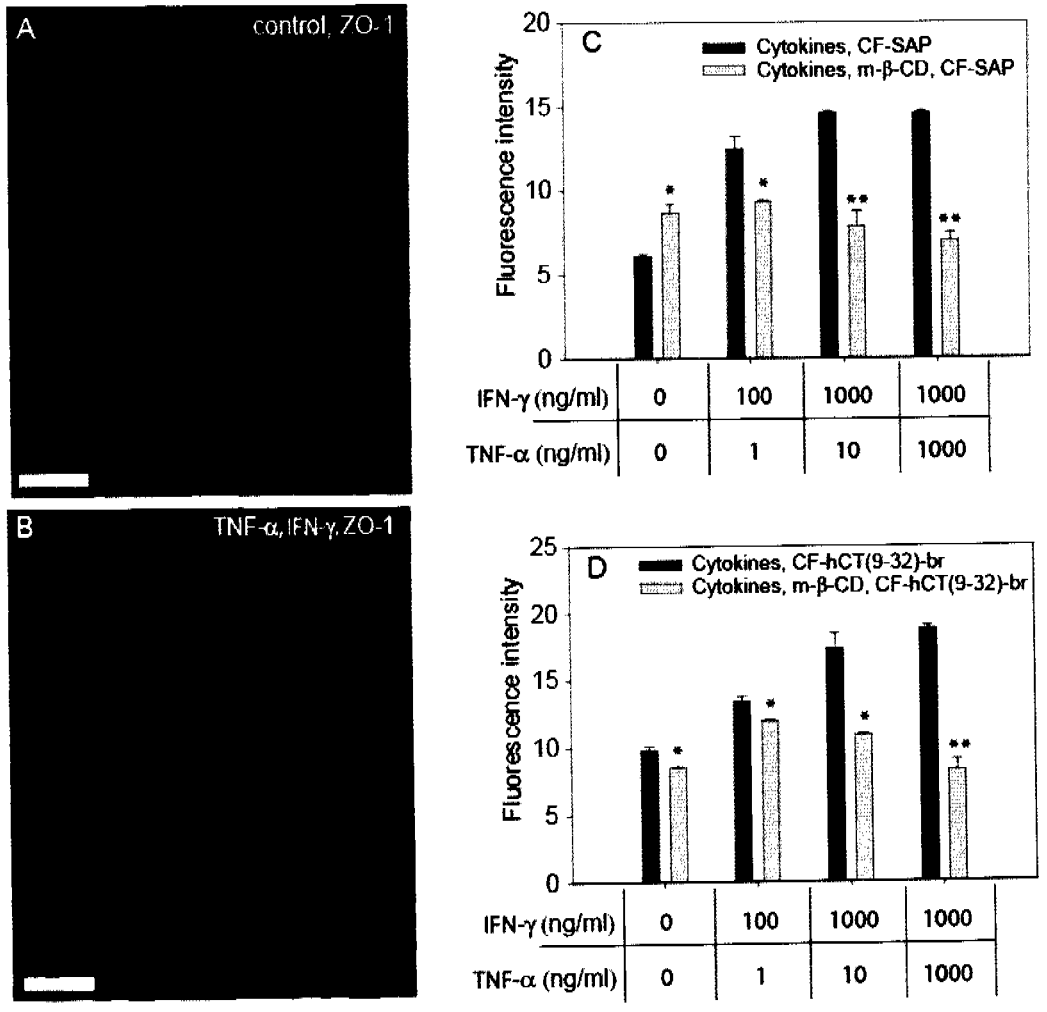

Figure 8. Redistribution of tight junctions. A and B. Distribution of the TJ protein ZO-1 with or without prior cytokine treatment (CLSM). ZO-1 staining in cytokine pre-treated confluent MDCK cells (IFN-γ/TNF-α 100/1 ng/ml) was compared to ZO-1 staining in control cells. Maximum intensity projection is shown. The scalebar is 20 μm.

C and D. Involvement of lipid rafts in enhanced translocation in inflammatory MDCK model (FACS). MDCK cells were pre-treated with IFN-γ and TNF-α in concentrations ranging from 0-1000 ng/ml prior to incubation for 3 hours with 50 μM CF-SAP (Fig. 8C) or 30 μM CF-hCT(9-32)-br (Fig. 8D). Additionally, cholesterol depletion was performed by pre-treating cells with 10 mM M-β-CD before incubation with CF-SAP or CF-hCT(9-32)-br. Fluorescence intensities are normalized to control cells. Significant and highly significant results are indicated as * or ** (t-test, n=5).

Cytokines induce redistribution of the tight junction protein ZO-1 – Cytokine-induced redistribution of tight junction proteins to the membrane has been observed by Bruewer et al. [67]. To investigate changes in the distribution of the tight junction protein ZO-1 due to cytokine treatment, we performed ZO-1 staining in cytokine pre-treated MDCK cells (IFN-γ/TNF-α 100:1 ng/ml) and compared it to ZO-1 staining in control cells. As shown in Fig. 8B, cytokine exposure induced no drastic but relevant redistribution of the plaque protein ZO-1 as compared to control cells (Fig. 8A). Redistribution was in a cytokine concentration-dependent way (data not shown).

Involvement of lipid rafts in enhanced translocation in inflammatory MDCK model - As demonstrated in Fig. 2A and 2B, lipid rafts play a significant role in the endocytosis of CPPs in proliferating but not in confluent MDCK cells. Cytokine pre-treatments, however, restored much of the propensity for lipid raft mediated endocytosis. This is demonstrated by the inhibitory effect of M-β-CD on the translocation of CF-SAP and CF-hCT(9-32)-br in cytokine pre-treated, confluent MDCK. The reduction in CPP translocation was in a cytokine concentration-dependent fashion (Fig. 8C and 8D). Our findings suggest – for the studied inflammatory model – that a redistribution of tight junction proteins associated with lipid raft microdomains [67, 68] led to a concomitant restoration of lipid rafts on confluent MDCK cultures which reinstates the propensity for lipid raft-mediated endocytosis of CPPs.

DISCUSSION

In recent years, increasing numbers of CPPs have been described and evaluated for their ability to deliver therapeutics into cells that otherwise cannot translocate cellular membranes. In this work, we investigated the effect of cell density and differentiation state on the translocation kinetics and pathways of two CPPs in epithelial cell models and elucidated the underlying cellular mechanism for the thereby observed differentiation restricted endocytic slow-down. Furthermore, based on translocation studies in a cytokine induced inflammatory epithelial model, we point towards inflamed epithelia as potential niche for a clinical utilization of CPPs as cellular vectors for therapeutic cargoes.

To date, *in vitro* CPP translocation studies are mostly carried out in proliferating, "leaky" cell models devoid of tissular characteristics or junctional complexes, s [19-23]. For our studies we chose the kidney epithelial MDCK cell line. When grown to confluence, MDCK cells feature typical characteristics of polarized epithelia and mimic, e.g., the epithelial organization of drug absorption sites, such as the respiratory and intestinal mucosae. Sharply

contrasting to the ready translocation of Tat peptides into proliferating cell cultures, Violini et al. [23] observed a lack of intracellular accumulation of fluorescein conjugated Tat-peptide in confluent MDCK and CaCo-2 cells. Otherwise, "leaky" cell models, such as HeLa and KB 3-1 cells, showed cytoplasmic and nuclear accumulation. In one of our previous studies to this subject, using linear human calcitonin derived CPPs, Tat(47-57) and penetratin(43-58), translocation into proliferating HeLa cells was superior to that in a fully polarized MDCK model [7]. Similarly, Zhang et al. [24] suggested a cell type-specific barrier to control the translocation of RI-Tat-9 into HeLa, MT2, MDCK and Caco-2 cells.

Previously we observed marked translocation efficiency in HeLa cells for the linear proline-rich sweet arrow peptide CF-SAP (Tab. I) [15-17] and the branched derivative of the linear human calcitonin derived CPP CF-hCT(9-32) [7], denoted as CF-hCT(9-32)-br (Tab. I) [14]. Both CPPs were readily taken up by HeLa cells through lipid raft-mediated endocytosis followed by endosomal escape [18]. In the current study in proliferating MDCK cells, we observed concomitant lipid raft-mediated endocytosis and endocytosis via clathrin coated pits, indicating a cell line specific contrast to the pathway found in HeLa cells. After reaching confluence, however, translocation of the investigated CPPs in MDCK monolayers dropped substantially. Previously, Hallbrink et al. [34] found similar differences in intracellular MAP and penetratin uptake in CHO cells to correlate to peptide-to-cell ratio, but due to differences in cell seeding densities, rather than culture time.

Therefore, we investigated in more detail the impact of cellular differentiation on efficiency and mechanism of CPP translocation. By comparing proliferating versus confluent MDCK cell cultures, we found the slow-down in endocytic activity on the one hand to relate to the increasing cell culture density and the formation of tight junctions on the other. The observed slow-down was not specific for the investigated two CPPs but compound unspecific as it was a common feature of several markers for cellular endocytosis.

To investigate the underlying cell biology controlling the endocytic slow-down, we analysed the occurence of active Rho-GTPases, Rho-A and Rac-1 in MDCK layers of different states of differentiation. Rho-GTPases are known to regulate a variety of cellular events such as actin polymerization, cell morphology and polarity, cell growth control, transcription and membrane trafficking events such as endocytosis [36-42]. Apparently, Rho-GTPases mediate the signalling interface between endocytic traffic and actin cytoskeleton and, through cytoskeletal modification, affect epithelial barrier function [43-45]. For several cellular functions inverse activities of Rho-A versus Rac-1 and Cdc42 GTPases have been observed [36, 62, 69, 70], such as in actin reorganization and endocytosis. In polarized MDCK cells,

Rho-A activation has been found to stimulate apical and basolateral endocytosis whereas Rac-1 activation led to decreases in apical and basolateral endocytosis [69, 70]. During the formation of epithelia, Cdc42 and Rac-1 play a prominent role in the generation of intimate cell-to-cell contacts [36, 71, 72]. With respect to the cellular uptake of selected CPPs, our findings indicate an intimate involvement of Rho-family GTPases in the differentiation restricted regulation of endocytic traffic. The extent of CPP endocytosis was directly correlated with active form Rho-A, whereas active form Rac-1 correlated with endocytic slow-down, cell density and cellular differentiation. This reflects the mentioned inverse roles of Rho-A and Rac-1 in the regulation of endocytosis. To our knowledge, this is the first study to cast light on the cell line and differentiation restricted translocation of CPPs into epithelial cell models and its underlying cellular mechanism.

We further elaborated an interesting relationship between endocytic slow-down and cellular differentiation in an inflammatory epithelial IFN-γ/TNF-α model that was used to mimic inflammatory conditions in epithelia. Typically, inflammatory epithelial diseases, such as inflammatory bowel disease, or airway diseases originating from cystic fibrosis or asthma bronchiale, are associated with elevated cytokine production and significant barrier dysfunction [46-52]. We found the translocation efficiency of CPPs in the inflammatory IFN-γ/TNF-α model to be significantly enhanced as compared to untreated control. Depending on cytokine concentration, endocytosis of CPP rose by up to 90 %, concomitant to an increase in permeability of [^{3}H]-mannitol as a marker for paracellular permeability. By analysis of cell viability we could show that increases in endocytosis and paracellular permeability, secondary to cytokine treatments, were not related to cell death, at least not under the conditions tested. Nevertheless, small transient conductive leaks are likely to occur [73]. Fish et al. [66] suggested that TNF-α may have synergistic effects on IFN-γ mediated alterations of epithelial cell function. In fact, the combined cytokine treatment of IFN-γ and TNF-α allowed lower concentrations of individual cytokine applications to favor lower toxicity profiles as compared to non-combined cytokine treatments.

Bruewer et al. [67] found the exposure of epithelia to cytokines to induce a redistribution of tight junctional proteins that was not associated with a significant change in the total levels of these proteins, suggesting protein redistribution rather than membrane degradation. Changes in tight junctional functionality have been implicated in the pathogenesis of several inflammatory epithelial diseases. For instance, redistribution of tight junction proteins has been observed in patients suffering from active inflammatory bowel disease (IBD), where proinflammatory cytokines such as IFN-γ and TNF-α are elevated [74,

75]. Increased levels of inflammatory cytokines have also been found on the bronchial epithelia of cystic fibrosis patients [76] and on the gastric epithelium of patients infected with Helicobacter pylori [77]. On the cellular level, changes in the integrity of tight junctions in combination with a redistribution of tight junctional proteins have been found in primary human airway epithelial cells from cystic fibrosis patients [51]. In conformity with these findings, we demonstrated in confluent MDCK that upon cytokine treatment the tight junctional plaque protein ZO-1 redistributed in a cytokine concentration dependent way. Previously, Nusrat et al. [68] denoted tight junctions as lipid raft membrane microdomains, enriched in cholesterol, and featuring an affiliation of the tight junction proteins with Triton X-100-insoluble membrane rafts. Their study on the influence of cytokine treatment on the affiliation of tight junction proteins with membrane lipid rafts revealed this affiliation to be only minimally affected. Furthermore, cytokines did not alter the overall biophysical properties of membrane rafts [67].

We have shown in this study that lipid rafts were crucial for CPP endocytosis in proliferating MDCK cells whereas they were not involved in the translocation process into confluent layers. Interestingly, even in confluent MDCK cells, when treated with cytokines, lipid rafts regained their role in mediating the endocytosis of CPPs. In fact, the cellular translocation of both CPPs was markedly reduced upon extraction with M-β-CD in a cytokine concentration dependent manner. We thus conclude that – under inflammatory conditions – the redistribution of tight junction proteins associated with lipid raft microdomains [67, 68] re-opens the lipid raft mediated pathway for CPPs in confluent MDCK cells. This makes our findings particularly interesting for CPP mediated, targeted delivery of antiinflammatory drugs, e.g., cyclosporin A, to inflammatory epithelia [78] or caveolin-1 scaffolding domain against vasodilatation and nitric oxide production [79]. Nevertheless, the therapeutic outcome of this approach has yet to be demonstrated.

ACKNOWLEDGMENTS

The authors acknowledge the following contributions: Professor Randall Mrsny (Welsh School of Pharmacy, Cardiff UK) for valuable discussions on cytokine induced inflammatory cell models. Professor Heidi Wunderli-Allenspach and Dr. Gabor Csúcs (ETH Zurich) for the opportunity to use their confocal laser scanning microscopes, and Ms. Hanna Barman for help and advice with the Western Blot experiments.

REFERENCES

1. Morris, M.C., et al., *Translocating peptides and proteins and their use for gene delivery.* Curr Opin Biotechnol, 2000. **11**(5): p. 461-6.
2. Wadia, J.S. and S.F. Dowdy, *Modulation of cellular function by TAT mediated transduction of full length proteins.* Curr Protein Pept Sci, 2003. **4**(2): p. 97-104.
3. Derossi, D., et al., *The third helix of the Antennapedia homeodomain translocates through biological membranes.* J Biol Chem, 1994. **269**(14): p. 10444-50.
4. Vives, E., P. Brodin, and B. Lebleu, *A truncated HIV-1 Tat protein basic domain rapidly translocates through the plasma membrane and accumulates in the cell nucleus.* J Biol Chem, 1997. **272**(25): p. 16010-7.
5. Futaki, S., *Arginine-rich peptides: potential for intracellular delivery of macromolecules and the mystery of the translocation mechanisms.* Int J Pharm, 2002. **245**(1-2): p. 1-7.
6. Trehin, R., et al., *Cellular uptake but low permeation of human calcitonin-derived cell penetrating peptides and Tat(47-57) through well-differentiated epithelial models.* Pharm Res, 2004. **21**(7): p. 1248-56.
7. Trehin, R., et al., *Cellular internalization of human calcitonin derived peptides in MDCK monolayers: a comparative study with Tat(47-57) and penetratin(43-58).* Pharm Res, 2004. **21**(1): p. 33-42.
8. Prochiantz, A., *Getting hydrophilic compounds into cells: lessons from homeopeptides.* Curr Opin Neurobiol, 1996. **6**(5): p. 629-34.
9. Schwarze, S.R., et al., *In vivo protein transduction: delivery of a biologically active protein into the mouse.* Science, 1999. **285**(5433): p. 1569-72.
10. Astriab-Fisher, A., et al., *Conjugates of antisense oligonucleotides with the Tat and antennapedia cell-penetrating peptides: effects on cellular uptake, binding to target sequences, and biologic actions.* Pharm Res, 2002. **19**(6): p. 744-54.
11. Singh, D., et al., *Peptide-based intracellular shuttle able to facilitate gene transfer in mammalian cells.* Bioconjug Chem, 1999. **10**(5): p. 745-54.
12. Pooga, M., et al., *Cell penetrating PNA constructs regulate galanin receptor levels and modify pain transmission in vivo.* Nat Biotechnol, 1998. **16**(9): p. 857-61.
13. Lewin, M., et al., *Tat peptide-derivatized magnetic nanoparticles allow in vivo tracking and recovery of progenitor cells.* Nat Biotechnol, 2000. **18**(4): p. 410-4.

14. Krauss, U., et al., *In vitro gene delivery by a novel human calcitonin (hCT)-derived carrier peptide.* Bioorg Med Chem Lett, 2004. **14**(1): p. 51-4.

15. Crespo, L., et al., *Peptide dendrimers based on polyproline helices.* J Am Chem Soc, 2002. **124**(30): p. 8876-83.

16. Fernandez-Carneado, J., et al., *Potential Peptide Carriers: Amphipathic Proline-Rich Peptides Derived from the N-Terminal Domain of gamma-Zein.* Angew Chem Int Ed Engl, 2004. **43**(14): p. 1811-1814.

17. Fernandez-Carneado, J., et al., *Amphipathic peptides and drug delivery.* Biopolymers, 2004. **76**(2): p. 196-203.

18. Foerg, C., et al., *Decoding the Entry of Two Novel Cell-Penetrating Peptides in HeLa Cells: Lipid Raft-Mediated Endocytosis and Endosomal Escape.* Biochemistry, 2005. **44**(1): p. 72-81.

19. Ferrari, A., et al., *Caveolae-mediated internalization of extracellular HIV-1 tat fusion proteins visualized in real time.* Mol Ther, 2003. **8**(2): p. 284-94.

20. Fischer, R., et al., *A stepwise dissection of the intracellular fate of cationic cell-penetrating peptides.* J Biol Chem, 2004. **279**(13): p. 12625-35.

21. Hallbrink, M., et al., *Cargo delivery kinetics of cell-penetrating peptides.* Biochim Biophys Acta, 2001. **1515**(2): p. 101-9.

22. Tyagi, M., et al., *Internalization of HIV-1 tat requires cell surface heparan sulfate proteoglycans.* J Biol Chem, 2001. **276**(5): p. 3254-61.

23. Violini, S., et al., *Evidence for a plasma membrane-mediated permeability barrier to Tat basic domain in well-differentiated epithelial cells: lack of correlation with heparan sulfate.* Biochemistry, 2002. **41**(42): p. 12652-61.

24. Zhang, X., et al., *Quantitative assessment of the cell penetrating properties of RI-Tat-9: evidence for a cell type-specific barrier at the plasma membrane of epithelial cells.* Mol Pharm, 2004. **1**(2): p. 145-55.

25. Cho, M.J., et al., *The Madin Darby canine kidney (MDCK) epithelial cell monolayer as a model cellular transport barrier.* Pharm Res, 1989. **6**(1): p. 71-7.

26. Rothen-Rutishauser, B., et al., *MDCK cell cultures as an epithelial in vitro model: cytoskeleton and tight junctions as indicators for the definition of age-related stages by confocal microscopy.* Pharm Res, 1998. **15**(7): p. 964-71.

27. Simons, K. and S.D. Fuller, *Cell surface polarity in epithelia.* Annu Rev Cell Biol, 1985. **1**: p. 243-88.

28. Balcarova-Stander, J., et al., *Development of cell surface polarity in the epithelial Madin-Darby canine kidney (MDCK) cell line.* Embo J, 1984. **3**(11): p. 2687-94.

29. Harhaj, N.S. and D.A. Antonetti, *Regulation of tight junctions and loss of barrier function in pathophysiology.* Int J Biochem Cell Biol, 2004. **36**(7): p. 1206-37.

30. van Meer, G., B. Gumbiner, and K. Simons, *The tight junction does not allow lipid molecules to diffuse from one epithelial cell to the next.* Nature, 1986. **322**(6080): p. 639-41.

31. van Meer, G. and K. Simons, *The function of tight junctions in maintaining differences in lipid composition between the apical and the basolateral cell surface domains of MDCK cells.* Embo J, 1986. **5**(7): p. 1455-64.

32. Cereijido, M., et al., *Cell-to-cell communication in monolayers of epithelioid cells (MDCK) as a function of the age of the monolayer.* J Membr Biol, 1984. **81**(1): p. 41-8.

33. Cereijido, M., et al., *Role of tight junctions in establishing and maintaining cell polarity.* Annu Rev Physiol, 1998. **60**: p. 161-77.

34. Hallbrink, M., et al., *Uptake of cell-penetrating peptides is dependent on peptide-to-cell ratio rather than on peptide concentration.* Biochim Biophys Acta, 2004. **1667**(2): p. 222-8.

35. Bourne, H.R., *GTPases. A turn-on and a surprise.* Nature, 1993. **366**(6456): p. 628-9.

36. Etienne-Manneville, S. and A. Hall, *Rho GTPases in cell biology.* Nature, 2002. **420**(6916): p. 629-35.

37. Fukata, M., M. Nakagawa, and K. Kaibuchi, *Roles of Rho-family GTPases in cell polarisation and directional migration.* Curr Opin Cell Biol, 2003. **15**(5): p. 590-7.

38. Hall, A., *Rho GTPases and the actin cytoskeleton.* Science, 1998. **279**(5350): p. 509-14.

39. Nobes, C.D. and A. Hall, *Rho, rac, and cdc42 GTPases regulate the assembly of multimolecular focal complexes associated with actin stress fibers, lamellipodia, and filopodia.* Cell, 1995. **81**(1): p. 53-62.

40. Rivero, F. and B.P. Somesh, *Signal transduction pathways regulated by Rho GTPases in Dictyostelium.* J Muscle Res Cell Motil, 2002. **23**(7-8): p. 737-49.

41. Symons, M. and N. Rusk, *Control of vesicular trafficking by Rho GTPases.* Curr Biol, 2003. **13**(10): p. R409-18.

42. Van Aelst, L. and C. D'Souza-Schorey, *Rho GTPases and signaling networks.* Genes Dev, 1997. **11**(18): p. 2295-322.

43. Qualmann, B., M.M. Kessels, and R.B. Kelly, *Molecular links between endocytosis and the actin cytoskeleton.* J Cell Biol, 2000. **150**(5): p. F111-6.

44. Qualmann, B. and H. Mellor, *Regulation of endocytic traffic by Rho GTPases.* Biochem J, 2003. **371**(Pt 2): p. 233-41.

45. Hopkins, A.M., et al., *Constitutive activation of Rho proteins by CNF-1 influences tight junction structure and epithelial barrier function.* J Cell Sci, 2003. **116**(Pt 4): p. 725-42.

46. Orlando, R.C., *Mechanisms of epithelial injury and inflammation in gastrointestinal diseases.* Rev Gastroenterol Disord, 2002. **2 Suppl 2**: p. S2-8.

47. Sanders, D.S., *Mucosal integrity and barrier function in the pathogenesis of early lesions in Crohn's disease.* J Clin Pathol, 2005. **58**(6): p. 568-72.

48. Schmitz, H., et al., *Epithelial barrier and transport function of the colon in ulcerative colitis.* Ann N Y Acad Sci, 2000. **915**: p. 312-26.

49. Schmitz, H., et al., *Tumor necrosis factor-alpha (TNFalpha) regulates the epithelial barrier in the human intestinal cell line HT-29/B6.* J Cell Sci, 1999. **112 (Pt 1)**: p. 137-46.

50. Siccardi, D., J.R. Turner, and R.J. Mrsny, *Regulation of intestinal epithelial function: a link between opportunities for macromolecular drug delivery and inflammatory bowel disease.* Adv Drug Deliv Rev, 2005. **57**(2): p. 219-35.

51. Coyne, C.B., et al., *Regulation of airway tight junctions by proinflammatory cytokines.* Mol Biol Cell, 2002. **13**(9): p. 3218-34.

52. Trautmann, A., et al., *Apoptosis and Loss of Adhesion of Bronchial Epithelial Cells in Asthma.* Int Arch Allergy Immunol, 2005. **138**(2): p. 142-150.

53. Wunderbaldinger, P., L. Josephson, and R. Weissleder, *Tat peptide directs enhanced clearance and hepatic permeability of magnetic nanoparticles.* Bioconjug Chem, 2002. **13**(2): p. 264-8.

54. Hemmings, D.G., et al., *Villous trophoblasts cultured on semi-permeable membranes form an effective barrier to the passage of high and low molecular weight particles.* Placenta, 2001. **22**(1): p. 70-9.

55. Mann, D.A. and A.D. Frankel, *Endocytosis and targeting of exogenous HIV-1 Tat protein.* Embo J, 1991. **10**(7): p. 1733-9.

56. Letoha, T., et al., *Membrane translocation of penetratin and its derivatives in different cell lines.* J Mol Recognit, 2003. **16**(5): p. 272-9.

57. Lamaze, C., et al., *Interleukin 2 receptors and detergent-resistant membrane domains define a clathrin-independent endocytic pathway.* Mol Cell, 2001. **7**(3): p. 661-71.

58. Nichols, B.J., et al., *Rapid cycling of lipid raft markers between the cell surface and Golgi complex.* J Cell Biol, 2001. **153**(3): p. 529-41.

59. Orlandi, P.A. and P.H. Fishman, *Filipin-dependent inhibition of cholera toxin: evidence for toxin internalization and activation through caveolae-like domains.* J Cell Biol, 1998. **141**(4): p. 905-15.

60. Puri, V., et al., *Clathrin-dependent and -independent internalization of plasma membrane sphingolipids initiates two Golgi targeting pathways.* J Cell Biol, 2001. **154**(3): p. 535-47.

61. Karp, G., *Cell and Molecular Biology.* 2nd ed. 1999: John Wiley & Sons, Inc. 292-325.

62. Pelkmans, L. and A. Helenius, *Endocytosis via caveolae.* Traffic, 2002. **3**(5): p. 311-20.

63. Pelkmans, L., J. Kartenbeck, and A. Helenius, *Caveolar endocytosis of simian virus 40 reveals a new two-step vesicular-transport pathway to the ER.* Nat Cell Biol, 2001. **3**(5): p. 473-83.

64. Richard, J.P., et al., *Cell-penetrating peptides. A reevaluation of the mechanism of cellular uptake.* J Biol Chem, 2003. **278**(1): p. 585-90.

65. Ellis, S. and H. Mellor, *Regulation of endocytic traffic by rho family GTPases.* Trends Cell Biol, 2000. **10**(3): p. 85-8.

66. Fish, S.M., R. Proujansky, and W.W. Reenstra, *Synergistic effects of interferon gamma and tumour necrosis factor alpha on T84 cell function.* Gut, 1999. **45**(2): p. 191-8.

67. Bruewer, M., et al., *Proinflammatory cytokines disrupt epithelial barrier function by apoptosis-independent mechanisms.* J Immunol, 2003. **171**(11): p. 6164-72.

68. Nusrat, A., et al., *Tight junctions are membrane microdomains.* J Cell Sci, 2000. **113 (Pt 10)**: p. 1771-81.

69. Jou, T.S., et al., *Selective alterations in biosynthetic and endocytic protein traffic in Madin-Darby canine kidney epithelial cells expressing mutants of the small GTPase Rac1.* Mol Biol Cell, 2000. **11**(1): p. 287-304.

70. Leung, S.M., et al., *Modulation of endocytic traffic in polarized Madin-Darby canine kidney cells by the small GTPase RhoA.* Mol Biol Cell, 1999. **10**(12): p. 4369-84.

71. Kuroda, S., et al., *Regulation of cell-cell adhesion of MDCK cells by Cdc42 and Rac1 small GTPases.* Biochem Biophys Res Commun, 1997. **240**(2): p. 430-5.

72. Takaishi, K., et al., *Regulation of cell-cell adhesion by rac and rho small G proteins in MDCK cells.* J Cell Biol, 1997. **139**(4): p. 1047-59.

73. Gitter, A.H., et al., *Leaks in the epithelial barrier caused by spontaneous and TNF-alpha-induced single-cell apoptosis.* Faseb J, 2000. **14**(12): p. 1749-53.

74. Gassler, N., et al., *Inflammatory bowel disease is associated with changes of enterocytic junctions.* Am J Physiol Gastrointest Liver Physiol, 2001. **281**(1): p. G216-28.

75. Kucharzik, T., et al., *Neutrophil transmigration in inflammatory bowel disease is associated with differential expression of epithelial intercellular junction proteins.* Am J Pathol, 2001. **159**(6): p. 2001-9.

76. Bonfield, T.L., M.W. Konstan, and M. Berger, *Altered respiratory epithelial cell cytokine production in cystic fibrosis.* J Allergy Clin Immunol, 1999. **104**(1): p. 72-8.

77. Naumann, M., et al., *Activation of activator protein 1 and stress response kinases in epithelial cells colonized by Helicobacter pylori encoding the cag pathogenicity island.* J Biol Chem, 1999. **274**(44): p. 31655-62.

78. Rothbard, J.B., et al., *Conjugation of arginine oligomers to cyclosporin A facilitates topical delivery and inhibition of inflammation.* Nat Med, 2000. **6**(11): p. 1253-7.

79. Bucci, M., et al., *In vivo delivery of the caveolin-1 scaffolding domain inhibits nitric oxide synthesis and reduces inflammation.* Nat Med, 2000. **6**(12): p. 1362-7.

DISCUSSION AND OUTLOOK

The objective of the present PhD thesis is to elucidate cellular translocation, trafficking and metabolic cleavage of two recently developed CPPs, namely SAP and hCT(9-32)-br, when in contact with epithelial cell cultures. In addition and for comparison, we also included two members of the so-called MPG family, [Pα] and [Pβ].

Concerning the internalization process and the downstream fate of cell-penetrating peptides, we succeeded in contributing to a more detailed understanding of their translocation mechanism as well as to broaden the knowledge on the still largely unexplored field of their intracellular trafficking. Our findings of both CPPs being internalized via a clathrin-independent mechanism that originates from plasma membrane lipid rafts corroborate recent observations of other groups on already established cationic peptides, revealing comparable clathrin-independent, lipid raft-mediated mechanisms. Nevertheless, in disagreement with recent proposals of a mandatory combination of proteoglycan interaction and lipid raft dependent uptake, our results suggest that irrespective of charge and interaction with the extracellular matrix, the lipid raft-mediated pathway represents the preferred port of entry for various classes of CPPs and is not exclusive for oligocationic peptides, as shown for the weakly cationic, linear hCT(9-32). Furthermore, we propose that early endosomes are involved in the uptake and initial intracellular trafficking of the two oligocationic peptides SAP and hCT(9-32)-br. Having passed the cellular membrane, the two cationic compounds were found to transiently sojourn in endosomal compartments where sorting steps take place, but, within a period of three hours, most of the internalized CF-SAP or CF-hCT(9-32)-br moved to other compartments within the cytosol or was metabolically degraded. Nevertheless, for a future therapeutic application of cell-penetrating peptides, it is still a main prerequisite to study the mechanism of CPP internalization as well as their intracellular trafficking routes in greater detail.

In terms of metabolic stability, we found that for all investigated CPPs, namely SAP, hCT(9-32)-br, [Pα] and [Pβ], the stability was strongly cell line dependent. Assuming that protein and enzyme activity levels correlate, we conclude that the increased protein levels in Calu-3 layers, for example, contribute to the enhanced metabolism of the four CPPs in this model. Inspite of large differences in the rates, there was no major difference in the cleavage patterns between the three cell lines for each of the investigated CPP. In this context we also compared the cellular translocation of the four cell-penetrating peptides. Interestingly, there was no direct relationship between metabolic stability and translocation efficiency, indicating that stability is not a main limiting factor in cellular translocation, at least in the investigated

cell cultures. Nevertheless, translocation of individual CPPs may be improved by structural modifications aiming at increased metabolic stability. To our knowledge, this study is the first to aim towards a relation between metabolic stability and translocation efficiency of CPPs. Our data broaden the knowledge on metabolic stability of CPPs, a momentous subject on which information is still rare. For future therapeutic application, we expect the balance between (i) sufficient CPP stability to deliver a cargo to its destination as well as (ii) sufficient metabolic clearance of the CPPs after delivery in order to free the cargo once internalized and to avoid systemic toxicity, to require careful molecular engineering and development.

In order to emphasize the importance of sufficiently differentiated cell models to study the translocation of CPPs, we investigated the impact of the cellular differentiation state upon efficiency and mechanism of CPP translocation. By comparing proliferating versus confluent MDCK cell cultures, we found the slow-down in endocytic activity on the one hand to relate to the increasing cell culture density and the formation of tight junctions on the other. The observed slow-down was not specific for the investigated two CPPs but compound-unspecific as it was a common feature of several markers for cellular endocytosis. With respect to the cellular translocation of selected CPPs, our findings indicate an intimate involvement of Rho-family GTPases in the differentiation-restricted regulation of endocytic traffic. The extent of CPP endocytosis was directly correlated with active form Rho-A, whereas active form Rac-1 correlated with endocytic slow-down, cell density and cellular differentiation. To our knowledge, this is the first study to cast light on the cell line and differentiation-restricted translocation of CPPs into epithelial cell models and its underlying cellular mechanism.

Our findings further elaborated an interesting relationship between endocytic slow-down and cellular differentiation in an inflammatory epithelial IFN-γ/TNF-α model which we used to mimic inflammatory conditions in epithelia. We found the translocation efficiency of CPPs in the inflammatory IFN-γ/TNF-α model to be significantly enhanced as compared to untreated control. Interestingly, in the inflammatory model of cytokine treated, confluent MDCK cells, lipid rafts were shown to regain their role in mediating the endocytosis of CPPs. This results in our proposal that – under inflammatory conditions – the redistribution of tight junction proteins associated with lipid raft microdomains reopens the lipid raft-mediated pathway for CPPs into confluent MDCK cells. To our knowledge, this indicates for the first time that CPPs may have a role as vehicles for the delivery of therapeutics to inflamed tissue.

In summary, the present PhD study contributes to a more detailed understanding of the translocation process, the involved intracellular trafficking routes and the metabolic stability of CPPs. For a future therapeutic application of CPPs, our studies on the cell line and

differentiation state-dependent translocation of CPPs are of importance. Based on the observed correlation between the slow-down in CPP translocation on the one hand and cell density as well as tight junction formation on the other, we strongly suggest tissue-like cellular models involving junctional complexes to be more justified for translocation studies under therapeutic considerations, as compared to "leaky" cell lines that do not form tight junctions. Furthermore, we propose to revise the notion of an unrestricted cellular delivery by the CPP approach. The observed limitations of CPP translocation may instead by used to identify potential niches for the therapeutic application of CPPs in drug delivery. Our findings of the enhanced CPP translocation in an inflammatory MDCK model are of particular interest with regard to recent studies in the field of cell-penetrating peptides that report on the delivery of anti-inflammatory drugs by CPPs, such as cyclosporin A against cutaneous inflammation or caveolin-1 scaffolding domain against vasodilatation and nitric oxide production. Nevertheless, the therapeutic outcome of this approach has yet to be demonstrated.

CHRISTINA FÖRG
born in Augsburg, Germany
on Dec 16th, 1977

Education

Postgraduate studies

January 2003 until today	**Swiss Federal Institute of Technology (ETH) Zurich, Switzerland** PhD studies at the Institute of Pharmaceutical Sciences Drug Formulation & Delivery (Prof. H. P. Merkle) Teaching assistant in the area of disperse and semi-solid dosage forms.

Undergraduate studies

Nov 1997 – Oct 2001	**University of Würzburg, Germany** Studies in Pharmaceutical Sciences
Dec 2002	Approbation as a pharmacist
1988-1997	**Gymnasium bei St. Anna, Augsburg, Germany**

Working experience

May 2002 - Oct 2002	**Internship at the retail pharmacy "Wittelsbacher-Apotheke", Passau, Germany**
Nov 2001 – April 2002	**Internship at EonPharma, LLC, Wilson, NC, USA;**
April 2000	**Internship at the Calcutta Medical Research Institute, Calcutta, India**
August 1998	**Internship at the pharmaceutical division of Lichtenberg hospital, Berlin, Germany**

Scientific contributions

ARTICLES

Foerg, C., et al. (2005) Decoding the Entry of Two Novel Cell-Penetrating Peptides in HeLa Cells: Lipid Raft-Mediated Endocytosis and Endosomal Escape, *Biochemistry 44*, 72-81.

Fischer, S., Foerg, C., et al. (2006) One-step preparation of polyelectrolyte-coated PLGA microparticles and their functionalization with model ligands, *J Control Release 111*, 135-144

ORAL PRESENTATIONS

Foerg C., et al. *Cellular uptake of cell penetrating peptides is differentiation restricted.* Pepvec meeting, Satellite meeting of the joint 15th JUPAB & 5th EBSA International Biophysics Congress, Montpellier, **France**, August **2005**

Foerg C., et al. *Cellular uptake of cell penetrating peptides (CPP) is differentiation restricted.* 19th American Peptide Symposium, San Diego, **USA**, June **2005**

Foerg C., et al. *Cell penetrating peptides: Cell line and differentiation state specific uptake?* European Project Consortium Meeting, Montpellier, **France**, November **2004**

Foerg C., et al. *Cell penetrating peptides: Cell line and differentiation state specific uptake?* Zurich-Geneva Joint Seminar Series on Drug Formulation & Drug Delivery, Zurich, **Switzerland**, October **2004**

Foerg C., et al. *Cyclodextrins and cell-penetrating peptides: synergistic enhancement of uptake in an epithelial cell model.* 12th International Cyclodextrin Symposium, Montpellier, **France**, May **2004**

Foerg C., et al. *Uptake and translocation mechanisms of two novel cell penetrating peptides* European Project Consortium Meeting, Zurich, **Switzerland**, April **2004**

Foerg C., et al. *Promising new CPPs: CF-(VRLPPP)$_3$OH and hCT(9-32)-branched. Uptake studies in epithelial cell models.* European Project Consortium Meeting, Leipzig, **Germany**, October **2003**

POSTER PRESENTATIONS

Foerg C., et al. *Uptake and translocation mechanisms of two novel cell penetrating peptides in Hela cells.* Joining Forces Symposium, Zurich, **Switzerland**, October **2004**

Foerg C., et al. *Uptake and translocation mechanisms of two novel cell penetrating peptides in Hela cells.*
3rd International and 28th European Peptide Symposium, Prag, **Czech Republic**, September **2004**

Foerg C., et al. *Uptake and translocation mechanisms of two novel cell penetrating peptides in Hela cells.*
2nd Pharmaceutical Sciences World Congress (PSWC), Kyoto, **Japan**, June **2004**

Foerg C., et al. *Uptake and translocation mechanisms of two novel cell penetrating peptides in Hela cells.* 5th GPEN Meeting (Globalization of Pharmaceutics Education Network), Kyoto, **Japan**, May **2004**

Foerg C., et al. *Proline-rich peptides as potential cell-penetrating peptides: uptake studies in epithelial cell lines.* Meeting of the European Light Microscopy Initiative, Barcelona, **Spain**, June **2003**.

Acknowledgements

First of all, I want to thank my supervisor, Professor Hans Peter Merkle for accepting me in his research group. He gave me scientific support and motivation and he was always available for constructive discussions. It was a great pleasure to work in his group!

My sincere thanks also go to Dr. Urs Ziegler for granting me "guest-worker status" in the anatomy group. His support and continuous encouragement were of great help. I want to thank Claudia, Hanna, Sonja, Gerry, Michael and the whole anatomy group for the nice working atmosphere and the valuable discussions.

I am very grateful to Professor Ernest Giralt for being my co-referee. His scientific inputs as well as his personal encouragement were a great contribution to my PhD thesis.

Cordial thanks also go to Dr. Jimena Fernandez-Carneado for the helpful scientific contributions given during her stay in Zurich and the fruitful discussions.

I want to thank Professor Annette Beck-Sickinger and her working group for the valuable collaboration during my PhD thesis.

Thank you also to Dr. René Brunisholz and Helen Rechensteiner for supporting me during the metabolism study, as well as to the group of Professor Heidi Wunderli-Allenspach for support in confocal microscopy.

Special thanks go to all (former) members of the Galenic group at the ETH Zurich, especially Kathrin, Annette, Rachel, Michael, Uta, Stefan, Sandra, Esther, Lukas, Lorenz, Ruth, Christina and, last but not least, Professor Bruno Gander. You all made my stay in Zurich a great time!

Dankeschön!

Mein ganz besonderer Dank geht an Thomas für seine Geduld und Unterstützung in jeglicher Hinsicht – nicht nur während meiner Doktoratszeit in Zürich! Ohne seine Motivation wäre ich nicht so schnell in Berlin gelandet!

Vor allem möchte ich mich ganz herzlich bei meinen Eltern und meinen Schwestern Eva-Maria und Sylvia bedanken! Sie haben mir den nötigen Ehrgeiz und Optimismus und alles, was man sonst fürs Leben braucht, mit auf den Weg gegeben.